NOT FOR PUBLICATION

NEANDC(J)-61/U

INDC(JAP)-47/U

PROGRESS REPORT

(July 1978 to June 1979 inclusive)

September 1979

Editor

S. Kikuchi

Japanese Nuclear Data Committee

Japan Atomic Energy Research Institute

Tokai Research Establishment

Tokai-mura, Ibaraki-ken, Japan

NOT FOR PUBLICATION

NEANDC(J)-61/U

INDC(JAP)-47/U

PROGRESS REPORT

(July 1978 to June 1979 inclusive)

September 1979

Editor

S. Kikuchi

Japanese Nuclear Data Committee

Japan Atomic Energy Research Institute

Tokai Research Establishment

Tokai-mura, Ibaraki-ken, Japan

Editor's Note

This is a collection of reports which have been submitted to the Japanese Nuclear Data Committee at the Committee's request. The request was addressed to the following individuals who might represent or be in touch with groups doing researches related to the nuclear data of interest to the development of the nuclear energy program.

Although the editor tried not to miss any appropriate addressees, there may have been some oversight. Meanwhile, contribution of a report rested with discretion of its author. The coverage of this document, therefore, may not be uniform over the related field of research.

In this progress report, each individual report is generally reproduced as it was received by the JNDC Secretariat, and the editor also let pass some simple obvious errors in the manuscripts if any.

This edition covers a period of July 1, 1978 to June 30, 1979. The information herein contained is of a nature of "Private Communication". Data contained in this report should not be quoted without the author's permission.

Addressees of the request to submit report:

(in Alphabetical order)

1) Electrotechnical Laboratory
Tanashi Branch / 5-4-1, Mukaidai, Tanashi-shi, Tokyo 188
(E. Teranishi)

2) Hiroshima University
Faculty of Science / 1-1-89 Higashi-senda, Hiroshima 730
(Y. Yoshizawa)

3) Hitachi Ltd.
Atomic Energy Research Laboratory / Oozenji, Tama-ku, Kawasaki-shi, Kanagawa 215
(S. Kobayashi)

4) Hokkaido University
Faculty of Engineering / Kitajunijo, Kita-ku, Sapporo 060
(Y. Ozawa, H. Tanaka)

5) Hosei University
2-17-1 Fujimi, Chiyoda-ku, Tokyo 102
(R. Nakasima)

6) Japan Atomic Energy Research Institute
Tokai Research Establishment / Tokai-mura, Naka-gun, Ibaraki 319-11
(T. Abe, H. Amano, A. Asami, T. Asaoka, T. Fuketa, Y. Goto, Y. Hamaguchi, K. Harada, K. Hidaka, J. Hirota, S. Honma, Y. Ishiguro, N. Itoh, S. Katsuragi, H. Kuroi, H. Nakamura, H. Natsume, K. Nishimura, M. Nozawa, Y. Obata, H. Okashita, N. Shikazono, J. Shimokawa, S. Tanaka, K. Tsukada, K. Ueno, T. Yasuno, S. Yasukawa, H. Yoshida, et al.)

7) Konan University
Faculty of Science / Okamoto, Motoyama-cho, Higashinada-ku, Kobe 658
(K. Yuasa)

8) Kyoto University
   a) Faculty of Engineering / Yoshida Hon-cho, Sakyo-ku, Kyoto 606
   (H. Nishihara)

   b) Faculty of Science / Kitashirakawa Oiwaki-cho, Sakyo-ku, Kyoto 606
   (J. Muto)

   c) Institute of Atomic Energy / Gokanosho, Uji-shi, Kyoto 611
   (T. Nishi)

   d) Keage Laboratory of Nuclear Science, Institute for Chemical Research / 2 Torii-cho, Awataguchi, Sakyo-ku, Kyoto 606
   (H. Takekoshi)

   e) Research Reactor Institute / Kumatori, Sennan-gun, Osaka 590-04
   (I. Kimura, K. Okano, S. Okamoto)

9) Kyushu University
   a) Faculty of Engineering / Hakozaki-cho, Higashi-ku, Fukuoka 812
   (A. Katase, I. Kumabe, M. Ohta)

b) Faculty of Science/ Hakozaki-cho, Higashi-ku, Fukuoka 812
(A. Isoya, M. Kawai)

c) Graduate School of Engineering Science / Hakozaki-cho, Higashi-ku, Fukuoka 812
(Y. Kanda)

10) Mitsubishi Atomic Power Industries, Inc.
Engineering and Development Division / Kitafukuro, Omiya-shi, Saitama 330
(Y. Seki)

11) Nagoya University
Faculty of Engineering / Furo-cho, Chigusa-ku, Nagoya 464
(T. Katoh)

12) National Institute of Radiological Sciences
4-9-1 Anagawa, Chiba 280
(K. Kitao)

13) National Laboratory for High Energy Physics
Ooho-cho, Tsukuba-gun, Ibaraki 300-32
(K. Kato, K. Takahashi)

14) Nippon Atomic Industry Group Co., Ltd.
NAIG Nuclear Research Laboratory / 4-1, Ukishima-cho, Kawasaki-shi Kanagawa 210
(S. Iijima)

15) Osaka University
a) Faculty of Engineering / Yamadaue, Suita-shi, Osaka 565
(T. Sekiya, K. Sumita)

b) Faculty of Science / 1-1, Machikaneyama, Toyonaka-shi, Osaka 560
(M. Muraoka)

c) Research Center for Nuclear Physics / Yamadaue, Suita-shi, Osaka 565
(H. Ikegami, S, Yamabe)

16) Radiation Center of Osaka Prefecture
704 Shinke-cho, Sakai-shi, Osaka 593
(K. Fukuda)

17) Rikkyo (St. Paul's) University
a) Department of Physics / 3, Ikebukuro, Toshima-ku, Tokyo 171
(I. Ogawa, S. Shirato)

b) Institute for Atomic Energy / 2-5-1, Nagasaka, Yokosuka-shi, Kanagawa 240-01
(M. Hattori)

18) Ship Research Institute
38-1, 6-chome, Shinkawa, Mitaka-shi, Tokyo 181
(H. Yamakoshi)

19) Sumitomo Atomic Energy Industries, Ltd.
2-10, Kandakaji-cho, Chiyoda-ku, Tokyo 101
(H. Matsunobu)

20) The Institute of Physical and Chemical Research
2-1, Hirosawa, Wako-shi, Saitama 351
(A. Hashizume)

21) Tohoku University
a) Faculty of Engineering / Aza-Aoba, Aramaki, Sendai 980
(K. Sugiyama)

b) Faculty of Science / Aza-Aoba, Aramaki, Sendai 980

c) Laboratory of Nuclear Science / 1 Kanayama, Tomisawa, Sendai 982
(Y. Torizuka)

22) Tokai University
Faculty of Engineering / 2-28-4 Tomigaya, Shibuya-ku, Tokyo 151
(Y. Kuroda)

23) Tokyo Institute of Technology
a) Faculty of Science / 2-12-1 Ohokayama, Meguro-ku, Tokyo 152
(K. Hisatake, Y. Oda, H. Ohnuma, H. Taketani)

b) Research Laboratory for Nuclear Reactors / 2-12-1 Ohokayama, Meguro-ku, Tokyo 152
(N. Yamamuro)

24) University of Tokyo
a) College of General Education / 3-8-1 Komaba, Meguro-ku, Tokyo 153
(T. Terasawa)

b) Faculty of Engineering / 7-3-1 Hongo, Bunkyo-ku, Tokyo 113
(S. An, A. Sekiguchi)

c) Faculty of Science / 7-3-1 Hongo, Bunkyo-ku, Tokyo 113
(Y. Nogami)

d) Institute for Nuclear Study / 3-2-1 Midori-cho, Tanashi-shi, Tokyo 188
(T. Hasegawa, Y. Ishizaki, H. Kamitsubo, M. Sakai, K. Sugimoto)

e) The Institute for Solid State Physics / 7-22-1 Roppongi, Minato-ku, Tokyo 106
(K. Ohno)

25) University of Tsukuba
Institute of Physics / Ooaza-Saiki, Sakura-mura, Niihari-gun, Ibaraki 300-31
(J. Sanada)

26) Waseda University
School of Science and Engineering / 4-170 Nishi-Ohkubo, Shinjuku-ku, Tokyo 160
(M. Yamada)

TABLE OF CONTENTS

Contents of the Japanese Progress Report

The content table in the CINDA format was compiled by the JNDC CINDA group;

S. Tanaka (JAERI),

R. Nakasima (Hosei Univ.),

Y. Kawarasaki (JAERI),

M. Sakamoto (JAERI),

M. Kawai (NAIG),

T. Nakagawa (JAERI).

ELEMENT S	A	QUANTITY	ENERGY MIN	MAX	LAB	TYPE	DOCUMENTATION REF	VOL	PAGE	DATE	COMMENTS
BE	009	N, 2N	14+7		YOK	EXPT-PROG	NEANDC-J61U	108		SEP 79	SHIRATO+,ALPHA-ALPHA CORRELATION,FIG
MG	024	N, PROTON	FISS		KTO	EXPT-PROG	NEANDC-J61U	81		SEP 79	KOBAYASHI+,FOR U235,CF252 FISS-N.TBL
MG	024	N, PROTON	FAST		TKO	EXPT-PROG	NEANDC-J61U	81		SEP 79	KOBAYASHI+,1.35+-0.07MB
AL	027	NONELA GAMMA	53+6	70+6	TOH	EXPT-PROG	NEANDC-J61U	112		SEP 79	HINO+,DYNAMITRON,GE-DET,125DEG-SIGS
AL	027	N, PROTON	FISS		KTO	EXPT-PROG	NEANDC-J61U	81		SEP 79	KOBAYASHI+,FOR U235,CF252 FISS-N.TBL
AL	027	N, PROTON	FAST		TKO	EXPT-PROG	NEANDC-J61U	81		SEP 79	KOBAYASHI+,3.64+-0.21MB
P	031	N, PROTON	FISS		KTO	EXPT-PROG	NEANDC-J61U	81		SEP 79	KOBAYASHI+,33.5+-2.0MB FOR U235 FISS
P	031	N, PROTON	FAST		TKO	EXPT-PROG	NEANDC-J61U	81		SEP 79	KOBAYASHI+,34.0+-2.5MB
S	032	N, PROTON	FISS		KTO	EXPT-PROG	NEANDC-J61U	81		SEP 79	KOBAYASHI+,FOR U235,CF252 FISS-N.TBL
TI		TOTAL	30+5	20+7	JAE	EVAL-PROG	NEANDC-J61U	18		SEP 79	KAWAI.OPT-MDL FIT IN FIG
TI		STRNTH FNCTN	10+3		JAE	EVAL-PROG	NEANDC-J61U	18		SEP 79	KAWAI.OPT-MDL CALC. CFD C EXP.DATA
TI	046	N, PROTON	15+7		KYU	EXPT-PROG	NEANDC-J61U	94		SEP 79	KAYASHIMA+,ACTIVATION. 230+-50MB
TI	048	N, PROTON	15+7		KYU	EXPT-PROG	NEANDC-J61U	94		SEP 79	KAYASHIMA+,ACTIVATION. 55.0+-5.0MB
TI	050	N, ALPHA	15+7		KYU	EXPT-PROG	NEANDC-J61U	94		SEP 79	KAYASHIMA+,ACTIVATION. 11.5+-5.3MB
V	051	EVALUATION		20+7	JAE	EVAL-PROG	NEANDC-J61U	11		SEP 79	TANAKA,RES,TOT,SEL,SIN,NG,NX'S,FIG
V	051	TOTAL	30+5	20+7	JAE	EVAL-PROG	NEANDC-J61U	18		SEP 79	KAWAI.OPT-MDL FIT.NDG
V	051	N, PROTON	FISS		KTO	EXPT-PROG	NEANDC-J61U	81		SEP 79	KOBAYASHI+,0.71+-.11MB IN CF252 FISS
V	051	STRNTH FNCTN	10+3		JAE	EVAL-PROG	NEANDC-J61U	18		SEP 79	KAWAI.OPT-MDL CALC. CFD C EXP.DATA
CR		EVALUATION	10-5	20+7	JAE	EVAL-PROG	NEANDC-J61U	14		SEP 79	ASAMI+,RES,TOT,SEL,SIN,NG,NX'S,NDG
CR		TOTAL	20+5	20+7	JAE	EVAL-PROG	NEANDC-J61U	18		SEP 79	KAWAI.OPT-MDL FIT IN FIG

ELEMENT S	A	QUANTITY	ENERGY MIN	MAX	LAB	TYPE	DOCUMENTATION REF	VOL	PAGE	DATE	COMMENTS
CR		STRNTH FNCTN	10+3		JAE	EVAL-PROG	NEANDC-J61U	18		SEP 79	KAWAI.OPT-MDL CALC. CFD C EXP.DATA
CR	050	EVALUATION	10-5	20+7	JAE	EVAL-PROG	NEANDC-J61U	14		SEP 79	ASAMI+.RES.TOT.SEL.SIN.NG.NX'S.NDG
CR	050	LVL DENSITY	NDG		JAE	EVAL-PROG	NEANDC-J61U	16		SEP 79	YOSHIDA.DETERMINATION OF PARS.TABLE
CR	051	LVL DENSITY	NDG		JAE	EVAL-PROG	NEANDC-J61U	16		SEP 79	YOSHIDA.DETERMINATION OF PARS.TABLE
CR	052	EVALUATION	10-5	20+7	JAE	EVAL-PROG	NEANDC-J61U	14		SEP 79	ASAMI+.RES.TOT.SEL.SIN.NG.NX'S.NDG
CR	052	N. PROTON	FAST		TKO	EXPT-PROG	NEANDC-J61U	81		SEP 79	KOBAYASHI+.1.07+-0.07MB
CR	052	N. PROTON	FISS		KTO	EXPT-PROG	NEANDC-J61U	81		SEP 79	KOBAYASHI+.1.06+-0.11MB IN U235 FISS
CR	052	LVL DENSITY	NDG		JAE	EVAL-PROG	NEANDC-J61U	16		SEP 79	YOSHIDA.DETERMINATION OF PARS.TABLE
CR	053	EVALUATION	10-5	20+7	JAE	EVAL-PROG	NEANDC-J61U	14		SEP 79	ASAMI+.RES.TOT.SEL.SIN.NG.NX'S.NDG
CR	053	N. PROTON	FAST		TKO	EXPT-PROG	NEANDC-J61U	81		SEP 79	KOBAYASHI+.0.306+-0.027MB
CR	053	LVL DENSITY	NDG		JAE	EVAL-PROG	NEANDC-J61U	16		SEP 79	YOSHIDA.DETERMINATION OF PARS.TABLE
CR	054	EVALUATION	10-5	20+7	JAE	EVAL-PROG	NEANDC-J61U	14		SEP 79	ASAMI+.RES.TOT.SEL.SIN.NG.NX'S.NDG
CR	054	LVL DENSITY	NDG		JAE	EVAL-PROG	NEANDC-J61U	16		SEP 79	YOSHIDA.DETERMINATION OF PARS.TABLE
MN	055	TOTAL	30+5	20+7	JAE	EVAL-PROG	NEANDC-J61U	18		SEP 79	KAWAI.OPT-MDL FIT.NDG
MN	055	N. 2N	15+7		KYU	EXPT-PROG	NEANDC-J61U	94		SEP 79	KAYASHIMA+.ACTIVATION. 884+-58MB
MN	055	STRNTH FNCTN	10+3		JAE	EVAL-PROG	NEANDC-J61U	18		SEP 79	KAWAI.OPT-MDL CALC. CFD C EXP.DATA
FE		TOTAL	50+4	20+7	JAE	EVAL-PROG	NEANDC-J61U	18		SEP 79	KAWAI.OPT-MDL FIT IN FIG
FE		DIFF INELAST	14+7		KYU	THEO-PROG	NEANDC-J61U	86		SEP 79	FUKUDA+.MULTI-STEP DIRECT REACT.FIG
FE		RESON PARAMS		51+5	JAE	EVAL-PROG	NEANDC-J61U	30		SEP 79	YAMAKOSHI+.EVL FOR JENDL-2.FIGS
FE	054	N. PROTON	FAST		TKO	EXPT-PROG	NEANDC-J61U	81		SEP 79	KOBAYASHI+.76.7+-4.6MB

ELEMENT S A	QUANTITY	ENERGY MIN	ENERGY MAX	LAB	TYPE	DOCUMENTATION REF	VOL	PAGE	DATE	COMMENTS
FE 054	N, PROTON	FISS		KTO	EXPT-PROG	NEANDC-J61U	81	SEP	79	KOBAYASHI+,FOR U235,CF252 FISS-N.TBL
FE 054	RESON PARAMS		51+5	JAE	EVAL-PROG	NEANDC-J61U	30	SEP	79	YAMAKOSHI+,EVL FOR JENDL-2.NDG
FE 054	STRNTH FNCTN	10+3		JAE	EVAL-PROG	NEANDC-J61U	18	SEP	79	KAWAI,OPT-MDL CALC, CFD C EXP.DATA
FE 054	LVL DENSITY	NDG		JAE	EVAL-PROG	NEANDC-J61U	16	SEP	79	YOSHIDA,DETERMINATION OF PARS.TABLE
FE 055	LVL DENSITY	NDG		JAE	EVAL-PROG	NEANDC-J61U	16	SEP	79	YOSHIDA,DETERMINATION OF PARS.TABLE
FE 056	DIFF ELASTIC	20+4		JAE	THEO-PROG	NEANDC-J61U	22	SEP	79	IIJIMA,ANISOTROPY IN RESONANCE.FIGS
FE 056	N, PROTON	FISS		KTO	EXPT-PROG	NEANDC-J61U	81	SEP	79	KOBAYASHI+,FOR U235,CF252 FISS-N.TBL
FE 056	N, PROTON	FAST		TKO	EXPT-PROG	NEANDC-J61U	81	SEP	79	KOBAYASHI+,0.996+-0.06MB
FE 056	RESON PARAMS		40+5	JAE	EVAL-PROG	NEANDC-J61U	30	SEP	79	YAMAKOSHI+,EVL FOR JENDL-2.NDG
FE 056	STRNTH FNCTN	10+3		JAE	EVAL-PROG	NEANDC-J61U	18	SEP	79	KAWAI,OPT-MDL CALC, CFD C EXP.DATA
FE 056	STRNTH FNCTN		10+7	JAE	EVAL-PROG	NEANDC-J61U	18	SEP	79	KAWAI,OPT-MDL CALC, CFD C EXP.IN FIG
FE 056	LVL DENSITY	NDG		JAE	EVAL-PROG	NEANDC-J61U	16	SEP	79	YOSHIDA,DETERMINATION OF PARS.TABLE
FE 057	RESON PARAMS		19+5	JAE	EVAL-PROG	NEANDC-J61U	30	SEP	79	YAMAKOSHI+,EVL FOR JENDL2.SIN IN FIG
FE 057	STRNTH FNCTN	10+3		JAE	EVAL-PROG	NEANDC-J61U	18	SEP	79	KAWAI,OPT-MDL CALC, CFD C EXP.DATA
FE 057	LVL DENSITY	NDG		JAE	EVAL-PROG	NEANDC-J61U	16	SEP	79	YOSHIDA,DETERMINATION OF PARS.TABLE
FE 058	LVL DENSITY	NDG		JAE	EVAL-PROG	NEANDC-J61U	16	SEP	79	YOSHIDA,DETERMINATION OF PARS.TABLE
CO 059	TOTAL	30+5	20+7	JAE	EVAL-PROG	NEANDC-J61U	18	SEP	79	KAWAI,OPT-MDL FIT.NDG
CO 059	N, ALPHA	FAST		TKO	EXPT-PROG	NEANDC-J61U	81	SEP	79	KOBAYASHI+,0.143+-0.008MB
CO 059	N, ALPHA	FISS		KTO	EXPT-PROG	NEANDC-J61U	81	SEP	79	KOBAYASHI+,.217+-015MB IN CF252 FISS
CO 059	STRNTH FNCTN	10+3		JAE	EVAL-PROG	NEANDC-J61U	18	SEP	79	KAWAI,OPT-MDL CALC, CFD C EXP.DATA

ELEMENT S	A	QUANTITY	ENERGY MIN	MAX	LAB	TYPE	DOCUMENTATION REF	VOL	PAGE	DATE	COMMENTS
NI		EVALUATION	10-5	20+7	JAE	EVAL-PROG	NEANDC-J61U	43		SEP 79	SEKINE+.RES.TOT.SEL.SIN.NG.NX'S.FIGS
NI		TOTAL	30+5	20+7	JAE	EVAL-PROG	NEANDC-J61U	18		SEP 79	KAWAI.OPT-MDL FIT IN FIG
NI		NONELA GAMMA	53+6	70+6	TOH	EXPT-PROG	NEANDC-J61U	112		SEP 79	HINO+.DYNAMITRON.GE-DET.NDG
NI		STRNTH FNCTN	10+3		JAE	EVAL-PROG	NEANDC-J61U	18		SEP 79	KAWAI.OPT-MDL CALC. CFD C EXP.DATA
NI	058	N. PROTON	FISS		KTO	EXPT-PROG	NEANDC-J61U	81		SEP 79	KOBAYASHI+.119+-6MB IN CF252 FISS-N
NI	058	LVL DENSITY	NDG		JAE	EVAL-PROG	NEANDC-J61U	16		SEP 79	YOSHIDA.DETERMINATION OF PARS.TABLE
NI	059	LVL DENSITY	NDG		JAE	EVAL-PROG	NEANDC-J61U	16		SEP 79	YOSHIDA.DETERMINATION OF PARS.TABLE
NI	060	LVL DENSITY	NDG		JAE	EVAL-PROG	NEANDC-J61U	16		SEP 79	YOSHIDA.DETERMINATION OF PARS.TABLE
NI	061	LVL DENSITY	NDG		JAE	EVAL-PROG	NEANDC-J61U	16		SEP 79	YOSHIDA.DETERMINATION OF PARS.TABLE
NI	062	LVL DENSITY	NDG		JAE	EVAL-PROG	NEANDC-J61U	16		SEP 79	YOSHIDA.DETERMINATION OF PARS.TABLE
NI	063	LVL DENSITY	NDG		JAE	EVAL-PROG	NEANDC-J61U	16		SEP 79	YOSHIDA.DETERMINATION OF PARS.TABLE
NI	064	LVL DENSITY	NDG		JAE	EVAL-PROG	NEANDC-J61U	16		SEP 79	YOSHIDA.DETERMINATION OF PARS.TABLE
NI	065	LVL DENSITY	NDG		JAE	EVAL-PROG	NEANDC-J61U	16		SEP 79	YOSHIDA.DETERMINATION OF PARS.TABLE
CU		TOTAL	30+5	20+7	JAE	EVAL-PROG	NEANDC-J61U	18		SEP 79	KAWAI.OPT-MDL FIT.NDG
CU		DIFF INELAST	14+7		KYU	THEO-PROG	NEANDC-J61U	86		SEP 79	FUKUDA+.MULTI-STEP DIRECT REACT.FIG
CU		NONELA GAMMA	53+6	70+6	TOH	EXPT-PROG	NEANDC-J61U	112		SEP 79	HINO+.DYNAMITRON.GE-DET.125DEG-SIGS
CU		STRNTH FNCTN	10+3		JAE	EVAL-PROG	NEANDC-J61U	18		SEP 79	KAWAI.OPT-MDL CALC. CFD C EXP.DATA
CU	063	N. ALPHA	15+7		KYU	EXPT-PROG	NEANDC-J61U	94		SEP 79	KAYASHIMA+.ACT.GND SIG=50.4+-5.7MB
ZN	064	N. PROTON	FISS		KTO	EXPT-PROG	NEANDC-J61U	81		SEP 79	KOBAYASHI+.41.7+-2.7MB IN CF252 FISS
ZN	066	N. 2N	15+7		KYU	EXPT-PROG	NEANDC-J61U	94		SEP 79	KAYASHIMA+.ACTIVATION. 588+-65MB

ELEMENT S	A	QUANTITY	ENERGY MIN	MAX	LAB	TYPE	DOCUMENTATION REF	VOL	PAGE	DATE	COMMENTS
AS		DIFF INELAST	14+7		KYU	THEO-PROG	NEANDC-J61U	86		SEP 79	FUKUDA+,MULTI-STEP DIRECT REACT,FIG
BR	079	TOTAL		15+4	JAE	EXPT-PROG	NEANDC-J61U	5		SEP 79	OHKUBO+,LINAC,TRANSMMISION,NDG
BR	079	N, GAMMA		15+4	JAS	EXPT-PROG	NEANDC-J61U	5		SEP 79	OHKUBO+,LINAC,TOF,M-R DET,NDG
BR	079	RESON PARAMS		10+4	JAE	EXPT-PROG	NEANDC-J61U	5		SEP 79	OHKUBO+,WN,WG FOR ABOUT 150 LVLS,NDG
BR	081	TOTAL		15+4	JAE	EXPT-PROG	NEANDC-J61U	5		SEP 79	OHKUBO+,LINAC,TRANSMMISION,NDG
BR	081	N, GAMMA		15+4	JAE	EXPT-PROG	NEANDC-J61U	5		SEP 79	OHKUBO+,LINAC,TOF,M-R DET,NDG
BR	081	RESON PARAMS		15+4	JAS	EXPT-PROG	NEANDC-J61U	5		SEP 79	OHKUBO+,WN,WG FOR ABOUT 100 LVLS,NDG
SR	086	N, 2N	15+7		KYU	EXPT-PROG	NEANDC-J61U	94		SEP 79	KAYASHIMA+,ACT,GND SIG=918+-74MB
SR	086	N, PROTON	15+7		KYU	EXPT-PROG	NEANDC-J61U	94		SEP 79	KAYASHIMA+,ACTIVATION, 34.9+-8.4MB
Y	089	N, 2N	15+7		KYU	EXPT-PROG	NEANDC-J61U	94		SEP 79	KAYASHIMA+,ACTIVATION, 962+-78MB
Y	089	N, ALPHA	15+7		KYU	EXPT-PROG	NEANDC-J61U	94		SEP 79	KAYASHIMA+,ACT,GND SIG=4.8+-2.1MB
NB	093	TOT INELAST	FISS		KTO	EXPT-PROG	NEANDC-J61U	78		SEP 79	KOBAYASHI+,122+-9MB (ISOMER)
NB	093	DIFF INELAST	14+7		KYU	THEO-PROG	NEANDC-J61U	86		SEP 79	FUKUDA+,MULTI-STEP DIRECT REACT=69G
NB	093	NONELA GAMMA	53+6	70+6	TOH	EXPT-PROG	NEANDC-J61U	112		SEP 79	HINO+,DYNAMITRON,GE-DET,NDG
NB	093	N EMISSION	16+7		TOH	EXPT-PROG	NEANDC-J61U	117		SEP 79	IWASAKI+,DYNAMITRON,SIG IN FIG
AG		DIFF INELAST	14+7		KYU	THEO-PROG	NEANDC-J61U	86		SEP 79	FUKUDA+,MULTI-STEP DIRECT REACT,FIG
CD	110	N, PROTON	15+7		KYU	EXPT-PROG	NEANDC-J61U	94		SEP 79	KAYASHIMA+,ACT,ISOM SIG=27.1+-4.7MB
CD	116	N, 2N	15+7		KYU	EXPT-PROG	NEANDC-J61U	94		SEP 79	KAYASHIMA+,ACT,ISOM AND GND SIGS GVN
IN	113	TOT INELAST	FAST		TKO	EXPT-PROG	NEANDC-J61U	81		SEP 79	KOBAYASHI+,155+-13MB FOR ISOMER
IN	113	TOT INELAST	FISS		KTO	EXPT-PROG	NEANDC-J61U	81		SEP 79	KOBAYASHI+,ISOM SIG FOR CF252 FISS-N

ELEMENT S	A	QUANTITY	ENERGY MIN	ENERGY MAX	LAB	TYPE	DOCUMENTATION REF	VOL	PAGE	DATE	COMMENTS
IN	115	TOT INELAST	FISS		KTO	EXPT-PROG	NEANDC-J61U	81		SEP 79	KOBAYASHI+.ISOM SIG FOR CF252 FISS-N
IN	115	N. 2N	15+7		KYU	EXPT-PROG	NEANDC-J61U	94		SEP 79	KAYASHIMA+.ACT.ISOM SIG=1331+-110MB
IN	115	N. PROTON	15+7		KYU	EXPT-PROG	NEANDC-J61U	94		SEP 79	KAYASHIMA+.ACT.GND SIG=5.1+-0.8MB
IN	115	N. PROTON	14+7		KYU	THEO-PROG	NEANDC-J61U	90		SEP 79	FUKUDA+.MULTI-STEP DIRECT REACT.FIG
SB	124	N. GAMMA	PILE		JAE	EXPT-PROG	NEANDC-J61U	67		SEP 79	NISHIMURA+.TBP IN NST.17.4+-3 BARNS
TE	120	N. 2N	15+7		KYU	EXPT-PROG	NEANDC-J61U	94		SEP 79	KAYASHIMA+.ACT.ISOM AND GND SIGS GVN
TE	122	N. 2N	15+7		KYU	EXPT-PROG	NEANDC-J61U	94		SEP 79	KAYASHIMA+.ACT.ISOM AND GND SIGS GVN
TE	122	N. PROTON	15+7		KYU	EXPT-PROG	NEANDC-J61U	94		SEP 79	KAYASHIMA+.ACTIVATION. 14.5+-3.1MB
TE	124	N. 2N	15+7		KYU	EXPT-PROG	NEANDC-J61U	94		SEP 79	KAYASHIMA+.ACT.ISOM SIG=863+-69MB
TE	124	N. PROTON	15+7		KYU	EXPT-PROG	NEANDC-J61U	94		SEP 79	KAYASHIMA+.ACT.GND SIG=8.4+-1.1MB
TE	128	N. ALPHA	15+7		KYU	EXPT-PROG	NEANDC-J61U	94		SEP 79	KAYASHIMA+.ACT.GND SIG=0.78+-0.45MB
TE	130	N. 2N	15+7		KYU	EXPT-PROG	NEANDC-J61U	94		SEP 79	KAYASHIMA+.ACT.ISOM SIG=1203+-97MB
CS	133	N. GAMMA	50+3	30+5	JAE	EXPT-PROG	NEANDC-J61U	101		SEP 79	KAWANO+.LINAC.TOF.LIQUID-SCINT.NDG
ND	143	N. GAMMA	50+3	40+5	JAE	EXPT-PROG	NEANDC-J61U	1		SEP 79	NAKAJIMA+.ABST FOR 78HAR.LINAC.NDG
ND	145	N. GAMMA	50+3	40+5	JAE	EXPT-PROG	NEANDC-J61U	1		SEP 79	NAKAJIMA+.ABST FOR 78HAR.LINAC.NDG
ND	146	N. GAMMA	50+3	40+5	JAE	EXPT-PROG	NEANDC-J61U	1		SEP 79	NAKAJIMA+.ABST FOR 78HAR.LINAC.NDG
ND	148	N. GAMMA	50+3	40+5	JAE	EXPT-PROG	NEANDC-J61U	1		SEP 79	NAKAJIMA+.ABST FOR 78HAR.LINAC.NDG
SM	147	TOTAL	+0	30+5	JAE	EXPT-PROG	NEANDC-J61U	3		SEP 79	MIZUMOTO+.LINAC.TRANSMISSION.NDG
SM	147	N. GAMMA	30+3	30+5	JAE	EXPT-PROG	NEANDC-J61U	3		SEP 79	MIZUMOTO+.LINAC.TOF.LIQUID-SCINT.NDG
SM	147	RESON PARAMS		20+3	JAE	EXPT-PROG	NEANDC-J61U	3		SEP 79	MIZUMOTO+.WN.WG FOR 250 LVLS.NDG

ELEMENT S A	QUANTITY	ENERGY MIN	ENERGY MAX	LAB	TYPE	DOCUMENTATION REF	VOL	PAGE	DATE	COMMENTS
SM 149	TOTAL	+0	30+5	JAE	EXPT-PROG	NEANDC-J61U		3	SEP 79	MIZUMOTO+,LINAC,TRANSMISSION,NDG
SM 149	N, GAMMA	30+3	30+5	JAE	EXPT-PROG	NEANDC-J61U		3	SEP 79	MIZUMOTO+,LINAC,TOF,LIQUID-SCINT,NDG
SM 149	RESON PARAMS		50+2	JAE	EXPT-PROG	NEANDC-J61U		3	SEP 79	MIZUMOTO+,WN,WG FOR 150 LVLS,NDG
EU 151	N, GAMMA	30+3	10+5	JAE	EXPT-PROG	NEANDC-J61U		2	SEP 79	MIZUMOTO+,TBP IN NST,LINAC,NDG
EU 153	N, GAMMA	30+3	10+5	JAE	EXPT-PROG	NEANDC-J61U		2	SEP 79	MIZUMOTO+,TBP IN NST,LINAC,NDG
AU 197	N, 2N	FAST		TKO	EXPT-PROG	NEANDC-J61U		81	SEP 79	KOBAYASHI+,3,09+-0,17MB
AU 197	N, 2N	FISS		KTO	EXPT-PROG	NEANDC-J61U		81	SEP 79	KOBAYASHI+,FOR U235,CF252 FISS-N,TBL
HG 199	TOT INELAST	FISS		KTO	EXPT-PROG	NEANDC-J61U		78	SEP 79	KOBAYASHI+,SIG FOR ISOMER IN TABLE
HG 199	TOT INELAST	FAST		TKO	EXPT-PROG	NEANDC-J61U		78	SEP 79	KOBAYASHI+,SIG FOR ISOMER IN TABLE
TH 232	EVALUATION	+3	20+7	KYU	EVAL-PROG	NEANDC-J61U		96	SEP 79	OHSAWA+,TOT,SEL,SIN,NG,NF,2N,3N,FIG
U 233	EVALUATION	10+2	20+7	JAE	EVAL-PROG	NEANDC-J61U		47	SEP 79	MATSUNOBU+,TOT,SEL,SIN,NF,NG,ETC,FIG
U 235	EVALUATION	10+2	20+7	JAE	EVAL-PROG	NEANDC-J61U		50	SEP 79	MATSUNOBU+,TOT,SEL,SIN,NF,NG,ETC,NDG
U 235	RESON PARAMS		10+2	JAE	EVAL-PROG	NEANDC-J61U		64	SEP 79	ASAMI+,EVL FOR JENDL-2,NDG
U 236	EVALUATION	10-5	20+7	JAE	EVAL-PROG	NEANDC-J61U		52	SEP 79	YOSHIDA,TOT,SEL,SIN,NF,NG,2N,3N,FIG
U 238	EVALUATION	10+2	20+7	JAE	EVAL-PROG	NEANDC-J61U		50	SEP 79	MATSUNOBU+,TOT,SEL,SIN,NF,NG,ETC,NDG
U 238	RESON PARAMS		47+3	JAE	EVAL-PROG	NEANDC-J61U		64	SEP 79	ASAMI+,EVL FOR JENDL-2,TOT IN FIG
U 238	RESON PARAMS	20+1	47+3	JAE	EXPT-PROG	NEANDC-J61U		6	SEP 79	NAKAJIMA,TBP IN ANE
U 238	STRNTH FNCTN	20+1	47+3	JAE	EXPT-PROG	NEANDC-J61U		6	SEP 79	NAKAJIMA,TBP IN ANE,S0=1,13+-0,13
NP 237	EVALUATION		20+7	KYU	EVAL-PROG	NEANDC-J61U		102	SEP 79	WACHI+,TOT,SEL,SIN,NG,NF,2N,3N,FIG
PU 239	EVALUATION	10+2	20+7	JAE	EVAL-PROG	NEANDC-J61U		50	SEP 79	MATSUNOBU+,TOT,SEL,SIN,NF,NG,ETC,NDG

ELEMENT S A	QUANTITY	ENERGY MIN	ENERGY MAX	LAB	TYPE	DOCUMENTATION REF	VOL	PAGE	DATE	COMMENTS
PU 239	RESON PARAMS		60+2	JAE	EVAL-PROG	NEANDC-J61U	64		SEP 79	ASAMI+.EVL FOR JENDL-2.NDG
PU 240	EVALUATION	10+2	20+7	JAE	EVAL-PROG	NEANDC-J61U	50		SEP 79	MATSUNOBU+.TOT.SEL.SIN.NF.NG.ETC.NDG
PU 240	RESON PARAMS	NDG		JAE	EVAL-PROG	NEANDC-J61U	64		SEP 79	ASAMI+.EVL FOR JENDL-2.NDG
PU 241	EVALUATION	10+2	20+7	JAE	EVAL-PROG	NEANDC-J61U	50		SEP 79	MATSUNOBU+.TOT.SEL.SIN.NF.NG.ETC.NDG
PU 241	EVALUATION	10+2	20+7	JAE	EVAL-PROG	NEANDC-J61U	54		SEP 79	KIKUCHI+.TOT.SEL.SIN.NF.NG.(N.XN)FIG
PU 242	EVALUATION	25-2	20+7	JAE	EVAL-PROG	NEANDC-J61U	58		SEP 79	KAWAI+.TOT.SEL.SIN.NF.NG.(N.XN).FIG
CM 242	EVALUATION	10-5	20+7	JAE	EVAL-PROG	NEANDC-J61U	60		SEP 79	IGARASI+.TOT.SEL.SIN.NF.NG.(N.XN)FIG
MANY	N. PROTON	14+7		KYU	THEO-PROG	NEANDC-J61U	92		SEP 79	KUMABE.RE-ANALYSIS BY PRE-COMP TH

I. JAPAN ATOMIC ENERGY RESEARCH INSTITUTE

A. Linac Laboratory, Division of Physics

I-A-1 Neutron Capture Cross Section Measurements of Nd-143, Nd-145, Nd-146 and Nd-148

Yutaka Nakajima, Akira Asami, Yuuki Kawarasaki, Yutaka Furuta, Tooru Yamamoto* and Yukinori Kanda**

A paper on this subject was presented at the International Conference on Neutron Physics and Nuclear Data for Reactors and other Applied Purposes, held at Harwell, United Kingdom in 25 - 29 September, 1978 with an abstract as follow:

The capture cross sections of Nd-143, Nd-145, Nd-146 and Nd-148 have been measured in the energy region of 5 keV to 400 keV with a large liquid scintillation detector using the JAERI LINAC time-of-flight spectrometer. To obtain accurate cross section data much attention was paid to background determination. Corrections were made for the effects of neutron multiple scattering in samples and resonance self-shielding. The results of Nd-143 agree very well with those Musgrove et al. For Nd-145, the present measurements in this energy region are apparently the first. For Nd-146 and Nd-148, energy dependences differ between the present and Musgrove et al.'s and Kononov et al.'s data.

---

* Tohoku University, Sendai, Miyagi-ken.

** Kyusyu University, Fukuoka, Fukuoka-ken.

I-A-2 Average Neutron Capture Cross Sections of ^{151}Eu and ^{153}Eu from 3 to 100 keV.

M. Mizumoto, A. Asami, Y. Nakajima, Y. Kawarasaki,
T. Fuketa and H. Takekoshi*

A paper on this subject was submitted for publicalition in Journal of Nuclear Science and Technology with an abstract as follows:

Neutron capture cross sections of europium isotopes, ^{151}Eu and ^{153}Eu, were measured in the neutron energy region from 3 to 100 keV. Experiments were carried out with the time-of-flight facility at the 52 m station of the JAERI Electron Linear Accelerator. Prompt capture gamma rays were detected by a large liquid scintillation detector and the neutron flux shape was determined with a ^{6}Li glass scintillation detector. The average capture cross sections were examined in terms of energy independent strength functions for ^{151}Eu and ^{153}Eu.

---

*Kéage Laboratory of Nuclear Science, Institute for Chemical Research, Kyoto University, Kyoto.

I-A-3 Neutron Radiative Capture and Transmission Measurements of ^{147}Sm and ^{149}Sm.

M. Mizumoto, M. Sugimoto*, Y. Nakajima, Y. Kawarasaki,
Y. Furuta and A. Asami

The neutron capture and total cross sections of ^{147}Sm and ^{149}Sm were measured at the 55 m time-of-flight station of the Japan Atomic Energy Research Institute Electron Linear Accelerator. Measurements were carried out with a large liquid scintillation detector, a ^{6}Li glass detector and a ^{10}B-NaI detector using enriched samples of ^{147}Sm (98.34%) and ^{149}Sm (97.82%). The average capture cross sections were deduced from 3 to 300 keV with an estimated accuracy of 5 to 15 % and fitted with energy independent strength functions. The transmission data were analyzed with a multilevel Breit-Wigner formula to obtain neutron widths of resonances up to 2 keV for ^{147}Sm (250 resonances) and 500 eV for ^{149}Sm (150 resonances). Radiation widths for some strong resonances were extracted with the area analysis of the capture data.

---

*Department of Nuclear Engineering, Tohoku University.

I-A-4 Capture Cross Section Analysis Program

M. Sugimoto* and M. Mizumoto

The FORTRAN program CPCS (Computer Program to analyze Capture TOF Spectra) was developed to deduce effective neutron capture cross sections from raw data obtained by the time-of-flight facility at the JAERI Electron Linear Accelerator. The data processing system for capture experiments consists of three different stages which are Data Acquisition, Data Handling (summing, listing, plotting etc.) and Data Analysis (background determination, flux determination, normalization etc.). At each stage of processing, three separate computers are used; USC-3, FACOM U-200 and FACOM 230/75. The CPCS program is included in the stage of Data Analysis. One of the characteristic features of this program is that the magnetic disk file is effectively utilized as INPUT/OUTPUT data storage interconnecting with other programs to determine neutron dlux, to average calculated cross sections and to fit data with strength functions. This program is able to handle eight sets of TOF spectra with 8192 channels including channel block option simultaneously. Paticular attension is paid to determine precise backgrounds in the wide neutron energy range.

---

*Department of Nuclear Engineering, Tohoku University

I-A-5

Neutron Resonance Parameters of ^{79}Br and ^{81}Br up to 15 keV

Makio OHKUBO, Yuuki KAWARASAKI and Motoharu Mizumoto

Neutron transmission and capture measurements were carried out on separated isotopes of ^{79}Br and ^{81}Br(NaBr, ~98% enrichment, ~100g each, loaned by ORNL) using the JAERI linac TOF spectrometer. Measurements were made with a ^{6}Li-glass and a Moxon-Rae detectors at 47-m station with a resolution ~1 ns/m. Resonance parameter analyses were made on transmission data with the Harvey-Atta area analysis code, and on capture data with a Monte-Carlo program CAFIT. For ^{79}Br $g\Gamma_n^0$ values for about 150 levels below 10 keV are obtained, and for ^{81}Br about 100 levels below 15 keV. Preliminary results are followings.

^{79}Br ; $\langle D \rangle = 45 \pm 6$ eV ($<$2.5keV), $S_0 = (1.3 \pm 0.1)10^{-4}$ ($<$10 keV),

^{81}Br $\langle D \rangle = 70 \pm 13$ eV($<$2.5 keV), $S_0 = (0.9 \pm 0.1)10^{-4}$ ($<$15 keV)

Γ_γ are obtained for large levels. Intermediate structures are observed in the resonances of ^{81}Br showing clusters of resonances at energies of 1.2, 10, 11.5 and 14 keV.

I-A-6 Neutron Resonance Parameters of ^{238}U

Yutaka Nakajima

A paper on this subject will be published in "Annals of Nuclear Energy" with an abstracrt as follows:

Neutron transmission measurements on natural uranium samples were performed in the energy region from 20 eV up to 4.7 keV on a 190 metre flight path of the JAERI 120 MeV linac neutron time-of-flight spectrometer. Samples were all metallic slabs with three thicknesses of 0.00725, 0.0144 and 0.0236 atoms/barn, respectively. One of them was cooled down to 77° K to reduce Doppler broadening effect. The best nominal resolution of the measurements was 0.3 nsec/m. Special attention has been paid to background determination, because its shape was found to depend on the thickness of the sample in the beam. Resonances parameters $\Gamma_n{}^\circ$ are obtained for 180 resonances in the energy region up to 4.7 keV with the Atta-Harvey area-analysis programme. Excluding p-wave resonances assigned by Corvi et al., the average level spacing, the average reduced neutron width and the strength function were determined to be $\overline{D}$ = 21.9 eV, $\overline{\Gamma}_n{}^\circ$ = 2.47 $\pm$ 0.33 meV and S_0 = (1.13 $\pm$ 0.13) x 10^{-4}, respectively. The statistics of the level spacings are in agreement with those predicted by the theory of Dyson and Mehta and are inconsistent with an uncorrelated Wigner distribution. Results are compared with currently available experimental data.

I-A-7

MCRTOF - A Monte-Carlo Program for Multiple Scattering of Neutrons in Resonance Energy Region

Makio OHKUBO

A report with the above title has been published in JAERI-M-7988(Nov.1978) with the following abstract.

Abstract

To study the capture and scattering probabilities of neutrons in the resonance energy region, a Monte-Carlo program is coded. Path of a neutron which impinges onto a inclined disk sample is simulated using neutron cross sections calculated from the resonance parameters. Capture, front and rear face scattering, transmission etc. probabilities are obtained from the average destinations of the incident neutrons. Incident neutron energy is changed step by step in order to reproduce these probabilities over resonances. In this report are described of the basic multiple scattering loop, coordinate transformations, cross section formulae, motion of the target nucleus, etc., also with flow chart, input card format, output example, and FORTRAN list in the appendix. Calculations were made with FACOM-230/75 computer at JAERI.

B. Nuclear Data Center, Division of Physics and Working Groups of Japanese Nuclear Data Committee

I-B-1 Summary of Benchmark Tests of JENDL-1

Y. Kikuchi, H. Takano, T. Kamei*, T. Hojuyama**,
Y. Seki**, M. Sasaki***, I. Otake***

Benchmark tests of JENDL-1 were continued in Working Group on Integral Tests for JENDL in JNDC. From various tests made since 1976, it is concluded that applicability of JENDL-1 is as satisfactory as that of the existing other sets. On the other hand, following drawbacks of JENDL-1 were also revealed.

1) Fission ratio of ^{239}Pu to ^{235}U is by about 3 % underestimated.
2) Anomalous C/E values of reaction rates are observed in the outer core and blanket regions. This tendency is enhanced when control rods are inserted in the outer core.
3) Prediction of sodium void coefficients is poor when sodium is removed from the outer core.

Concerning the problems (2) and (3), it was pointed out on the macroscopic cross sections of JENDL-1 that

1) the diffusion coefficients might be underestimated in the energy range above 10 keV,
2) the inelastic removal cross section might be underestimated, and
3) the elastic removal cross section might be overestimated above 10 kev and underestimated below 1 keV.

To investigate these problems, effects of the cross sections of Fe, Cr and Ni were investigated by replacing these cross section to those of ENDF/B-IV. It was suspected for Fe, Cr and Ni of JENDL-1:

1) The elastic scattering cross section might be overestimated in the energy range from a few hundred keV to a few MeV. This is caused by our adopting spherical optical potential which overestimates the total cross section in this energy range. The self-shielding effects cannot be taken into account in this energy range, since we ignored the structure observed in the unresolved resonance region.

2) The inelastic scattering cross section may be underestimated because of our ignorance of the direct inelastic scattering.

These comments were reflected on the evaluation of JENDL-2.

---

* NAIG Nuclear Research Laboratory, Nippon Atomic Industry Group Co. Ltd.

** Nuclear Development Center, Mitsubishi Atomic Power Industries Inc.

*** Power Reactor and Nuclear Fuel Development Corporation

I-B-2 On Compilation of Japanese Evaluated Nuclear Data Library, Version-2 (JENDL-2)

JENDL-2 Compilation Group

Since the first version of JENDL was released in autumn 1977, a lot of information have been reported on the merits and demerits of JENDL-1 through the use of it. JENDL-2 compilation work started at the beginning of 1978 fiscal year. Taking account of the above mentioned information, the JENDL-2 compilation group asked reevaluation to the evaluators who took charge of Cr, Fe, Ni, ^{235}U, ^{238}U, ^{239}Pu, ^{240}Pu and ^{241}Pu. Reports of the reevaluation for these nuclides will be presented in this progress report.

JENDL-2 includes the nuclear data for fast breeder reactors, shielding problems and fusion researches. Following nuclides are going to be stored in JENDL-2:

H	^{4}He	^{6}Li	^{7}Li	^{9}Be	^{10}B	^{11}B	^{12}C	^{16}O
^{19}F	^{23}Na	^{27}Al	Si	Ca	Ti	V	Cr	Mn
Fe	Co	Ni	Cu	67 FP Nuclides			Zr	Nb
Mo	Eu	Gd	Ta	Au	Pb	^{228}Th	^{230}Th	^{232}Th
^{233}Th	^{234}Th	^{231}Pa	^{233}Pa	^{234}Pa	^{233}U	^{234}U	^{235}U	^{236}U
^{238}U	^{237}Np	^{239}Np	^{238}Pu	^{239}Pu	^{240}Pu	^{241}Pu	^{242}Pu	^{241}Am
^{242}Am	^{242m}Am	^{243}Am	^{242}Cm	^{243}Cm	^{244}Cm	^{245}Cm		

I-B-3 Evaluation of Neutron Cross Sections for Vanadium

S. Tanaka

Neutron nuclear data for vanadium have been evaluated up to 20 MeV. The present work is to be submitted to Nuclear Data Center in JAERI as an elemental component in JENDL-2 Evaluated Nuclear Data File System. The energy range covered by the present work was divided into three regions; (1) resonance region up to 100 keV, (2) fluctuation region from 100 keV to 3.2 MeV and (3) continuum region higher than 3.2 MeV.

For the resonance region, the resonance parameters were obtained by modifying some values in those from BNL 325 (2nd Ed.) so that the results calculated with the Breit-Wigner multilevel formula were well fitted mainly to the experimental total cross sections. Fairly good fit was obtained, although addition and subtraction of artificial background cross sections were needed.

The evaluated total cross section in the fluctuation region was obtained based on the experimental data. The measured structures were incorporated into the file by use of an interactive CRT display system NDES developed by T. Nakagawa.

The spherical optical model was used to estimate the total and the elastic scattering cross sections above 3.2 MeV and the inelastic scattering cross sections above several MeV. Starting from the parameter set used in Ref. 1), the potential depth of the imaginary part and the radius parameter were changed to $W = 4.6 + 0.36E$ (MeV) and $r_0 = 1.23$ (fm), respectively, so that calculated total and differential elastic cross sections were fitted to experimental data. Fairly good fit was obtained for the total cross sections above several hundred keV.

The evaluation of the inelastic scattering cross sections was made for

"eight discrete levels" and continuous levels. The lowest energy region of the inelastic scattering for the first level was evaluated based on the experimental data. For the rest of the inelastic cross sections, Hauser-Feshbach calculations using the ELIESE-3 code[2] and the CASTHY code[3], and linear extrapolations were used for the evaluation. For the level density, Gilbert-Cameron's values[4] were employed.

The evaluation of the (n,γ) reaction cross section is given on the basis of experimental data below 0.6 MeV and, above this energy, given by a statistical model calculation using CASTHY code with normalization to the experimental value at 0.6 MeV.

The cross sections for the threshold reactions were evaluated based on the experimental data and Kitazawa's calculation[5] using the GROGI code.

Fig. 1 shows the result of the present evaluation in the energy range above 100 keV. The (n,γ) reaction cross section is not shown in the figure, because almost all values of the cross section are less than 0.01 barn. The inelastic scattering cross section to the continuum is obtained by $\sigma_T - \sum_{\text{all } i} \sigma_i$ where σ_T is the total cross section and σ_i a partial cross section other than the relevant cross section.

References:

1) S. Tanaka, JAERI-M 5984, P. 212 (1975)

2) S. Igarasi, JAERI 1224 (1972)

3) S. Igarasi, to be published

4) A. Gilbert and A. G. W. Cameron, Can. J. Phys. 43, 1446 (1965)

5) H. Kitazawa, Private communication

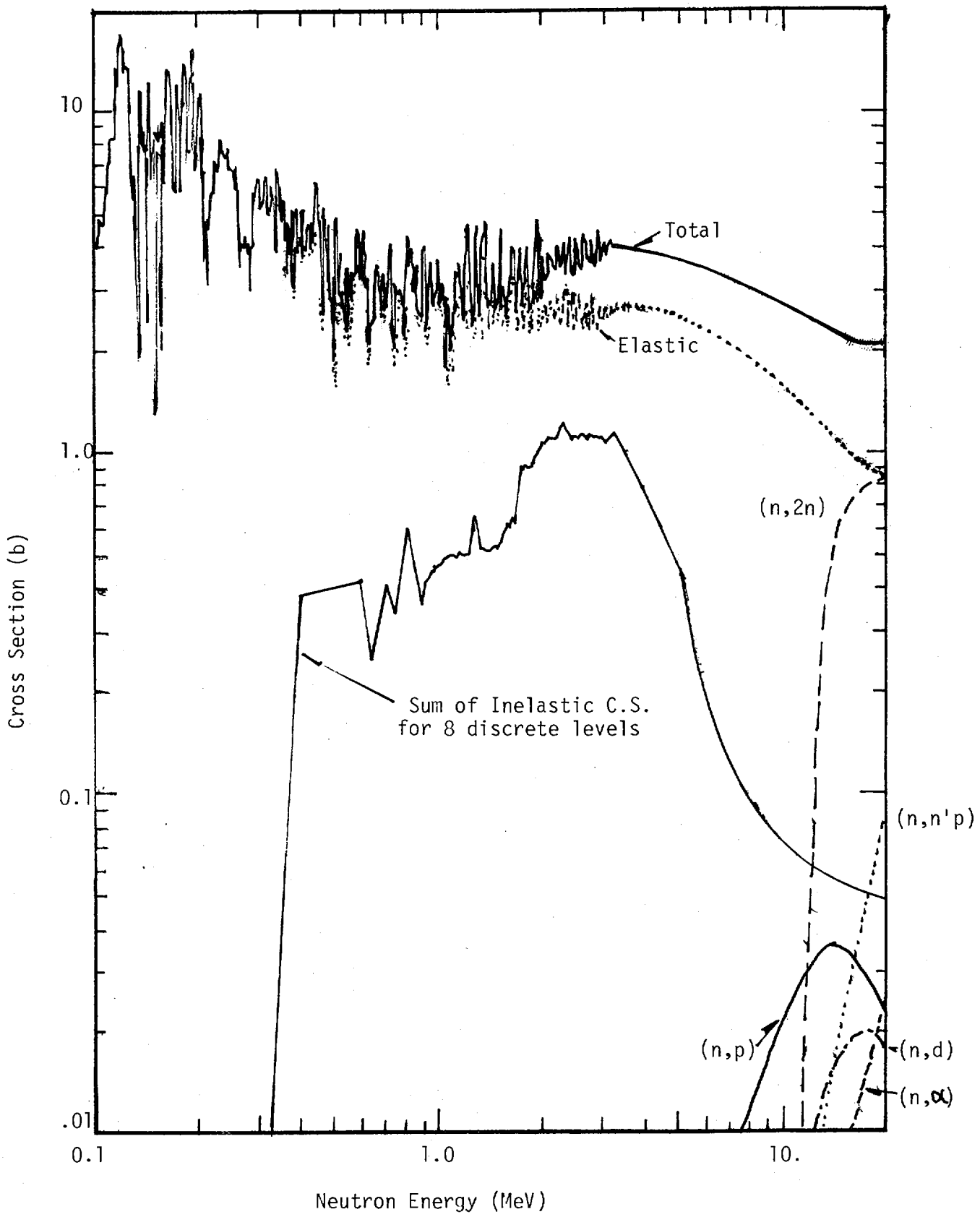

Fig. 1. Evaluated cross sections in the present work.

I-B-4

Evaluation of Cr Neutron Cross Sections for JENDL-2

T. Asami and N. Sekine

In the compilation of JENDL-2, the re-evaluation for the neutron cross sections of Cr was made to include new experimental and theoretical results and to extend the neutron energy range to 20 MeV. Another purpose of the re-evaluation is to refine the JENDL-1 data [1] on the total cross section of natural Cr in MeV region, including resonance structures observed in experiments, since the analysis has indicated[2] that even in MeV region these structures gave some effects in shielding calculations.

The neutron cross-section data for natural Cr and Cr isotopes (^{50}Cr, ^{52}Cr, ^{53}Cr and ^{54}Cr) were evaluated in the neutron energy range of 10^{-5} eV to 20 MeV.

In thermal and resonance regions, the neutron cross sections were generated with a multi-level Breit-Wigner formula by using the resonance parameters. The recent available experimental data on resonance parameters[3)-5)] were examined and a set of the parameters was selected so as to reproduce the experimental values of the total and capture cross sections for each isotope and for natural Cr. The resonance region for each isotope was extended to 300 keV except for ^{53}Cr(120 keV). Unknown radiative widths were assigned the average value for each isotope.

Fast neutron cross sections (total, capture, elastic and inelastic scattering) above 300 keV were estimated from the optical and statistical model calculations. The optical model parameters used were those of Kawai[6]. The level density parameters were taken from Yoshida's values[7], and the level schemes were based on Nakasima's recommendation[8]. Only the total cross sections above 300 keV for natural Cr were estimated from the experimental data of Cierjacks et al.[9] and Perey et al.[10], followed peaks and valleys

in the cross section below 6 MeV.

The cross sections for the (n,2n), (n,p), (n,α) and (n,n'p) reactions were estimated from experimental and/or theoretical calculations.

References:

1) S. Igrasi et al., JAERI 1261 (1979) p.28 ;
T. Asami et al.,Proc. of Specialists' Meeting on Neutron Data of Structural Materials for Fast Reactors (Geel, 5-8 Dec. 1977) p.118

2) K. Koyama et al., JAERI-M 8163 (1979) p.358 (in Japanese)

3) R.R. Spencer et al., KFK 1517 (1972)

4) M. J. Kenny et al., AAEC/E - 400 (1977)

5) B. J. Allen et al., Proc. of Specialists' Meeting on Neutron Data of Structural Materials for Fast Reactors (Geel, 5-8 Dec. 1977) p.447

6) M. Kawai, reported in this progress report.

7) T. Yoshida, reported in this progress report.

8) R. Nakasima, private communication (1979)

9) S. W. Cierjacks et al., KFK 1000 (1968)

10) F. G. Pérey et al., (1973) Data in NEUDADA File (NEA Data Bank, Saclay)

I-B-5 Systematic Determination of Level Density Parameters for Structural Materials (Cr,Fe,Ni)

T.Yoshida*

The level density parameters for 19 isotopes of Cr, Fe, and Ni have been determined systematically from the recent data of level schemes [1] and the average resonance spacings[2] for the use in the neutron cross section evaluations for JENDL-2.

The composite level density formula by Gilbert and Cameron[3] was used to fit the parameters, namely,

$$(E) = C\, e^{E/T} \qquad (E < E_x), \text{ and} \tag{1}$$

$$(E) = \sum_J \frac{\sqrt{\pi}}{12} \frac{\exp(2\sqrt{aU})}{a^{1/4}\, U^{5/4}} \frac{(2J+1)\, \exp(-(J+\frac{1}{2})^2/2\sigma^2)}{2\sqrt{2\pi}\,\sigma^3} \tag{2}$$

$$(E=U+E_p \geq E_x).$$

The smooth connection of the above two formulas (hereafter, CT and FG formulas, respectively) was elaborated in an iterative way (Step 1~3). The expression for spin cut-off factors in FG and CT regions was modified according to the recent parameterology study of Petten-Bologna-Cadarache group presented at FPND meeting at Petten, 1977. The resultant parameters are summarized in TABLE I.

The effect of this new evaluation of level density parameters on cross section calculation is being checked.

References

1) Nuclear Data Sheets

2) F. Fröhner, Proc. Harwell Conf. on Nucl Phys. and Data, NEA(1978) 268

3) A. Gilbert and A.G.W. Cameron, Can. J. Phys., 43(1965) 1446

---

* NAIG Nuclear Research Lab., Nippon Atomic Industry Group Co., Ltd.

TABLE I A Set of Level Density Parameters for Structural Materials

Isotope	a(MeV^{-1})	E_p(MeV)	B_{eff}(MeV)	D(keV)	C(MeV^{-1})	T(MeV)	E_x(MeV)	Step	σ^2 1) exp	σ^2 2) theo
Cr-50	6.80	2.89	12.94	syst 3)	0.847	1.42	11.0	1	7.55	14.71
Cr-51	6.84	1.35	9.44	15.4	0.596	1.14	7.0	2	7.74	12.48
Cr-52	6.92	2.65	12.04	syst	0.468	1.29	7.45	2	8.75	11.72
Cr-53	6.99	1.35	8.15	34.2	1.26	1.25	8.0	2	8.24	14.04
Cr-54	7.82	2.62	9.84	6.0	0.497	1.15	9.0	3	5.81	14.73
Cr-55	10.64	1.35	6.41	12.3	3.96	1.53	3.10	x 4)	–	9.11
Fe-54	6.19	2.84	13.38	syst	0.532	1.45	12.0	2	6.63	15.71
Fe-55	6.90	1.54	9.5	17.0	1.274	1.30	9.0	2	9.93	15.15
Fe-56	7.58	2.81	12.20	syst	0.746	1.27	10.0	1	5.59	15.78
Fe-57	8.27	1.54	7.85	19.3	1.694	1.14	7.70	3	4.88	15.43
Fe-58	8.45	2.83	10.1	5.4	0.742	1.16	10.0	1	4.18	17.03
Ni-58	6.45	2.47	12.20	syst	0.581	1.37	10.0	3	5.95	15.25
Ni-59	6.97	1.20	9.20	16.7	2.14	1.35	8.0	1	6.58	15.23
Ni-60	7.55	2.49	11.39	syst	0.864	1.26	10.0	2	4.47	16.85
Ni-61	8.14	1.20	8.02	15.1	2.303	1.17	7.0	2	5.17	15.54
Ni-62	8.77	2.61	10.63	1.61	0.621	1.08	9.0	2	4.26	17.12
Ni-63	9.37	1.20	7.04	14.6	2.059	1.36	3.0	x	4.34	9.49
Ni-64	9.98	2.70	9.66	syst	0.434	1.15	4.32	x	5.03	9.39
Ni-65	10.57	1.20	6.30	14.5	1.305	0.838	5.0	3	4.30	14.96

notes) $B_{eff} = B_n$(neutron binding energy) + one-half of resonance region

1) calculated with $\sigma^2 = \frac{1}{2N}\sum_{\lambda=1}^{N}(I_\lambda + \frac{1}{2})^2$, 2) at junction energy E_x with $\sigma^2 = 0.146\sqrt{aU}\,A^{2/3}$

3) determined by systematics; In these, the resonance region is set zero.

4) FG and CT formulas crossed (or, connected not smoothly).

I-B-6 Determination of Spherical Optical Model Parameters for Structural Materials

Masayoshi Kawai*

The spherical optical model parameters were determined for Ti, V, Cr, Mn, ^{54,56,57}Fe, Co, Ni and Cu in order to evaluate the fast neutron cross sections for JENDL-2. The optimum parameters were searched so as to reproduce experimental values of the total cross section over the energy interval of several hundred keV through 20 MeV. The results for Ti, Cr, Fe and Ni are illustrated in Fig. 1, and the determined parameters are given in Table 1. The neutron strength functions for s and p waves, and the scattering radius were also checked. It was found from Fig. 2 that the simultaneous fit to these data was extremely difficult, in particular, for ^{56}Fe. It was also noted that the above "SPRT" fit, which was observed to be effective in F.P. mass region[1], was not always sufficient to estimate reaction cross sections in structural materials mass region, because the d-wave transmission coefficient was large and important for the determination of the compound nucleus formation cross section. For example, Fig. 3 shows that the present parameters underestimate the total inelastic scattering cross section of ^{56}Fe.

Reference

1) J. P. Delaroche, et al. ; cited by S. Iijima: IAEA-213,"Fission Products Nuclear Data - 1977", vol. 1, p. 279 (1977).

* Nippon Atomic Industry Group Co., Ltd.

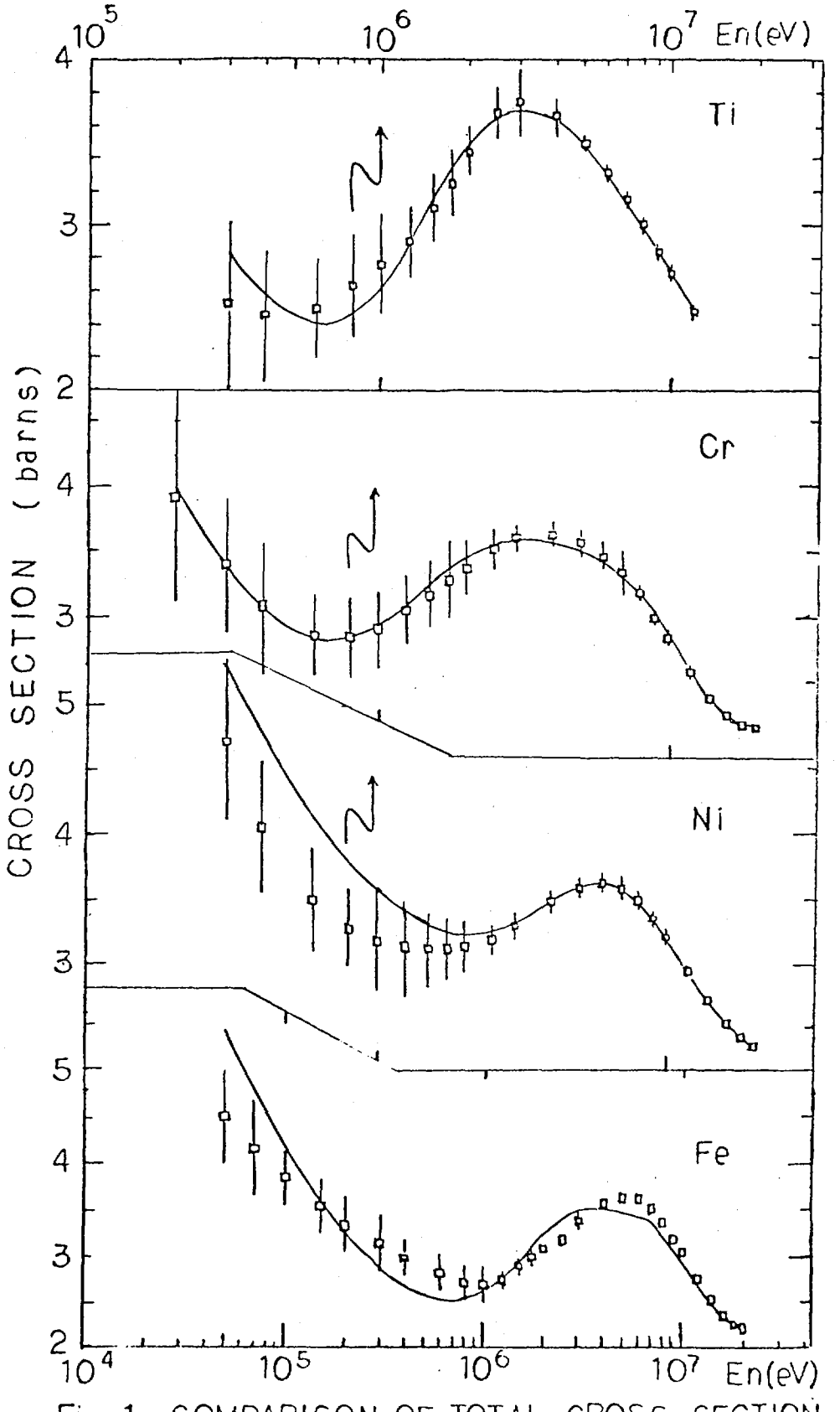

Fig. 1 COMPARISON OF TOTAL CROSS SECTION

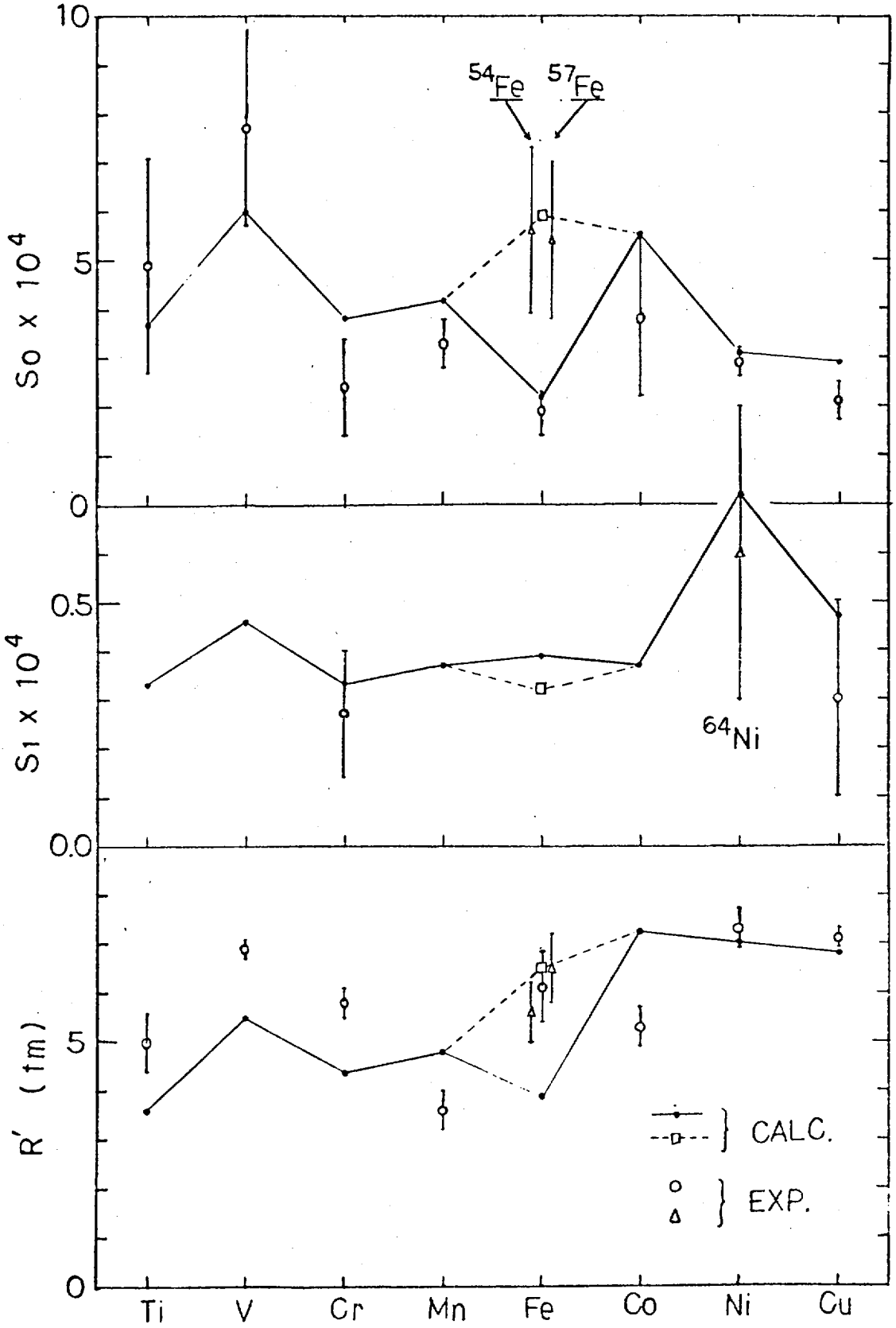

Fig. 2 COMPARISON OF So, S1 AND R'

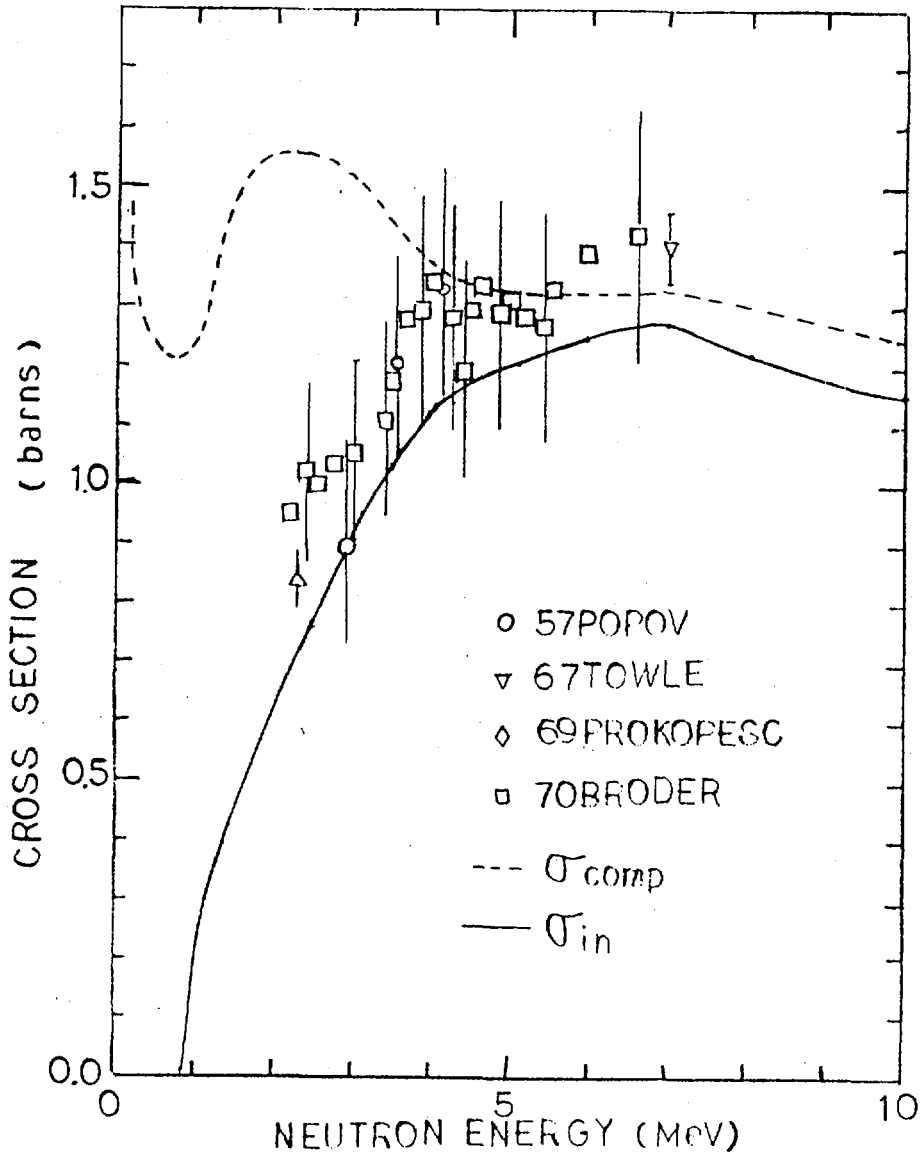

Fig. 3 COMPARISON OF σ-IN FOR IRON

Table 1 Selected Potential Parameters for Structural Materials

Nuclide	Real Potential r_o (fm)	a_o (fm)	V_o (MeV)	Surface Absorption(d.W.S.) r_s (fm)	b (fm)	W_s (MeV)	Spin-Orbit Force r_{so} (fm)	a_{so} (fm)	V_{so} (MeV)
Ti	1.240	0.520	51.41−0.353E	1.400	0.400	3.948+0.142E	1.240	0.520	7.00
^{51}V	1.240	0.480	49.57−0.385E	1.400	0.400	4.963+0.214E	1.240	0.480	7.00
Cr	1.240	0.480	50.05−0.262E	1.400	0.400	4.870+0.352E	1.240	0.480	7.00
^{55}Mn	1.240	0.522	47.856−.032E	1.410	0.392	5.288+0.342E	1.240	0.522	6.90
^{56}Fe	1.166	0.371	52.644−.002E−.006E^2	1.450	0.480	2.869+0.289E	1.166	0.371	6.138
^{54,57}Fe	1.240	0.500	50.136−0.150E	1.400	0.400	4.660+0.340E	1.240	0.500	7.00
^{59}Co	1.240	0.498	49.69−0.135E	1.400	0.400	4.931+0.198E	1.240	0.498	7.00
Ni	1.240	0.541	51.33−0.331E	1.400	0.400	8.068+0.112E	1.240	0.541	7.00
Cu	1.248	0.615	47.618−.003E−.004E^2	1.412	0.260	14.27−0.296E	1.248	0.615	6.50

I-B-7

Angular Distributions of Resonance Neutron Scattering from ^{56}Fe

S. Iijima*

F. G. Perey et al. at ORNL reported recently the fine resolution measurement of neutron angular distribution scattered from iron. They observed strong variation of angular distributions against energy even for 28 keV s-wave resonance of ^{56}Fe. This anisotropy of scattering in resonance region might cause a significant effect on the calculation of reactor shielding and fast reactor neutronics. The present note gives some typical results of calculation of angular distributions for ^{56}Fe based on Blatt-Biedenharn formula, and is intended to give account of characteristic features of the problem.

In case of isolated s-wave neutron resonance for even-even nucleus, the Blatt-Biedenharn formula reduces to the following expression.

$$\sigma_{el}(E,\theta) = \frac{\sigma_0}{4\pi} \sum_{\ell=0}^{\infty} B_\ell(E) P_\ell(\cos\theta).$$

Here, putting $x = (E - E_0)/(\Gamma/2)$,

$$\sigma_0 = 4\pi / k_0^2.$$

$$B_\ell = \frac{\Gamma_{n0}^2}{\Gamma^2} \cdot \frac{1}{1+x^2} \delta_{\ell,0} + H_\ell + \frac{\Gamma_{n0}}{\Gamma} \cdot \frac{2(2\ell+1)}{1+x^2} \cdot \sin\delta_\ell \left[x \cos(2\delta_0 - \delta_\ell) - \sin(2\delta_0 - \delta_\ell) \right],$$

$$H_0 = \sum_{\ell=0}^{\infty} (2\ell+1) \sin^2\delta_\ell ,$$

$$H_1 = 6 \sin\delta_1 \left[\sin\delta_0 \cos(\delta_0 - \delta_1) + 2 \sin\delta_2 \cos(\delta_1 - \delta_2) \right],$$

$$H_2 = 10 \sin\delta_2 \sin\delta_0 \cos(\delta_0 - \delta_2) + 6 \sin^2\delta_1 + \frac{50}{7} \sin^2\delta_2, \quad \text{etc.}$$

---

* NAIG Nuclear Research Laboratory, Nippon Atomic Industry Group Co., Ltd.

The phase shift δ_ℓ for hard sphere scattering is given by $\tan\delta_\ell = -\frac{j_\ell(\rho)}{n_\ell(\rho)}$, where ρ =kR' (R' is the scattering radius). Incidentally, the maximum and minimum total cross sections are approximately given by,

$$\sigma_{max} = \sigma_0 (1 + \Delta H), \quad at\ x = \tan\delta_0,$$

$$\sigma_{min} = \sigma_0 (\Delta H + \Gamma_\gamma/\Gamma \cdot \sin^2\delta_0), \quad at\ x = -\cot\delta_0,$$

where, $\Delta H = H_0 - \sin^2\delta_0$.

Numerical calculation was performed for ^{56}Fe assuming R' = 5.4 fm and $\Gamma_\gamma \ll \Gamma$. Calculation was terminated up to P_2 components. Fig. 1 shows the calculated total cross section near 24 keV valley in comparison with recent measurement of Liou et al. Γ_γ and Γ were taken as 1.4 eV and 1300 eV, respectively.

Figs. 2 and 3 show the B_ℓ and B_ℓ/B_0 values for resonances at E_0 = 27.67 keV and 300 keV (fictitious), respectively. Figs. 4 and 5 show the calculated angular distributions in the vicinity of these resonances. We observe from these figures the followings.

(1) B_1/B_0 and B_2/B_0 fluctuate considerably within a very narrow range ($\Delta x \sim 1$) of total cross section minimum ($x_{min} = -\cot\delta_0$), thus causing the rapid variation of angular distributions within this small energy interval.

(2) B_1 changes its sign within this interval due to the interference between s-wave resonance and p-wave hard sphere scattering. B_2 does not change sign (up to a few hundreds keV at least) since the hard sphere scattering is the major component. These are in agreement with experimental observation by Perey et al.

(3) B_2/B_0 shows a very narrow pronounced peak at the minimum of total cross section. The same may be true for the higher order B_ℓ/B_0. For the precise calculation of angular distributions near cross section minimum, the higher order P_ℓ components should be taken into account.

The study of the effect of the anisotropic resonance scattering from structural materials is being planned by JNDC shielding cross section working group.

References :

1. F. G. Perey et al.,Neutron Data of Structural Materials for Fast Reactors, Pergamon Press, Proc. of a Specialist Meeting, Geel, 1977, p.530
2. H. I. Liou, R. E. Chrien, R. C. Block and U. N. Singh, NSE 70 150 (1979)

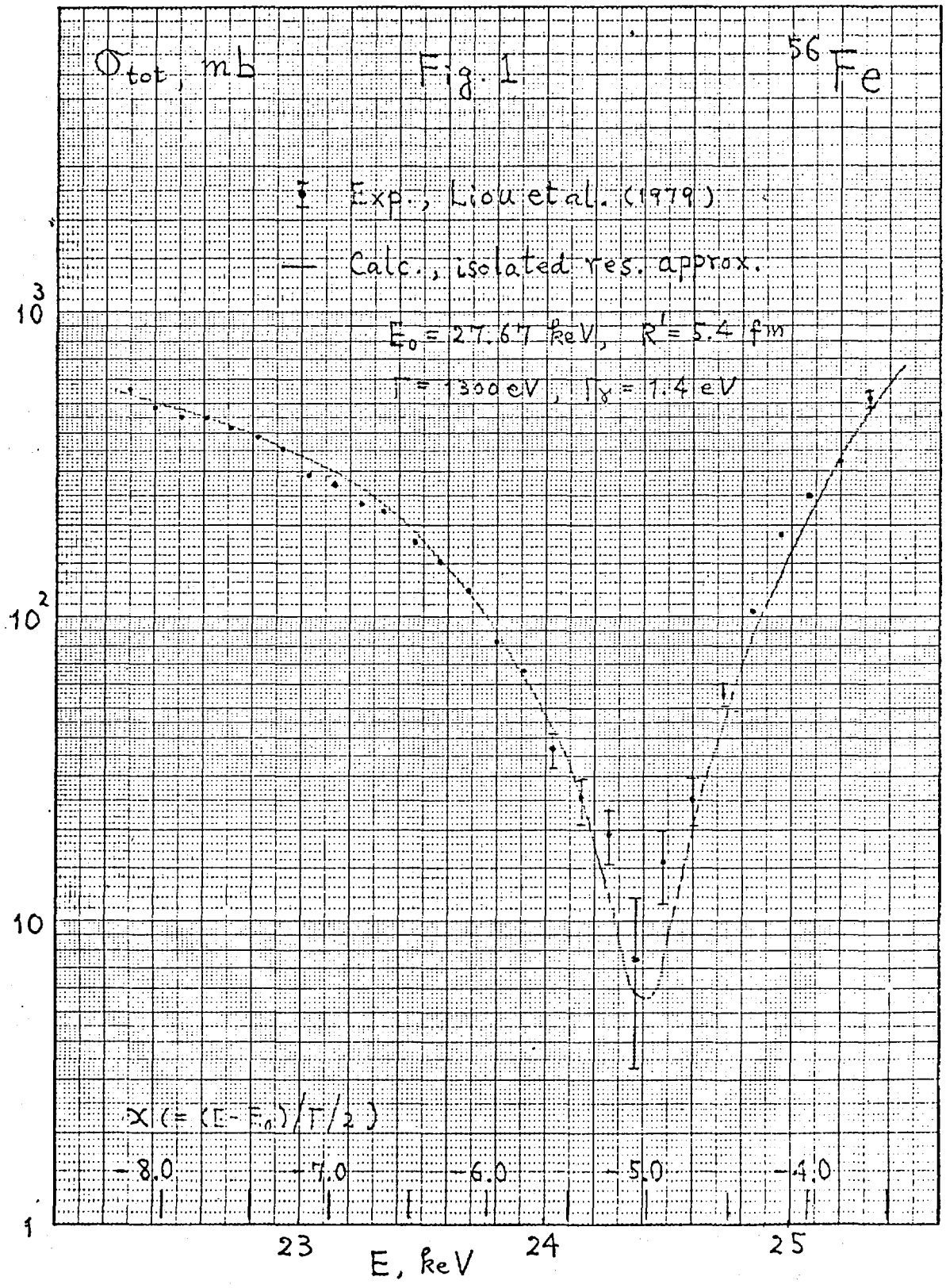
σtot, mb
Fig. 1
56Fe
Exp., Liou et al. (1979)
Calc., isolated res. approx.
E0 = 27.67 keV, R' = 5.4 fm
Γ = 1300 eV, Γγ = 1.4 eV
10^3
10^2
10
1
x (= (E - E0)/Γ/2)
-8.0
-7.0
-6.0
-5.0
-4.0
23
24
25
E, keV

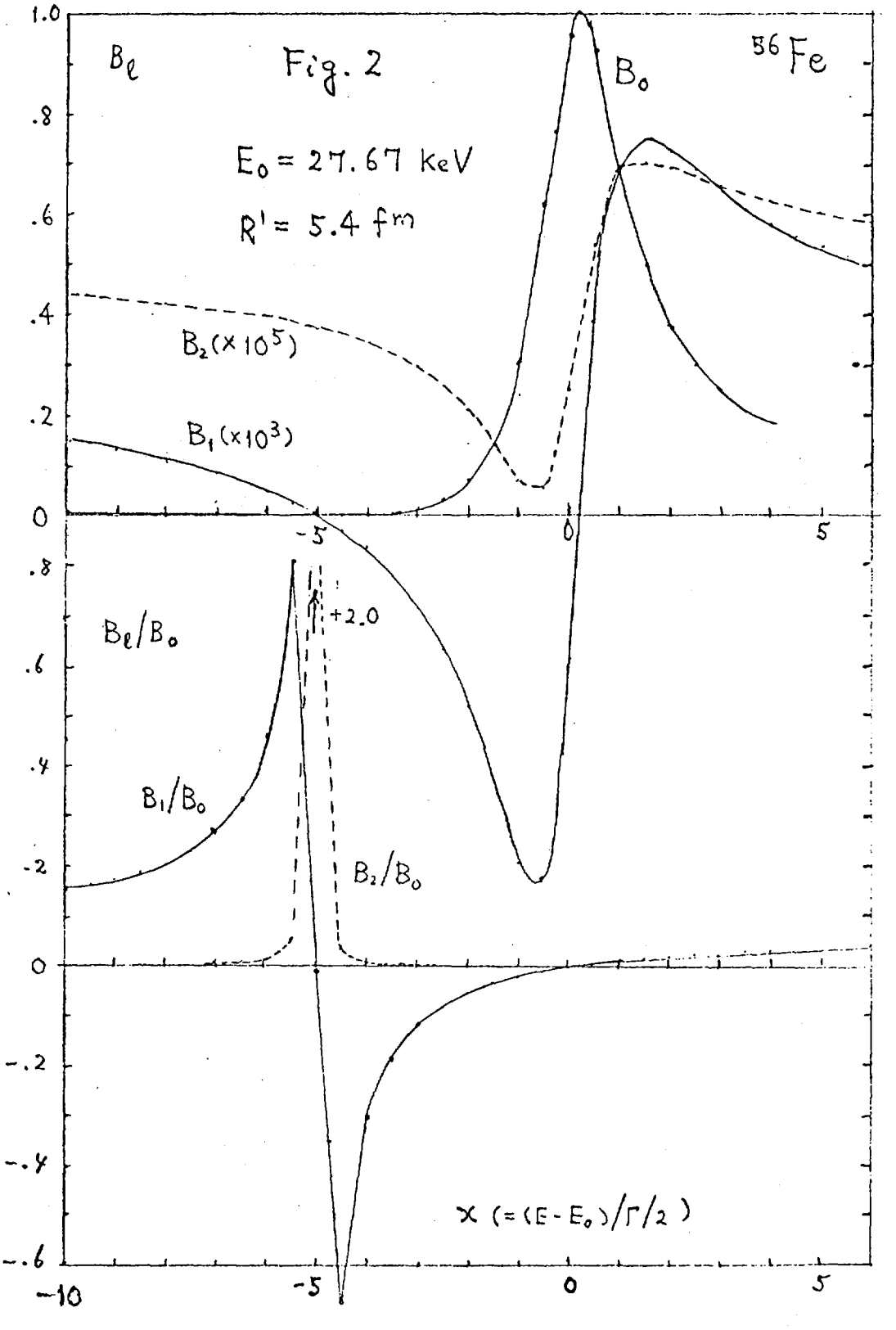
Fig. 2
B_ℓ
^{56}Fe
B_0
$E_0 = 27.67$ keV
$R' = 5.4$ fm
$B_2(\times 10^5)$
$B_1(\times 10^3)$
B_ℓ/B_0
B_1/B_0
B_2/B_0
+2.0
$x\ (=(E-E_0)/\Gamma/2)$
1.0
.8
.6
.4
.2
0
-.2
-.4
-.6
-10
-5
0
5

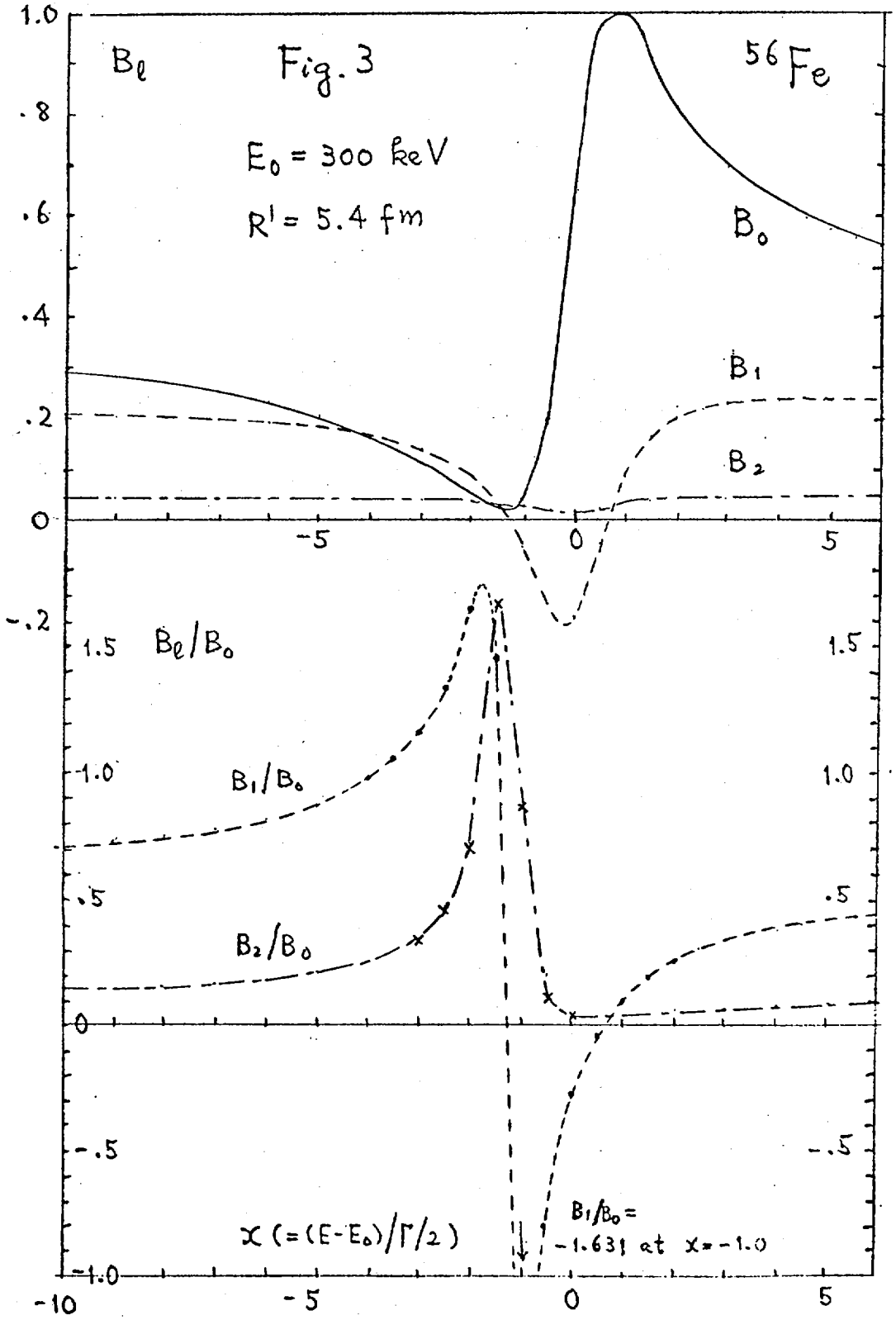
Fig. 3
B_ℓ
^{56}Fe
E_0 = 300 keV
R' = 5.4 fm
B_0
B_1
B_2
B_ℓ/B_0
B_1/B_0
B_2/B_0
x (= (E-E$_0$)/Γ/2)
B_1/B_0 =
-1.631 at x = -1.0

Fig.4 ^{56}Fe $\sigma_{el}(E,\theta)$, $E_0 = 27.67$ KeV, $R' = 5.4$ fm

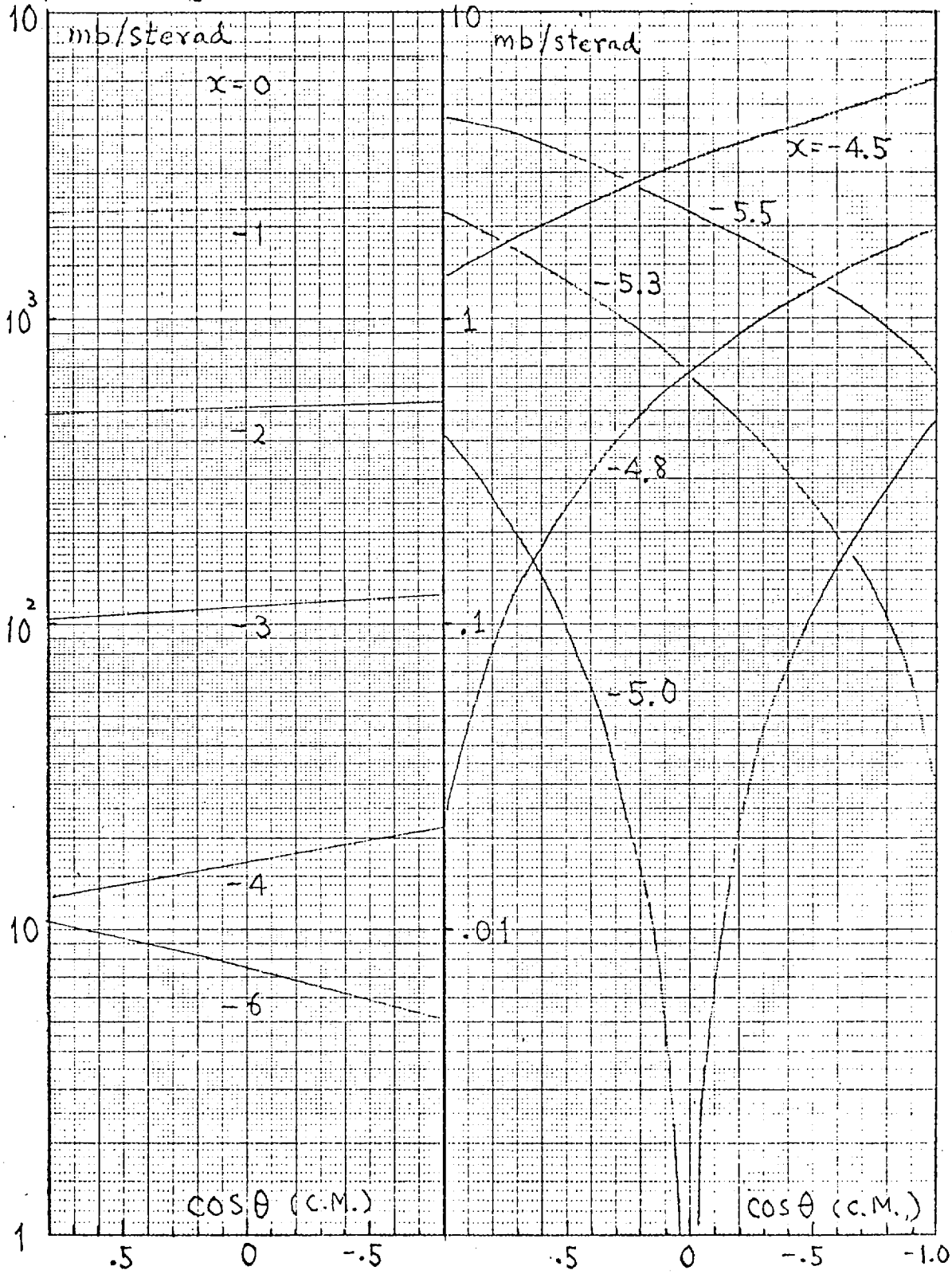

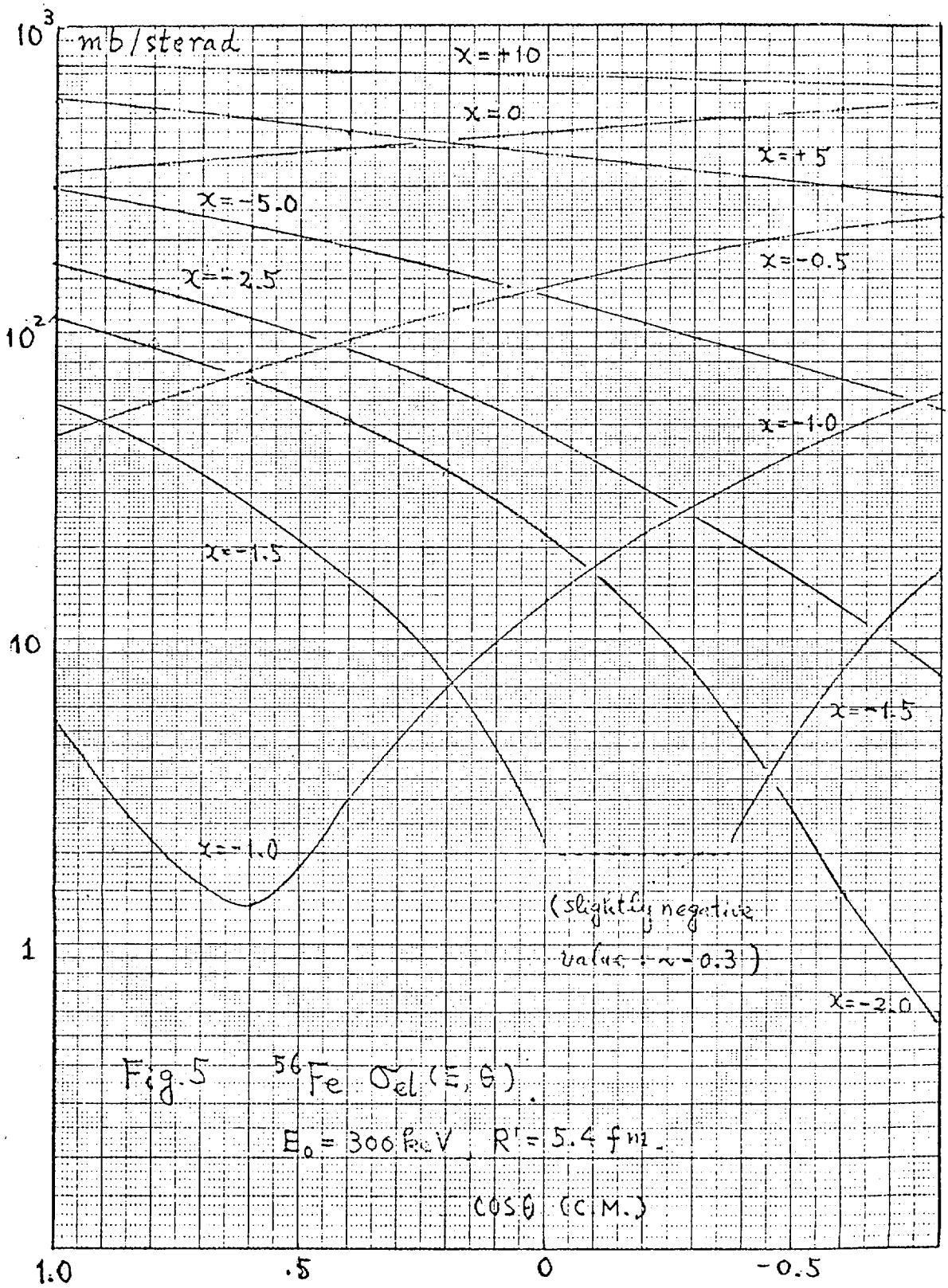

Fig.5 ^{56}Fe $\sigma_{el}(E, \theta)$.

$E_0 = 300$ MeV, $R' = 5.4$ fm.

I-B-8

Evaluation of Iron Neutron Cross Sections in Reonance Region

H. Yamakoshi* and S. Iijima**

A complete re-evaluation of iron neutron cross sections was performed for JENDL-2. This report gives a brief account of resonance and thermal region cross sections.

All cross sections in thermal and resonance regions were calculated by multi-level Breit-Wigner (MLBW) approximation. The effort was paid to obtain an overall good fit to the measured total cross section in order to minimize the background cross section correction. Resonance parameters were adopted from the following sources ;

^{54}Fe : Pandey et al.(1), up to 510.1 keV. R' = 5.6 fm.
^{56}Fe : Perey et al.(2), up to 400 keV. R' = 5.4 fm.
^{57}Fe : Allen et al.(3), for s-wave res., and
Beer et al. (4), for p- and d- wave res.,
up to 189.5 keV. R' = 6.5 fm.

To obtain a better fit with the measured total cross section in thermal region and near 28 keV resonance, the parameters of Perey et al. were slightly modified. A negative level was added at -3.75 keV with Γ_n = 100 eV and Γ_γ = 1.0 eV as in ENDF/B-4. Also, the Γ_n of 27.67 keV resonance was altered from 1520 eV to 1420 eV.

The scattering radius is often not given clearly by the evaluators of resonance parameters. First, we have assumed R' = 6.1 fm for ^{56}Fe from BNL-325, 3rd edition (6.1 $\pm$ 0.7 fm), resulting in a too large cross section above 100 keV. The choice of R' = 5.4 fm has resulted in a

---

* Ship Research Institute, Ministry of Transportaion
** NAIG Nuclear Research Laboratory, Nippon Atomic Industry Group Co., Ltd.

fairly good fit to the measured total cross section in 70 - 250 keV, but the cross section below 70 keV was significantly underestimated.

To avoid this difficulty, the sub-section structure of file 2 of ENDF/B format was utilized. The energy region was divided in two sub-sections, the one from 70 keV to 250 keV, and the other below 70 keV. In the former section, the cross sections were calculated from all resonace parameters of Perey et al. up to 400 keV. In the latter section, the cross sections were generated from the resonance parameters only below 70 keV. (Note that there is only one positive s-wave resonance at 27.67 keV in this energy region.) The result was quite successful. Fig. 1 shows the comparison of calculation of total cross section with recent measurement of Liou et al.[5] for almost pure ^{56}Fe sample in the vicinity of 24 keV cross section valley. It is seen that the agreement is excellent. This also supports that Γ_γ of 1.4 eV for 28 keV resonance is a reasonable value.

Figs. 2 to 4 show the comparison for elemental iron. Rather small and smoothe background cross section corrections of negative values were necessary to obtain a final evaluated data curve of total cross section in the energy regions of 30 - 70 keV and 225 - 250 keV. However, above 250 keV, we had to abandon to reproduce the cross section from resonance parameters since there occured persistent discrepancy between calculation and experiment which was not easily remedied in the framework of MLBW approximation.

Calculated capture cross section was in good agreement with the recommended value of Ribon[6]. Small correction was made for energy below 200 eV.

The resonance parameters for ^{57}Fe by Rohr et al.[7] and Allen et al.[3] contain the inelastic width for s-wave resonance with $J = 1^-$, which is of a comaparable order of magnitude with neutron width. The inelastic excitation threshold of ^{57}Fe is very low (14.4 keV). The study by JNDC shielding cross section working group indicates that the low energy neutron spectrum in large iron block is influenced significantly by the presence of the inelastic scattering due to this minor isotope, ^{57}Fe. We have therefore incorporated into file 3 of JENDL-2 the ^{57}Fe inelastic cross section as calculated from resonance parameters up to 200 keV (Fig.5), followed by the statistical theory calculation in higher energy region. The trouble was that we had to add fictitious "fission width" in resonance parameters of file 2, since there is no room for the inelastic width in ENDF/B format.

References :

1. M. S. Pandey et al., Proc. Conf. Nuclear Cross Sections and Technology, Washington, D.C., 1975, p.748
2. F. G. Perey et al., Neutron Data of Structural Materials for Fast Reactors, Geel Conf., 1977, p. 530
3. H. Beer and R. R. Spencer, KFK-2063 (1974)
4. B. J. Allen et al., Geel Conf., ibid., p. 476
5. H. I. Liou et al., Nucl. Sci. Eng. 70 150 (1979)
6. P. Ribon, Geel Conf., ibid., p.
7. G. Rohr and K. N. Müller, Z. Physik 227 1 (1969)

Fig. 1

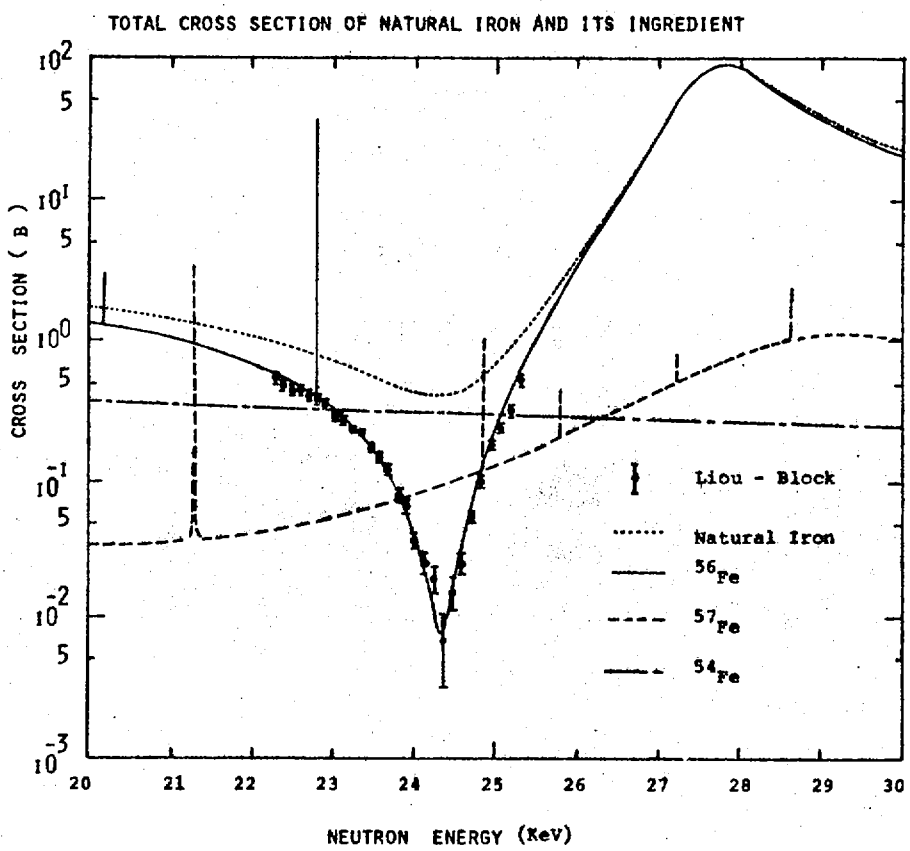
TOTAL CROSS SECTION OF NATURAL IRON AND ITS INGREDIENT
CROSS SECTION (B)
NEUTRON ENERGY (KeV)
Liou - Block
Natural Iron
56Fe
57Fe
54Fe

Fig. 2

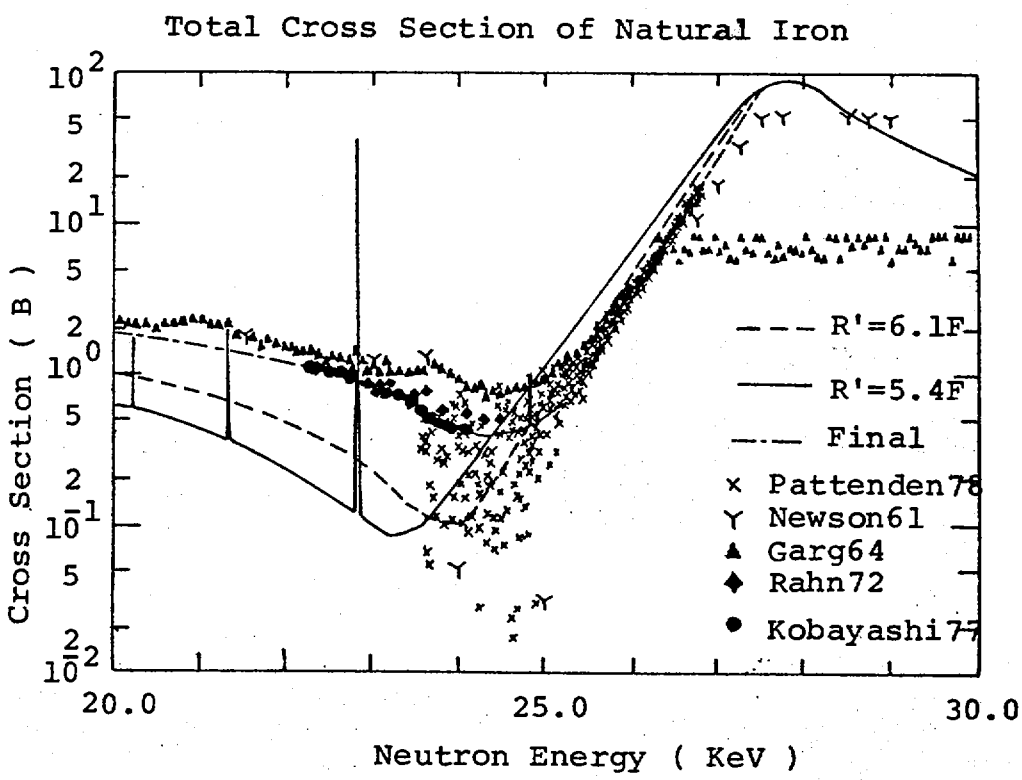
Total Cross Section of Natural Iron
Cross Section (B)
Neutron Energy (KeV)
R'=6.1F
R'=5.4F
Final
Pattenden78
Newson61
Garg64
Rahn72
Kobayashi77

Fig. 3

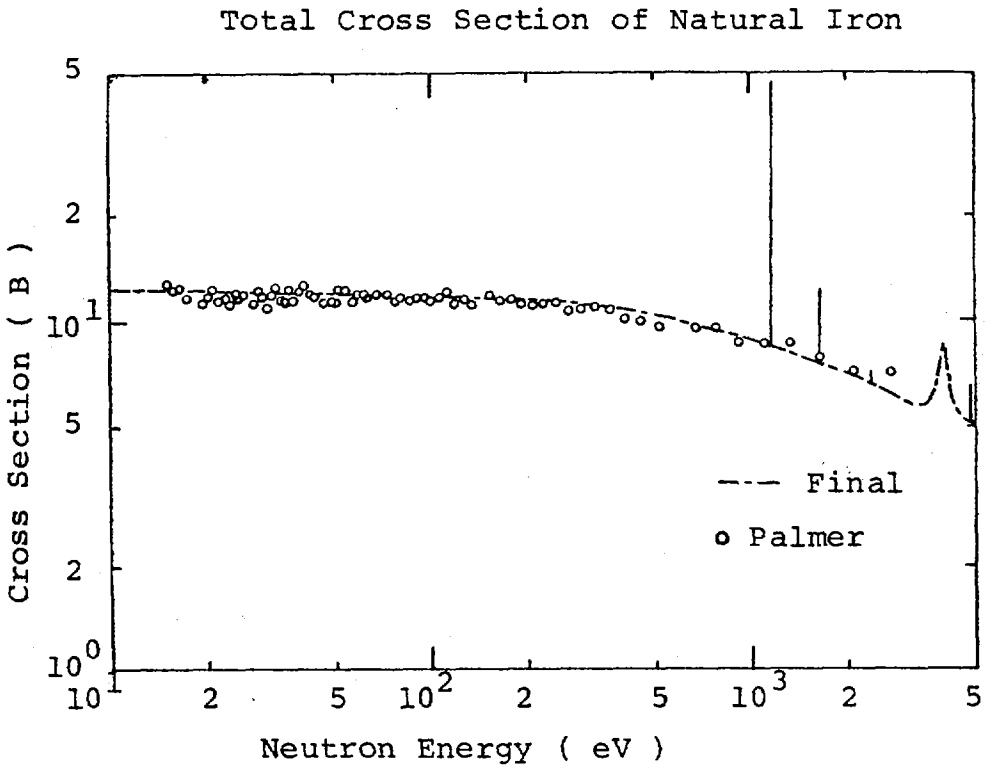
Total Cross Section of Natural Iron
Cross Section (B)
Neutron Energy (eV)
Final
Palmer

Fig. 4

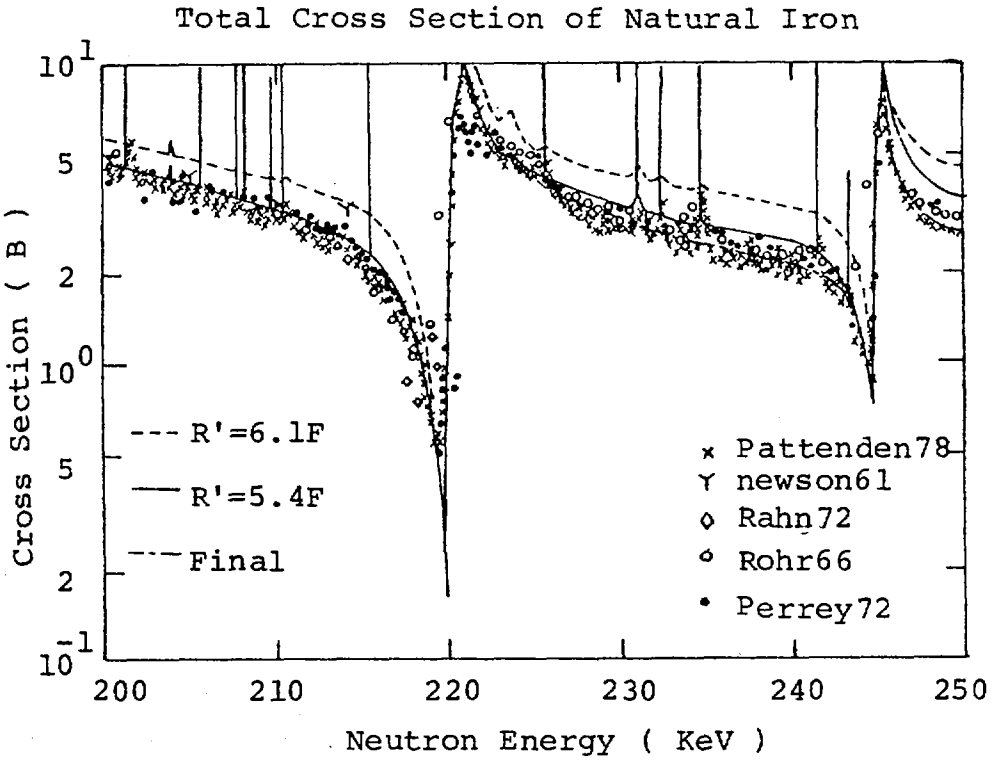
Total Cross Section of Natural Iron
Cross Section (B)
Neutron Energy (KeV)
R'=6.1F
R'=5.4F
Final
Pattenden78
newson61
Rahn72
Rohr66
Perrey72

Fig. 5 Excitation Curve for the First Level of ^{57}Fe

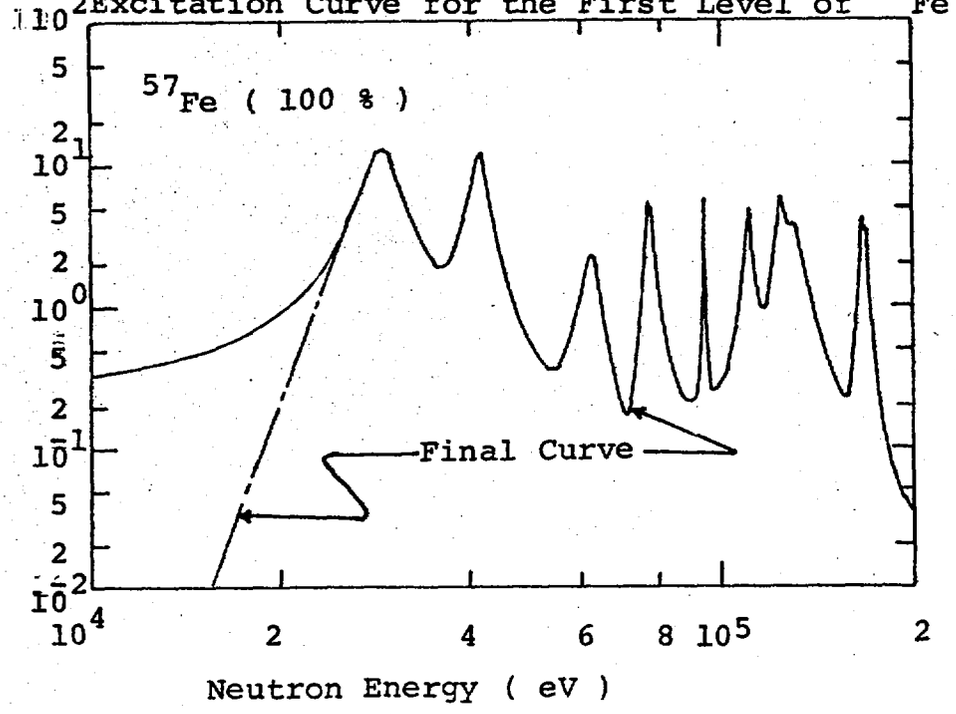

I-B-9 Problems in Iron Cross Sections on Shielding Application

Masayoshi Kawai[+], Naoki Yamano[++], and Kinji Koyama

This work has been performed for the purpose of pointing out the problems in structural material nuclear data from a viewpoint of shielding application. Nuclear data of structural materials play an important role for evaluating shielding design parameters, of which target accuracies are reported to be about 30 % for radiation damage and heating, and factor 2-3 for dose rate[1)]. Concerning the neutron cross section of iron which is used as a structural material, the following two large discrepancies are found between JENDL-1 and ENDF/B-IV : (1) Fine structure of total cross section in the energy region of unresolved resonance above 400 keV appeares in ENDF/B-IV, but is substituted by the smoothed mean value in JENDL-1. This difference gives a meaningful discrepancy of a self-shielded cross section for pure iron metal. (2) For the inelastic scattering cross section, JENDL-1 has maximum 40 discrete levels from the ^{57}Fe first exited level at 14.6 keV to the 3.90 MeV level of ^{56}Fe, while ENDF/B-IV has 26 levels from 861 keV to 4.59 MeV almost for ^{56}Fe. Secondary neutron energy spectrum of continuum level is expressed in the simple evaporation model in JENDL-1, but in the tabulated form in ENDF/B-IV. We have investigated how these differences affect on the neutron penetrating through bulk iron.

Cross section sensitivity analysis was performed to estimate the effect of resonance structure up to a few MeV in (n,n), (n,n') and capture cross sections on calculated neutron fluxes penetrating through iron slabs

---

+ Nippon Atomic Industry Group Co., Ltd.

++ Sumitomo Atomic Energy Industries, Ltd.

with the thickness from 10 cm to 100 cm. Calculations are carried out with S_{16}-transport theory by using one dimensional sensitivity code ROSETTA-1D[2] and the ENDF/B-IV file. The results in the case of 100 cm slab with a fission spectrum source are given in Fig.1, which shows the change of the detector response at 100 cm distance from the source correspondent to the cross section change due to the resonance self-shield. The neglect of resonance self-shield leads to underestimate of neutron dose rate by 90 % (for overall elastic scattering), 30 % (for elastic scattering in unresolved region), 5 % (for inelastic scattering), and 0.23 % (for capture). For the 1/v-detector , the contribution of fast neutron cross section decrease slightly. It was also found that contribution of self-shield for needle-like p-wave resonance was almost negligible in the energy range of resolved resonance below 400 keV.

The contribution of partial inelastic scattering cross section to neutron fluxes through iron sphere was examined by using the temporaly files consisting of ENDF/B-IV and JENDL-1 as shown in Table 1. Neutron penetration calculations were performed for the sphere of 100 cm diameter with three kinds of mono-energetic sources (0.65 MeV, 4.5 MeV, and 14 MeV) located at the center of sphere with S_{64}-P_{12} approximation using one dimensional S_N - transport theory, Results are shown in Fig. 2 and 3. It was found that the neutron flux at 30 cm from the center (below 10 keV) was increased about 60 % by considering low energy discrete level of ^{57}Fe and the fast neutron spectrum was much affected by the secondary neutron spectrum data of the continuum level.

From this study, it has been concluded that the following quantities should be considered for evaluating/compiling cross sections of structural materials : (1) unresolved resonance structure up to about 2 MeV, (2) the discrete inelastic scattering cross sections of an isotope even with a low

abundance, and (3) the detailed secondary neutron spectrum.

References :

(1) V. Herrnberger, et al. ; Proc. of the Specialists' Meet, on Sensitivity Studies and Shielding benchmarkes, paris, October 7-10, (1975) p, 224.

(2) S. Miyasaka, et al. ; ibid. p, 215 (1975)

Table 1 Contents of Temporary File

MAT No.	Contents
1260	JENDL-1 data
1192	ENDF/B-IV data
2600	replacing the data of MT=51-91 in MAT=1192 with those in MAT=1260
2601	replacing the secondary neutron spectrum of continuum level in MAT=1192 with the data in MAT=1260
2602	incorpolating the data of MT=67-76 in MAT=2601 into continuum level (MT=91)
2603	adding the data of MT=51 (first level of Fe-57) in MAT=1260 to the data in MAT=2601
2604	adding the data of MT=51-55 (discrete level of Fe-57 and Fe-58) in MAT=1260 to the data in MAT=2601

Fig. 1. Detector response change by neglecting the resonance self-shielding effect for iron cross sections.

Fig. 2. The change of neutron spectrum at the distance of 30 cm from the central source of 0.65 MeV. Differences are induced by the low-lying discrete levels of $^{57,58}Fe$.

Fig. 3. The change of neutron spectrum at the distance of 30 cm from the central source of 14 MeV. Differences above 1 MeV are mainly induced by the secondary neutron spectrum data of the continuum level.

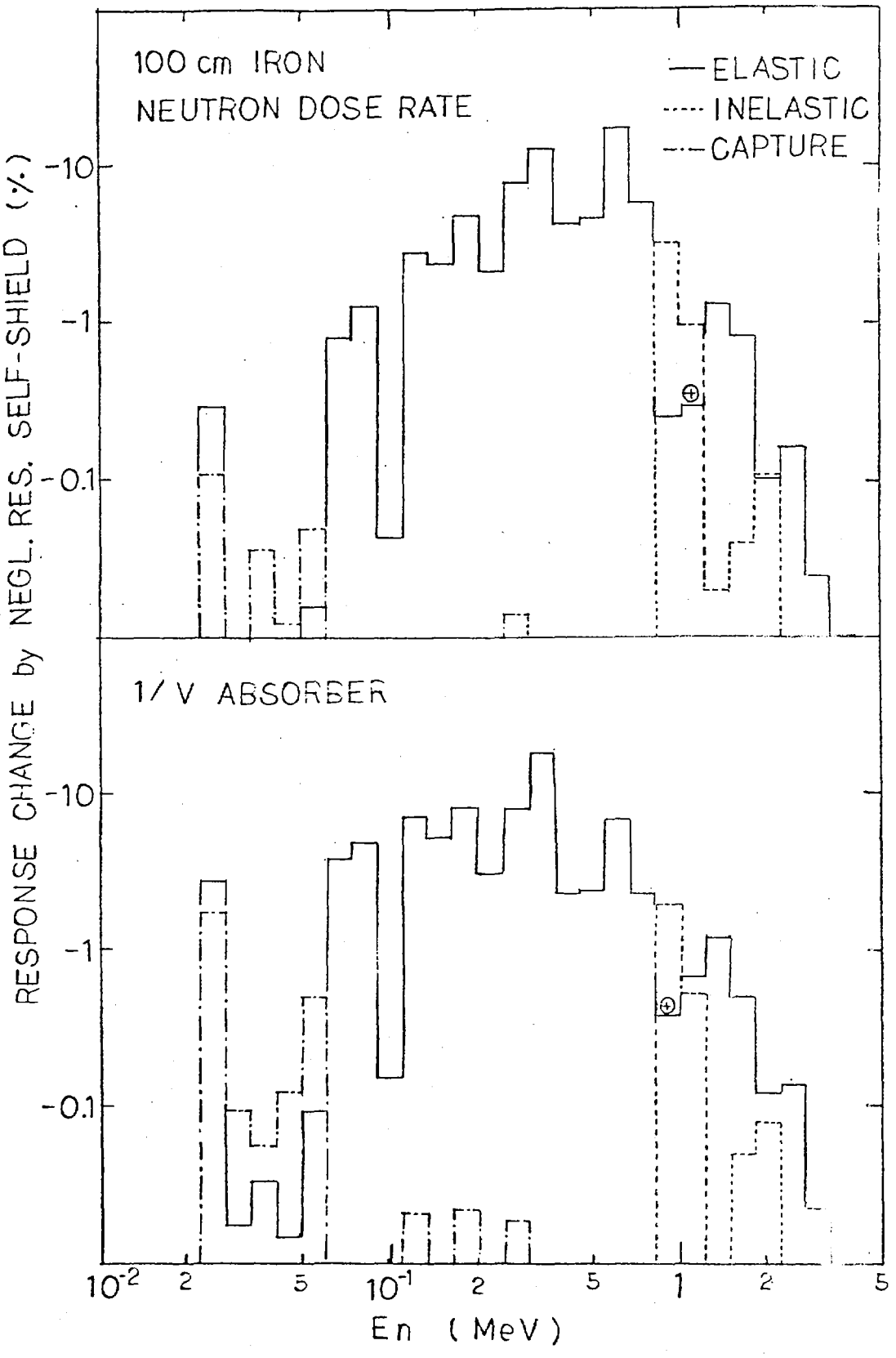
100 cm IRON
NEUTRON DOSE RATE
ELASTIC
INELASTIC
CAPTURE
1/V ABSORBER
RESPONSE CHANGE by NEGL. RES. SELF-SHIELD (%)
-10
-1
-0.1
10^-2
2
5
10^-1
2
5
1
2
5
En (MeV)

Fig.1

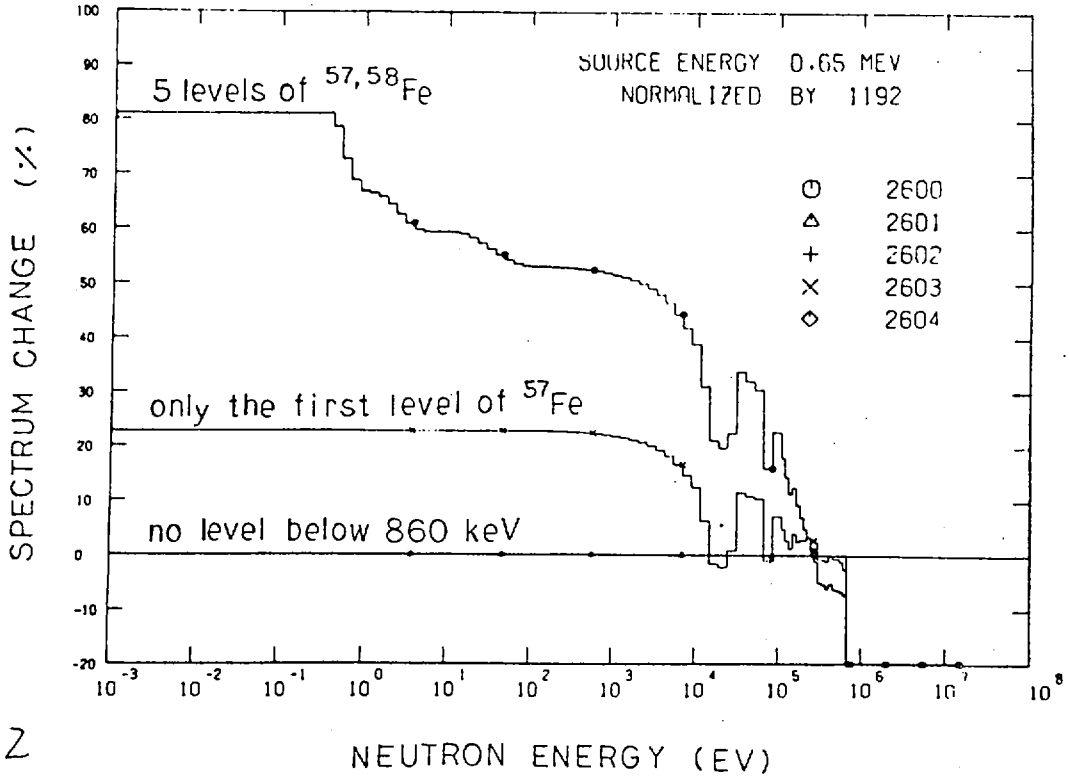
SOURCE ENERGY 0.65 MEV
NORMALIZED BY 1192
5 levels of 57,58Fe
only the first level of 57Fe
no level below 860 keV
2600
2601
2602
2603
2604
SPECTRUM CHANGE (%)
NEUTRON ENERGY (EV)

Fig. 2

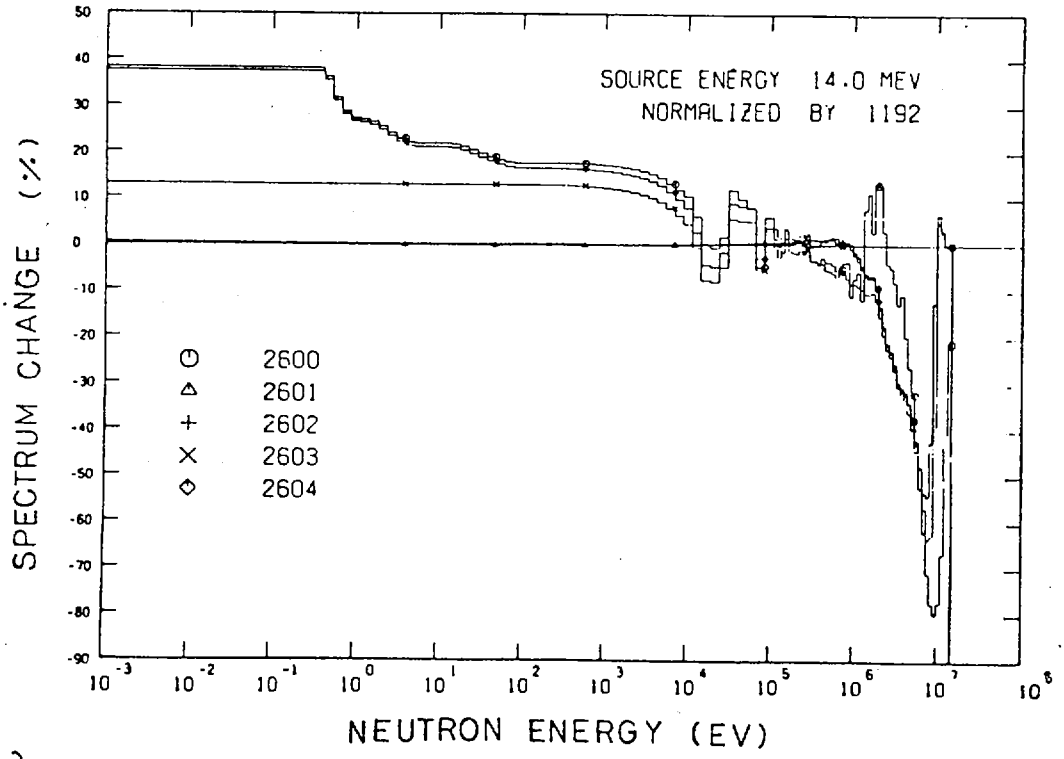
SOURCE ENERGY 14.0 MEV
NORMALIZED BY 1192
2600
2601
2602
2603
2604
SPECTRUM CHANGE (%)
NEUTRON ENERGY (EV)

Fig 3

I-B-10

Evaluation of Neutron Nuclear Data for Natural Nickel

N. Sekine and Y. Kikuchi

Evaluation of neutron nuclear data for natural nickel was made in the energy range of 10^{-5} eV to 20 MeV for JENDL-2. A region below 600 keV was regarded as resonance one for which resonance parameters were given on each isotope. The parameters for ^{58,60}Ni were re-evaluated based on recent experimental data, but those for ^{61,62,64}Ni followed almost the same values as adopted in JENDL-1. Due to the use of effective scattering radius independent on the energy, the calculated total cross sections become lower and higher than the experimental data at lower and higher energy, respectively. Therefore corrections were made by introducing positive and negative background cross sections at the lower and higher energy, respectively. The calculated capture cross sections were lower than experimental data above 200 keV due to missing P-wave resonances and positive background cross sections were applied above 200 keV.

In continuum region above 600 keV, the total cross sections were obtained by tracing the high resolution experimental data of Cierjacks et al.[1]. The results in the range of 600 keV to 3 MeV are shown in Fig. 1, together with the data of JENDL-1 as comparison. Capture and inelastic scattering cross sections were calculated by using the statistical model code CASTHY[2] treating the sum of (n,2n) and (n,p) reaction cross sections, which were taken from experimental data, as competing ones. The parameters used in the calculation are those determined by M. Kawai[3] and T. Yoshida[4]. The calculated capture cross sections were normalized at 450 keV to 9.6 mb obtained by averaging measured data. The present evaluated capture cross sections have somewhat lower values than those of JENDL-1, which is mainly due to the use of different level density functions from that used in JENDL-1. The calculated inelastic scattering cross sections were modified by taking into

account the contributions from direct processes and the results are shown in Fig. 2, together with the data of JENDL-2 and ENDF/B-IV. The present evaluated inelastic scattering cross sections agree well with the experimental data around at 4.5 MeV. The number of inelastic scattering cross sections corresponding the levels of each isotope up to the excitation energy 4.472 MeV were reduced to 40 levels so as to make closing levels into one level. In present evaluation, the cross sections such as (n,α), (n,n'p) reaction cross sections are not taken into account. Neglect of these cross sections is also the main source of increase of evaluated inelastic scattering cross sections above 10 MeV. The work of evaluation of these cross sections is in progress.

References:

1) Cierjacks, S. et al.: KFK-1000 (1968) sup. 1

2) Igarasi, S.: private communication

3) Kawai, M.: reported in this progress report

4) Yoshida, T.: reported in this progress report

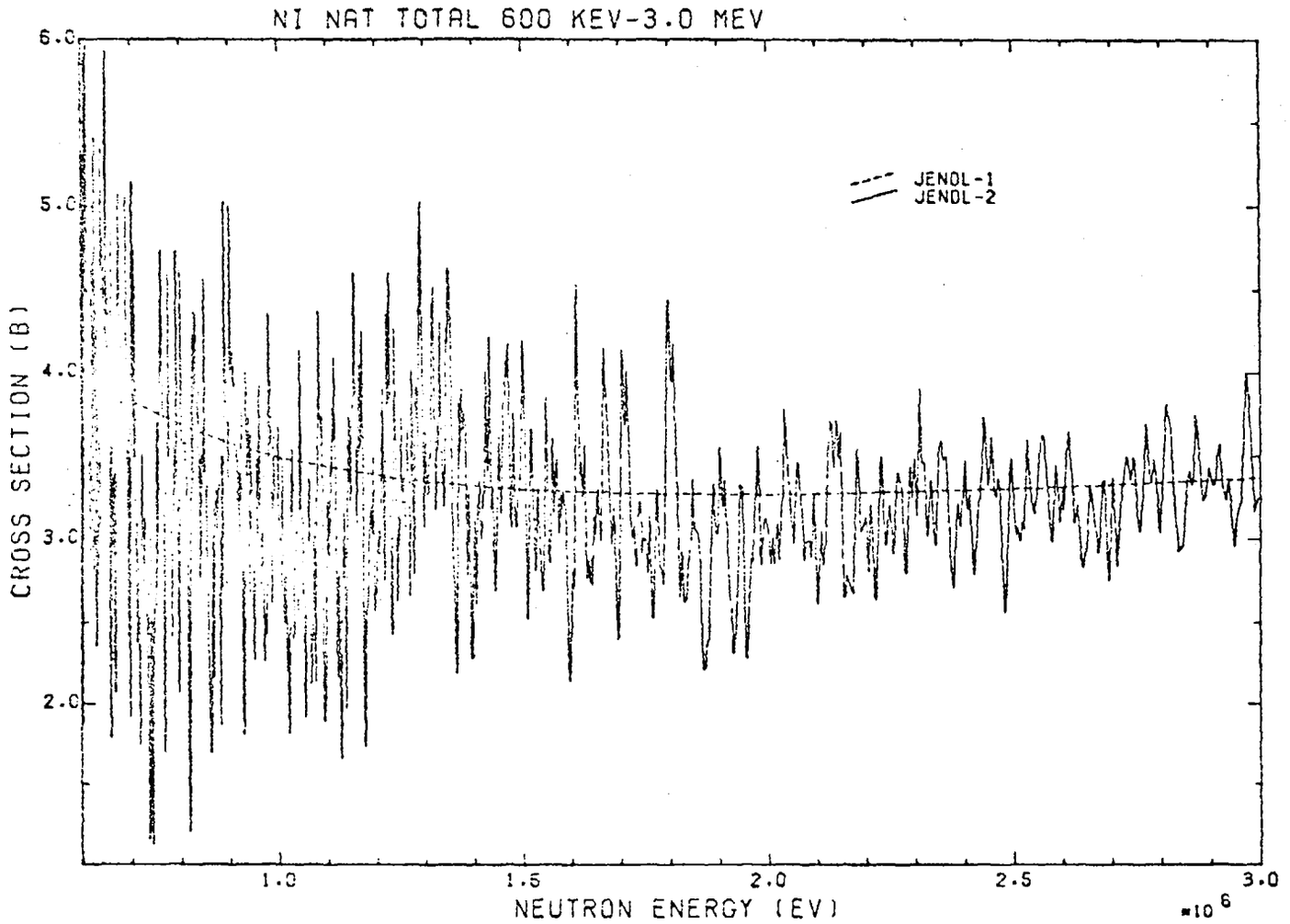

Fig. 1 Comparison of present evaluated total cross sections with the data of JENDL-1 in the energy range 600 keV - 3 MeV.

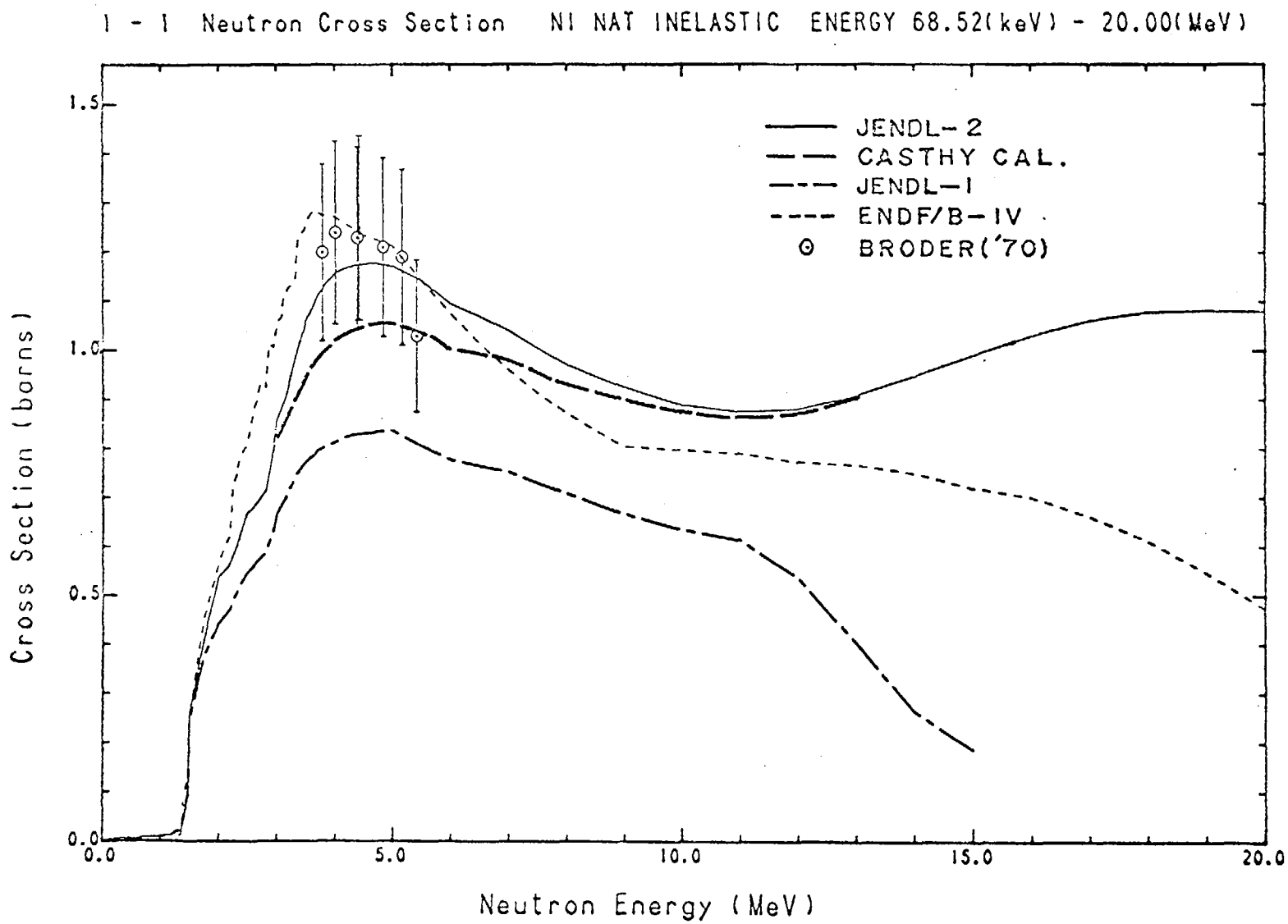

Fig. 2 Comparison of present evaluated inelastic scattering cross sections with experimental data and the data of JENDL-1 and ENDF/B-IV.

I-B-11 Evaluation of the Nuclear Data for ^{233}U

H. Matsunobu* and N. Asano*

Evaluation of the nuclear data for ^{233}U was performed in the energy range from 100 eV to 20 MeV as a part of the evaluated data preparation on thorium cycle nuclides for the Japanese Evaluated Nuclear Data Library-Version 2 (JENDL-2).

The fission cross section was evaluated with the simultaneous evaluation method used in the Working Group on Heavy-Nuclide Nuclear Data of Japanese Nuclear Data Committee. That is, the consistency of the fission cross sections between ^{233}U and ^{235}U was examined with the absolute and relative measurements of ^{233}U and the evaluated data of ^{235}U. The cross section was obtained on the basis of the experimental data selected by this examination.

The total cross section in the energy range from 10 keV to 20 MeV was obtained using the optical and statistical model calculation. The optical potential parameters used in this calculation were obtained by analysis of the recent experimental data. The total cross section below 10 keV was determined on the basis of the experimental data, because the fine structures of the cross section were not reproduced by the calculation in this energy range.

---

* Sumitomo Atomic Energy Industries, Ltd.

The neutron capture cross section was determined on the basis of the experimental data in the energy range below 2 keV, and using the above calculation in the energy range above 2 keV.

The elastic and inelastic scattering cross sections were also obtained using the calculation with the same potential parameters.

The (n, 2n) and (n, 3n) cross sections were calculated by Pearlstein's method. The neutron emission cross section used in this calculation was derived by subtracting the fission, neutron capture, and elastic scattering cross sections from the total cross section evaluated in this work, respectively.

The prompt and delayed neutron numbers per fission were evaluated on the basis of the experimental data. The structure of prompt neutron number per fission was taken into consideration in the energy range below 1 MeV. The evaluated values above 1 MeV were expressed by three straight lines with different energy dependences, of which the connecting points were given at 1.00, 2.73, and 7.95 MeV, respectively.

The following figure shows the results of the present work.

The authors were supported under the contract with Japan Atomic Energy Research Institute.

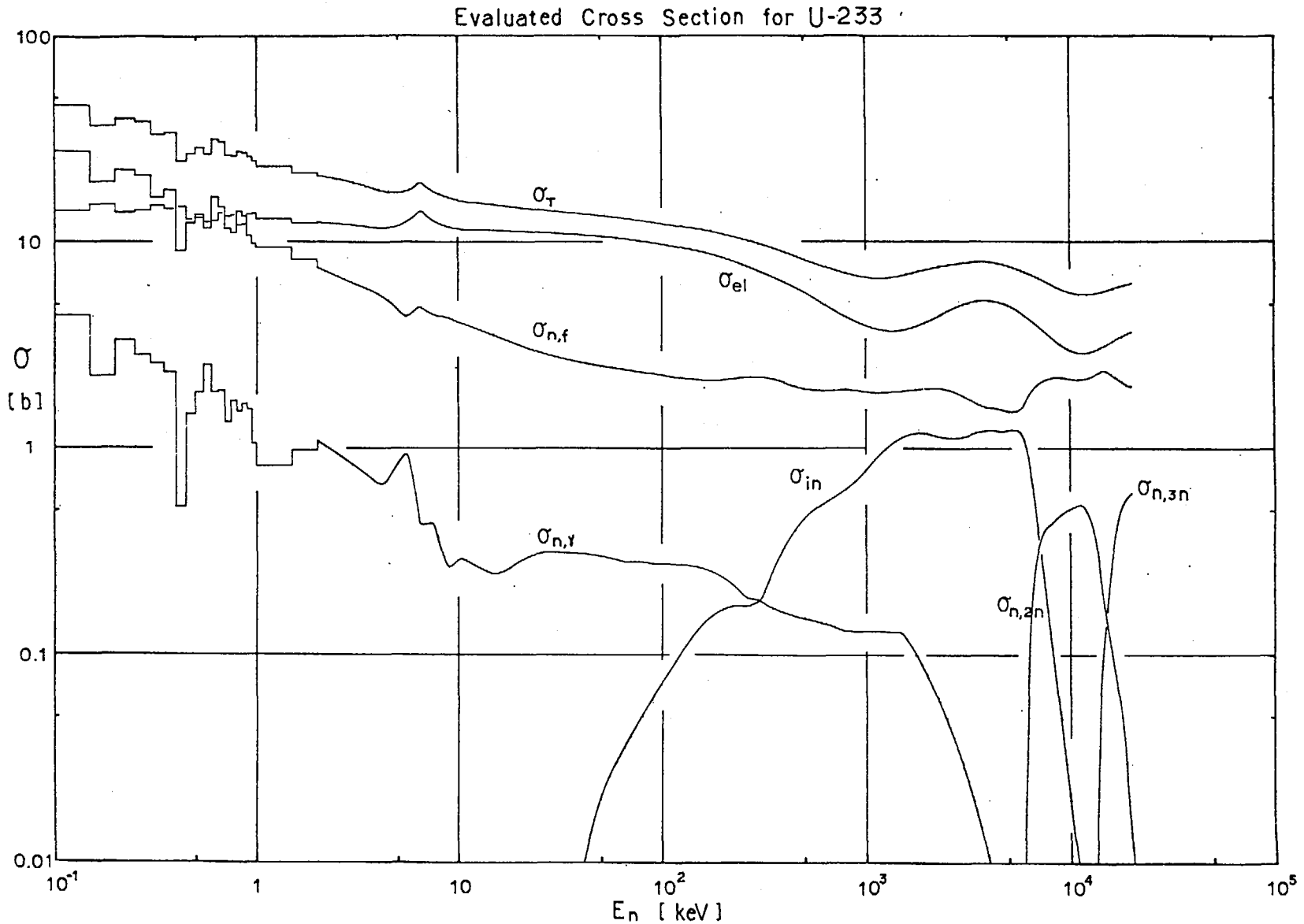
Evaluated Cross Section for U-233
100
10
1
0.1
0.01
σ
[b]
σ_T
σ_{el}
$\sigma_{n,f}$
σ_{in}
$\sigma_{n,\gamma}$
$\sigma_{n,2n}$
$\sigma_{n,3n}$
10^{-1}
1
10
10^2
10^3
10^4
10^5
E_n [keV]

I-B-12

Simultaneous Evaluation of the Nuclear Data for ^{235}U, ^{238}U, ^{239}Pu, ^{240}Pu, and ^{241}Pu

H. Matsunobu*, Y. Kanda**, M. Kawai†,
T. Murata†, and Y. Kikuchi††

Simultaneous evaluation of the nuclear data for ^{235}U, ^{238}U, ^{239}Pu, ^{240}Pu, and ^{241}Pu was recently completed in the energy range from 100 eV to 20 MeV. This work was performed as a part of the activities in the Working Group on Heavy-Nuclide Nuclear Data of Japanese Nuclear Data Committee in connection with preparation of the Japanese Evaluated Nuclear Data Library-Version 2 (JENDL-2).

A special care was paid in determining the fission cross sections of the above five nuclides. The fission cross section of ^{235}U was determined on the basis of the recent experimental data published after 1975 so that the consistency is kept between the ablolute data and the ratio data to fission cross section of ^{235}U in the other nuclides.

The total cross sections were evaluated using the experimental data, and the optical and statistical model calculations. In this work, a reference set of the optical potential parameters was used as the initial guess in order to search the best fit parameters with the experimental data. This reference set was

---

* Sumitomo Atomic Energy Industries, Ltd.

** Kyushu University

† Nippon Atomic Industry Group Co., Ltd.

†† Japan Atomic Energy Research Institute

determined so that the gross structures of the total cross section are reproduced for the five nuclides.

The above best fit parameters for each nuclide were used to calculate the capture, elastic and inelastic scattering cross sections. The experimental data for these cross sections were also used to normalize the calculated values.

The (n, 2n), (n, 3n), and (n, 4n) cross sections were evaluated using the experimental data and Pearlstein's method. In this evaluation, the neutron emission cross sections were obtained by subtracting the evaluated fission and capture cross sections from the non-elastic cross sections calculated with the optical and statistical models.

The results of evaluation will be presented to the International Conference on Nuclear Cross Sections for Technology to be held at Knoxville in October, 1979.

I-B-13

Evaluation of Neutron Cross Section of ^{236}U

T. Yoshida*

Neutron cross sections of ^{236}U have been evaluated for JENDL-2 in the energy range from 10^{-5} eV to 20 MeV. Reactions involved are total, fission, capture, (n,n'), (n,2n), and (n,3n).

The fission ratio curve (U-236/U-235) has been determined mainly based on data by Behrens and Carlson[1] and those by Meadows[2]. The results are multiplied by a ^{235}U fission curve by Matsunobu[3].

The capture cross section calculated with CASTHY code[4] has been adopted being normalized at 10 keV to a measured value by Carlson[5].

The inelastic cross section is based on a statistical model calculation carried out with CASTHY code. The method of Pearlstein has been applied to determine the (n,2n) and (n,3n) cross sections.

The adopted set of resonance parameters are mainly based on those by Carraro and Brusegan[6]. The thermal capture value is fixed to 5.2 barns.

References:

1) J. W. Behrens, G. W. Carlson, Nucl. Sci. Engn., 63 (1977) 250

2) J. W. Meadows, Nucl. Sci. Engn., 65 (1978) 171

3) H. Matsunobu, private communication (1979)

4) S. Igarasi, private communication

5) A. D. Carlson, GA-9057 (1968)

6) G. Carraro, A. Brusegan, Nucl. Phys., A275 (1976) 333

* NAIG Nuclear Research Lab., Nippon Atomic Industry Group Co., Ltd.

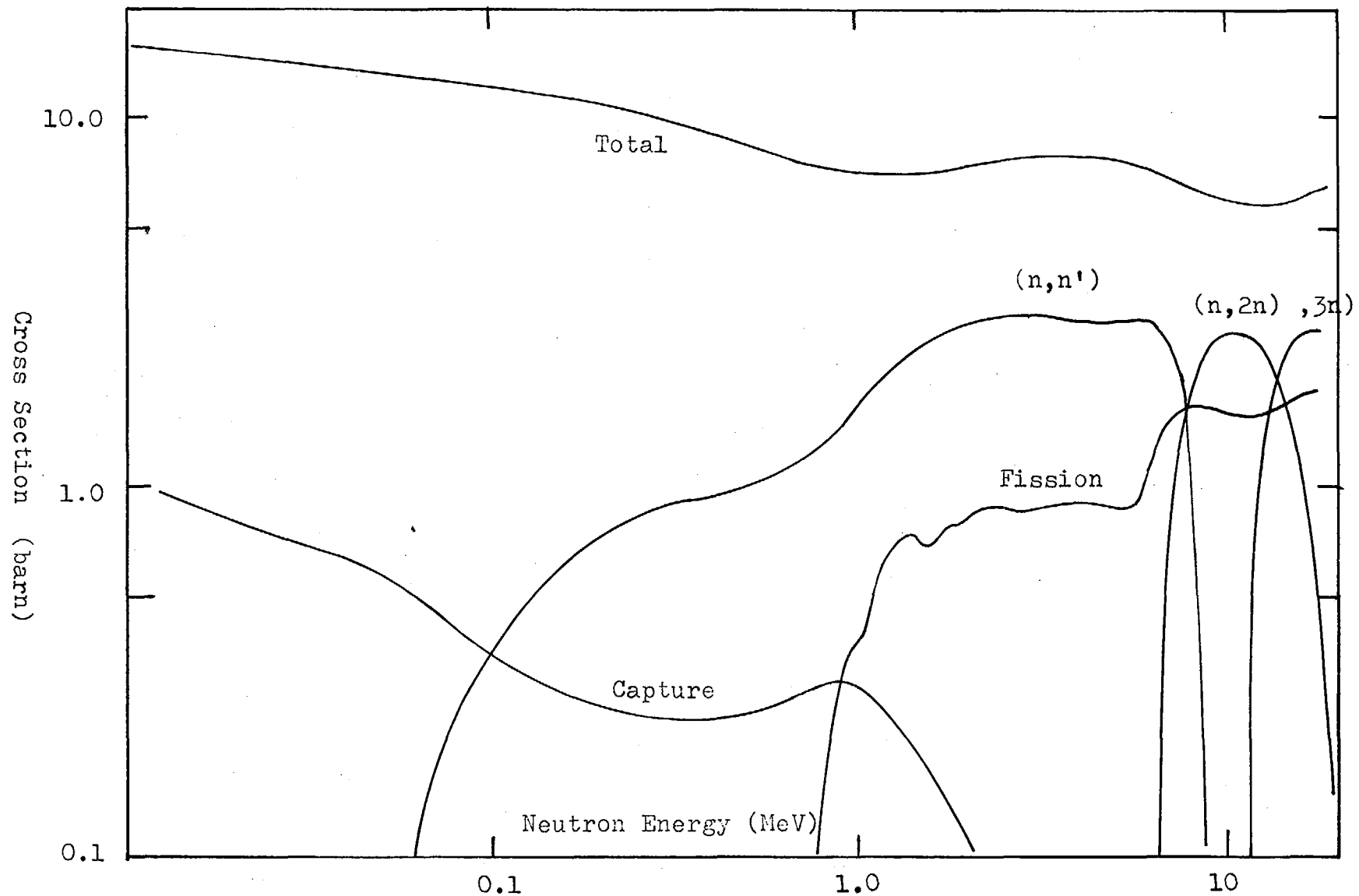

FIG. 1 NEUTRON CROSS SECTIONS OF ^{236}U

I-B-14

Evaluation of Neutron Cross Sections of ^{241}Pu for JENDL-2

Y. Kikuchi and N. Sekine

Neutron cross sections of ^{241}Pu were evaluated in the energy range from 10^{-5} eV to 20 MeV for JENDL-2.

The cross sections are given as point-wise data below 1 eV. We adopted the measured data of Wagemans and Deruytter[1] for fission and those of Young [2] for total cross section, and drew smooth curves by the eye-guide method. The elastic scattering cross section was calculated from the resonance parameters with assuming the effective scattering radius of 10 fm, and the capture cross section was obtained by subtracting the fission and elastic scattering cross sections from the total cross section. These cross sections agree well with the values of 1975 IAEA recommendation[3] and connect smoothly to those calculated from the resonance parameters at 1 eV.

The resonance parameters of JENDL-1 up to 100 eV, which was based on the recommendation of BNL-325 3rd edition, were modified so that the calculated cross sections may well reproduce the measured total cross section of Kolar et al.[4] and the measured fission cross section of Blons[5]. In spite of this modification, the background correction was required for the fission cross section, since the multi-level multi-channel representation is substantially necessary for fissile nuclides. The background cross section was also applied to the capture cross section so that the α-value measured by Weston and Todd[6] may be well reproduced.

The unresolved resonance parameters are given in the energy range between 100 eV and 30 keV. The parameters were determined so that the measured data of the fission cross section and the α-values may be well reproduced.

The fission cross section above 30 keV were evaluated mainly on the basis of the measured data of Kaeppeler and Pfletschinger[7], Behrens and

Carlson[8] and Szabo[9,10]. As the data of Kaeppeler and Pfletschinger[7] and Behrens and Carlson[8] are given as the ratio to the fission cross section of ^{235}U, the absolute values were deduced by multiplying the fission cross section of ^{235}U evaluated by Matsunobu[11] for JENDL-2.

The capture cross section was obtained up to 250 keV from the α-values measured by Weston and Todd[6]. Above 250 keV, the capture cross section was calculated with the optical and statistical models as well as the elastic and inelastic scattering cross section. The (n,2n), (n,3n) and (n,4n) reaction cross sections were calculated with Pearlstein's method[12] for which some modification was made on the level density parameters. The (n,2n), (n,3n) and (n,4n) reaction cross sections were used with the fission cross section as the competition cross sections in the statistical model calculations. The optical potential parameters were determined by Murata and Kawai[13] from the global trends of the total cross sections in this mass range. The γ-ray strength function was so obtained that the calculated value agrees with that obtained from the measurements of Weston and Todd[6] at 250 keV.

The evaluated cross sections are shown in Fig. 1.

Reference:

1) C. Wagemans and A. J. Deruytter: Nucl. Sci. Eng., 60, 44 (1976)

2) Young: Data in NEUDADA.

3) H. D. Lemmel: Nuclear Cross Section and Technology, Proc. Conf. Washington D. C., Mar. 3 - 7, 1975, P. 286, NBS Special Publication 425, (1975)

4) W. Kolar and G. Carraro: Neutron Cross Section Technology, Proc. Conf. Knoxville, Mar. 15 - 17, 1971, CONF-710301, P. 707 (1971)

5) J. Blons: Nucl. Sci. Eng., 51, 130 (1973)

6) L. W. Weston and J. H. Todd: Nucl. Sci. Eng., 65, 454 (1978)

7) F. Kaeppeler and E. Pfletschinger: Nucl. Sci. Eng., 51, 124 (1973)

8) J. W. Behrens and G. W. Carlson: Measurement of the Neutron induced fission cross section of ^{241}Pu relative to ^{235}U from 0.001 to 30 MeV, UCRL-51925, (1975)

9) I. Szabo, G. Filippi, J. L. Huet, J. L. Leroy and J. P. Marquette: Proc. EANDC Symp. Neutron Standards and Flux Normalization, ANL, Oct. 21 - 23, 1970, CONF-701002, P. 257 (1971)

10) I. Szabo, J. L. Leroy, J. P. Marquette: Proc. Conf. Nuclear Physics, Kiev, 28 May - 1 June, 1973, Vol. 3. P.27 (1973)

11) H. Matsunobu: Proc. 1978 Seminar on Nuclear Data, 20 - 21 Dec. 1978, Tokai, P. 209, JAERI-M 8163 (1979), (in Japanese)

12) S. Pearlstein: Nucl. Sci. Eng., 23, 238 (1965)

13) T. Murata and M. Kawai: private communication (1978)

1 - 1 Neutron Cross Section ^{241}Pu ENERGY 100.00(eV) - 20.00(MeV)

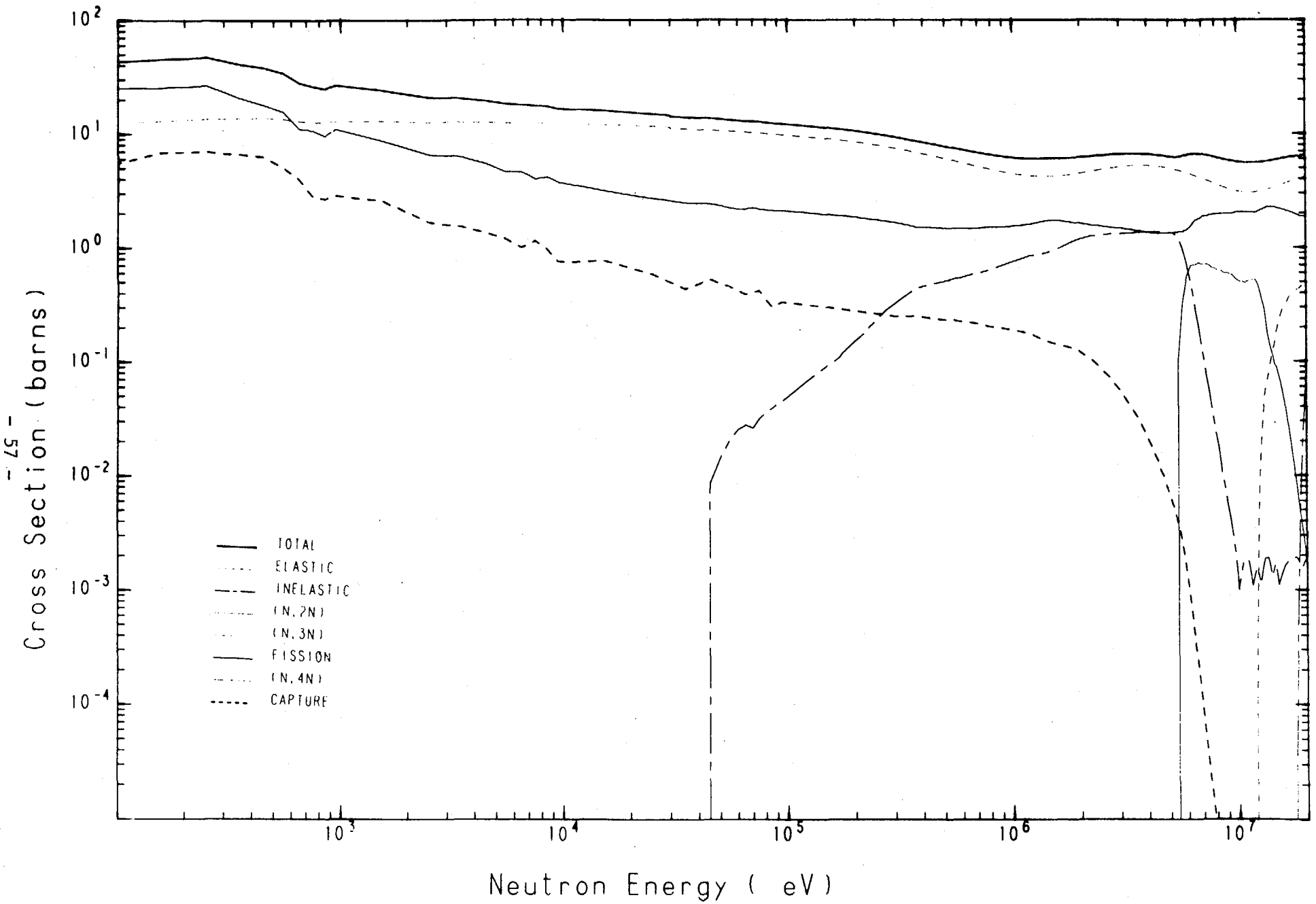

I-B-15 Evaluation of Neutron Cross Sections of ^{242}Pu

Masayoshi Kawai* and Tohru Murata*

Neutron cross sections have been evaluated for ^{242}Pu as an activity of Japanese Nuclear Data Committee (JNDC). The evaluated data are stored in the Japanese Evaluated Nuclear Data Library Version-2 (JENDL-2). The evaluated quantities are the resonance parameters, the total, elastic and inelastic scattering, capture, (n,2n), (n,3n), and (n,4n) cross sections from the thermal energy to 20 MeV.

Concerning the resonance parameters, 131 levels below 3.9 keV were evaluated by examing the experimental data reported by 1975. Neutron widths were determined with a weighted average method. The radiative widths were also obtained by the weighted average method for the levels to which some experimental data were given. An average value of these evaluated radiative widths was 24.2 MeV. This average value was used for the levels whose radiative width was not given. The fission widths were evaluated by taking account of the fission area. Using the resonance parameters mentioned above, the thermal and the resonance cross sections were reproduced. The reproduced cross section values were compared with the experimental data. Thus, the resolved resonance region was decided up to 1.29 keV. Average resonance parameters and the thermal cross sections are as follows:

$D = 13.04$ eV, $So = 0.85 \times 10^{-4}$, $\bar{\Gamma}_{rad} = 24{,}2$ MeV, $R' = 9.6$ fm

$\sigma_{cap} = 18{,}428$ b, $\sigma_{fis} = 0.013$ b, $\sigma_{el} = 8{,}2$ b.

Above the energy region of resolved resonance region, there are some but not sufficient experimental data for total, fission and capture cross sections for ^{242}Pu. For the total cross section, the spherical optical model was adopted above 6 keV. The global fit potential parameters[1] for heavy elements are adjusted so as to reproduce the experimental data below 6 keV.

The fission cross section was obtained mainly on the basis of the experimental data by Auchampaugh et al.[2] and Behrens et al.[3] From 370 eV to 110 keV, a shape of averaged fission cross section was assumed to be given by summing up Lorentzian shape resonances with the areas,

---

* Nippon Atomic Industry Group Co., Ltd.

whose trend was examined by using the data of Auchampaugh et al. The fission cross section thus obtained was normalized to the cross section values above 100 keV which were obtained by multiplying the fission ratio by the standard value[4] of ^{235}U fission cross section for JENDL-2. The capture cross sections were calculated with the Hauser-Feshbach theory and normalized to the experimental data of Hockenbury et al.[5] in the energy range from 6 keV to 40 keV. The (n,2n), (n,3n) and (n,4n) cross sections were estimated in the combination of the optical model and the Pearlstein's procedure. Elastic scattering cross section was determined as the difference between the total cross sections and the absorption cross sections below the threshold energy of inelastic scattering. Above the threshold energy, the elastic and the inelastic scattering cross sections were estimated with the statistical model.[6]

The results are shown in Fig. 1.

References:

1) T. Murata and M. Kawai ; 1978 Fall Meet. of the Atomic Energy Society of Japan, D19 (1978).
2) G. F. Auchampaugh, et al. ; Nucl. Phys. A171 (1971) 31.
3) J. W. Behrens, et al. ; Nucl. Sci. Eng. 66 (1978) 433.
4) H. Matsunobu, et al. ; JAERI-M 8163 p. 209 (1979).
5) R. W. Hockenbury, et al. ; Proc. of Conf. on Nuclear Cross Sections and Technology, Washington, D.C. 1975, (1975) 584
6) S. Igarashi ; J. Nucl. Sci. Tech. 12 (1975) 67.

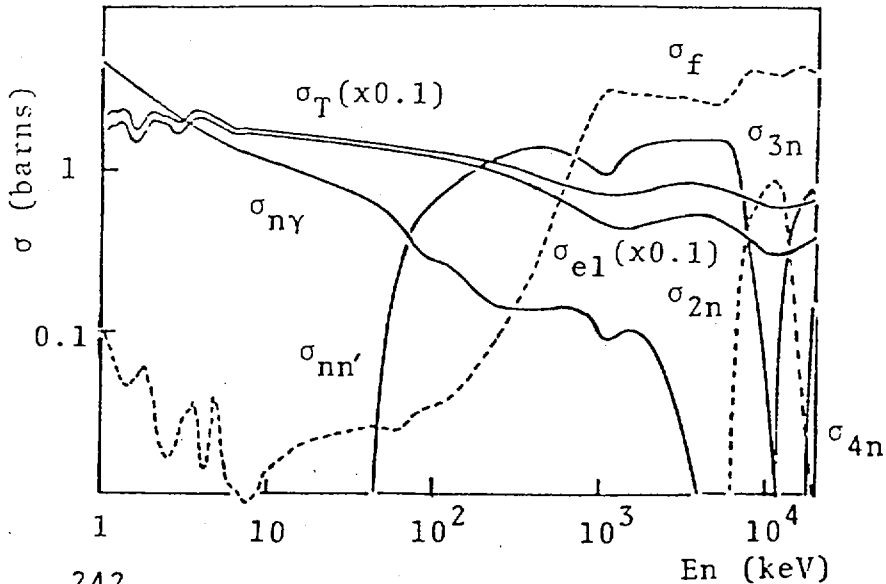

^{242}Pu Evaluated Cross Sections

I-B-16

Evaluation of Neutron Nuclear Data for ^{242}Cm

S. Igarasi and T. Nakagawa

Neutron nuclear data for ^{242}Cm were evaluated in the energy range of 10^{-5} eV to 20 MeV. The resonance region was defined below 275 eV. Artamonov et al.[1] measured 12 resonances in this region. These parameters were adopted and a negative resonance at -3.45 eV was taken into account in order to reproduce the capture cross section of 16.0 barns[2] at 0.0253 eV. Fission width for all resonances was assumed to be 0.0 and the fission cross section in the resonance region was presented by the expression as follows;

$$\sigma_{n,f} = 0.7952 / \sqrt{E(eV)} \quad .$$

This gives 5 barns[8] at 0.0253 eV. Cross sections at 0.0253 eV and resonance integrals above 0.5 eV are given in Table I.

Cross sections above 275 eV were mainly calculated with optical and statistical models by the use of the following potential parameters;

$$V = 43.4 - 0.107 \times E_n \ , \qquad \text{(MeV)}$$

$$W_s = 6.95 - 0.339 \times E_n + 0.0531 \times E_n^2 \ , \qquad \text{(MeV)}$$

$$V_{so} = 7.0 \ , \qquad \text{(MeV)}$$

$$r_o = r_{so} = 1.282 \ , \qquad \text{(fm)}$$

$$r_s = 1.29 \ , \qquad \text{(fm)}$$

$$a = a_{so} = 0.60 \ , \qquad \text{(fm)}$$

$$b = 0.50 \ . \qquad \text{(fm)}$$

The form factor for a surface term is the derivative Woods-Saxon type. These parameters were determined to reproduce well the total cross section of ^{241}Am measured by Phillips and Howe[3].

Fission cross section was obtained by using the evaluated cross section of ^{244}Cm[4] and systematics by Behrens and Howerton[5]. Cross sections of the (n,2n) and (n,3n) reactions were calculated with Pearlstein's method[6].

Total, elastic and inelastic scattering, and capture cross sections were calculated by taking account of the fission, (n,2n) and (n,3n) cross sections as competing processes. The level scheme recommended by Ellis and Haese[7] was adopted in this work. An average level spacing and capture width were assumed to be 16 eV and 36 meV, respectively. The results above 275 eV are shown in Fig. 1.

The result was published as JAERI-M 8342.

References:

1) Artamonov, V. S. et al.: "Neutron Resonances of ^{242}Cm", proc. of 4th All Union Conf. on Neutron Physics, Kiev, (1977), vol. 2, 257.

2) Mughabghab, S. F. and Garber, D. I.: "Neutron Cross Sections", vol. 1, BNL 325, 3rd Edition (1973).

3) Phillips, T. W. and Howe, R. E.: Nucl. Sci. and Eng. 69 (1979) 375.

4) Igarasi, S. and Nakagawa, T.: "Evaluation of the Neutron Nuclear Data for ^{244}Cm", (in Japanese) JAERI-M 7175 (1977).

5) Behrens, J.W. and Howerton, R. J.: Nucl. Sci. and Eng. 65 (1978) 464.

6) Pearlstein, S.: J. Nucl. Energy 27 (1973) 81.

7) Ellis, Y. A. and Haese, R. L.: Nucl. Data Sheets 21 (1977) 615.

8) Hanna, G. C. et al.: Phys. Rev. 81 (1951) 893.

Table I. Thermal cross section and resonance integral

	cross section at 0.0253 eV (barns)	resonance integral (barns)
elastic	11.6	
capture	16.0	116.2
fission	5.0	11.1
total	32.6	

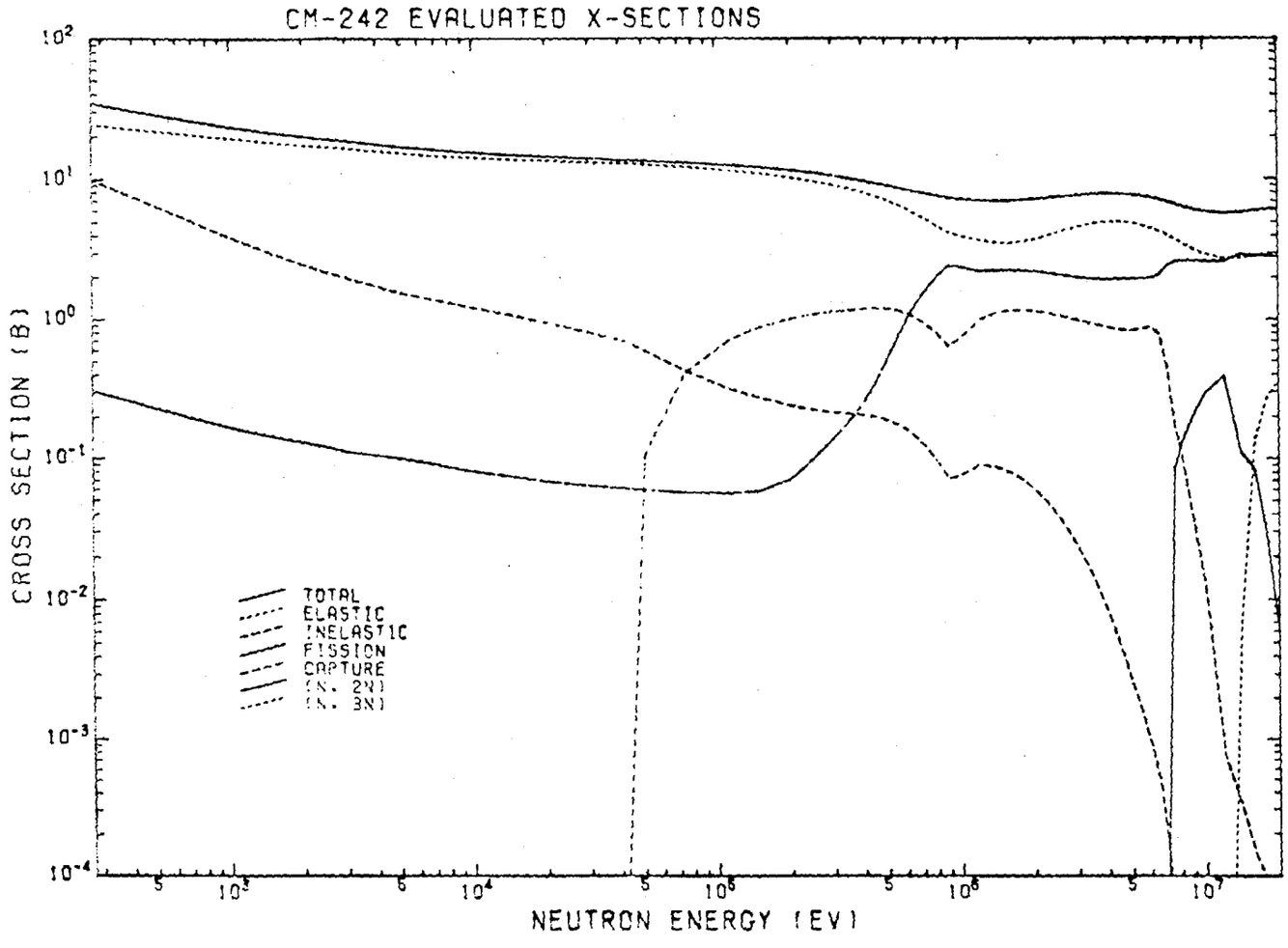

Fig. 1 Evaluated cross sections above 275 eV

I-B-17

Evaluation of Resonance Parameters of Heavy Nuclides

A. Asami, T. Nakagawa, T. Yoshida*, A. Zukeran**
and Y. Kikuchi

The resonance parameters of ^{235}U, ^{238}U, ^{239}Pu, ^{240}Pu and ^{241}Pu were evaluated for JENDL-2 by Resonance-Parameter Subworking Group of JNDC Working Group on Heavy-Nuclide Nuclear Data. Compilation of measured resonance parameters for each nuclide had been performed before this evaluation. Brief discriptions of the evaluation for each nuclide are as follows:

^{235}U

The data measured since 1964 were mainly used. The parameters evaluated in this work were obtained at first by suitably averaging the measured values. Then the calculated values with the parameters were compared with measured cross sections. After some corrections of parameters, background data for the evaluated resonance parameters were determined to reproduce the experimental cross sections.

The resonance region was determined below 100 eV.

^{238}U

About 10 newer measurements have been carried out since the evaluation was made for ENDF/B-IV. The resonance parameters of ^{238}U were evaluated up to 4.7 keV by the use of the newer measurements. Resonance energies were determined on the basis of the measurements at ORNL. Neutron and capture widths were evaluated with a simple area method. Fission widths were recommended for 27 s-wave resonances. The contribution of negative energy resonances and the correction for missing of p-wave resonances above 1.5 keV were taken into account as background data. Fig. 1 shows the comparison of calculated total cross section with measured values between 10 eV and 50 eV.

^{239}Pu

The parameters evaluated by Ribon and Le Coq[1)] were recommended. The

background data for the resonance parameters were evaluated by comparison with experimental cross sections. The resonance region was assigned below 598 eV.

^{240}Pu

After careful comparison of resonance parameters measured since 1966, the best parameters were selected from them. The cross sections calculated with the selected parameters were compared with experimental cross sections, and background data in resonance region were determined.

^{241}Pu

The discription of the evaluation is given by Kikuchi in a separate report on this progress report.

Reference:

1) Ribon, P., and Le Coq, G.: "Evaluation des Données Neutroniques de ^{239}Pu", CEA-N-1484 (1971)

---

* Nippon Atomic Industry Group Co., Ltd.

** Hitachi, Ltd.

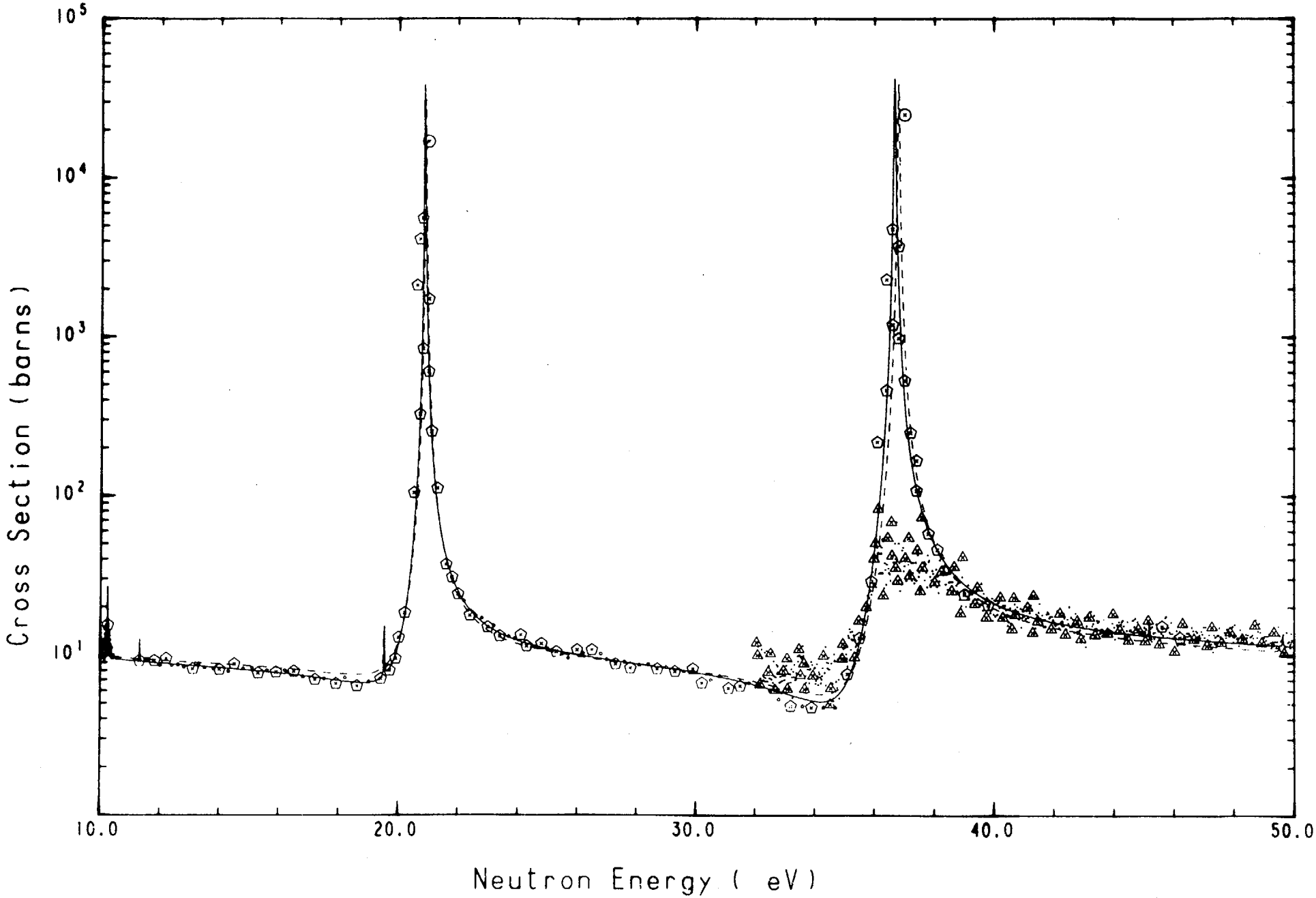

Fig. 1 Total cross section of ^{238}U. Solid curve shows the present result. Dashed curve is JENDL-1, and symbols are experimental values.

C. Radioisotope and Nuclear Engineering School

I-C-1 Reactor Neutron Capture Cross Section of 60.3-day Antimony-124

K. Nishimura, S. Ogawa and T. Tsutiya

A paper on this subject was submitted for publication to the Journal of Nuclear Science and Technology. It is now in press with an abstract as follows:

The radioactive nuclides ^{124}Sb ($T_{1/2}$=60.3 days) and ^{125}Sb ($T_{1/2}$=2.77 years) were produced from natural antimony by JRR-3 reactor irradiation of 283.5 hours through the single and double capture processes. After cooling of 3.50 years, the γ-ray spectrum of the antimony sample irradiated was measured by a 50 cc coaxial type Ge(Li) detector, and the photo-peak yield ratio of ^{125}Sb (E_γ=428 keV) to ^{124}Sb (E_γ=1.691 MeV) was obtained. By using a relation between this photo-peak yield ratio and the $^{124}Sb(n,\gamma)^{125}Sb$ cross section, the reactor neutron capture cross section of 60.3-day ^{124}Sb was obtained as $17.4^{+2.8}_{-2.5}$ barns. The thermal neutron flux at the position of antimony sample irradiated was estimated as $(4.92 \pm 0.38)\times10^{12}$ n/cm^{2}sec by measuring the 1.333-MeV photo-peak yield of ^{60}Co, which was activated by reactor irradiation of cobalt impurity contained in the antimony sample.

II. KYOTO UNIVERSITY

A. Institute of Atomic Energy

II-A-1 Mass Yield Curve of ^{232}Th Fission Induced by 80 MeV α-particle

T. Nishi, I. Fujiwara, N. Imanishi and Y. Horikawa*

Mass yield curve of ^{232}Th fission were measured at an incident α-particle energy of 80 MeV. The experimental method was similar to the one given in the previous report[1].

Cumulative or independent yields were measured for 23 nuclides ranging from A = 91 to 147. As shown in Fig. 1, the charge dispersion curve for the mass chains 131, 133 and 134 was composed of the yield of Sb, Te, I and Cs isotopes. The width σ of the charge dispersion curve was found out to be equal to 1.10. Assuming that the same charge dispersion curve at all mass chains and applying the UCD assumption referring to known data[2] of numbers of pre- and post-fission neutrons, we have deduced the values of chain yields from the measured cumulative yields. The results are shown in Fig. 2 along with the data for the ^{232}Th fission induced by 40 and 110 MeV α-particles[3,1].

Yields of the symmetric fission increase rapidly and the width of the mass yield curve becomes broader with increasing incident energy. The total fission cross section is obtained to be 2.2 b from the present mass yield curve and is in good agreement with data of 2.1 b obtained by using a solid state track detector[4].

---

* Present Address: Kansai Electric Power Co.

References:

1) T. Nishi et al., Progress Report NEANDC(J)-56/U (1978) 18, 22

2) T. C. Raginski et al. Phys. Rev. C4 (1971) 1361

3) M. Diksic et al. J. Inorg. Nucl. Chem. 36 (1976) 7;
E. Cheifetz and Z. Fraenkel, Phys. Rev. C2 (1970) 256

4) J. Ralarosky et al. Phys. Rev. C8 (1973) 2372

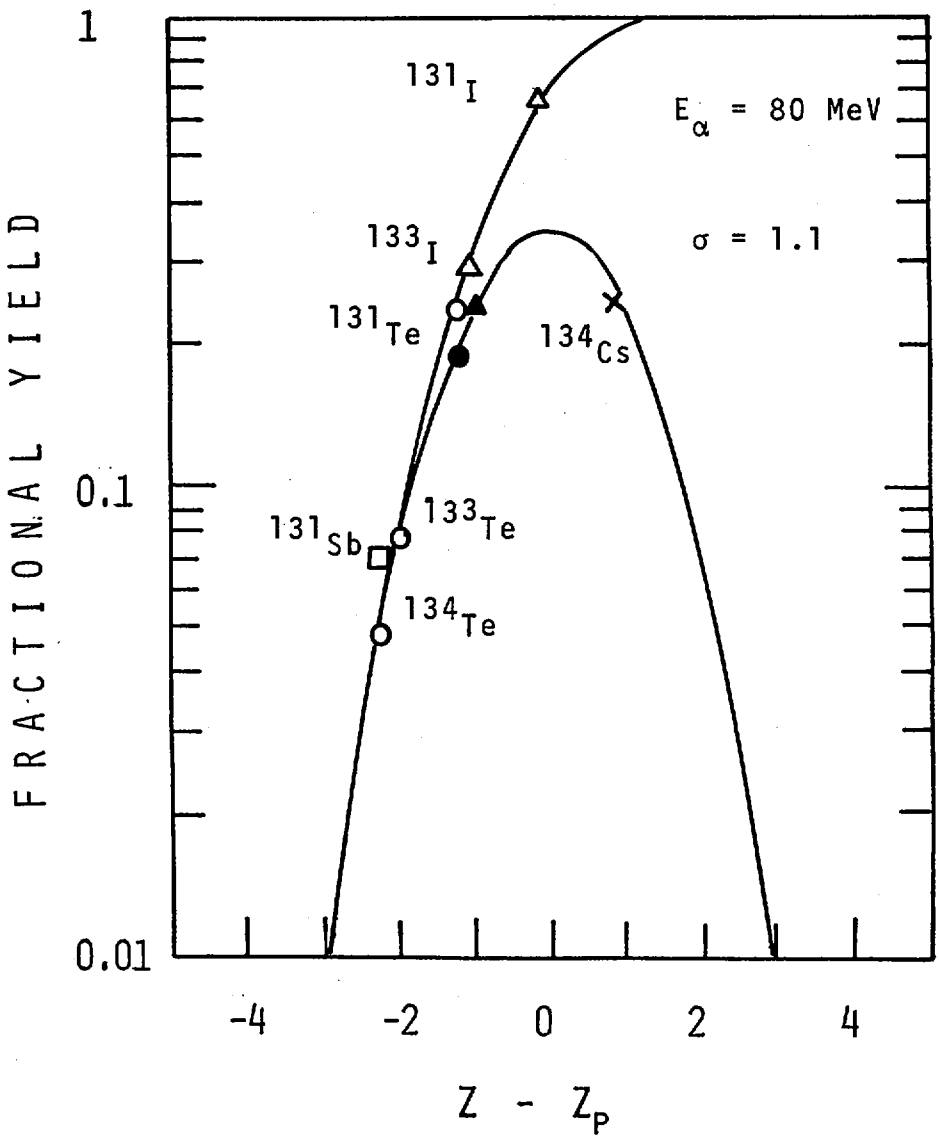

Fig. 1. Charge dispersion for fission products with A around 130.

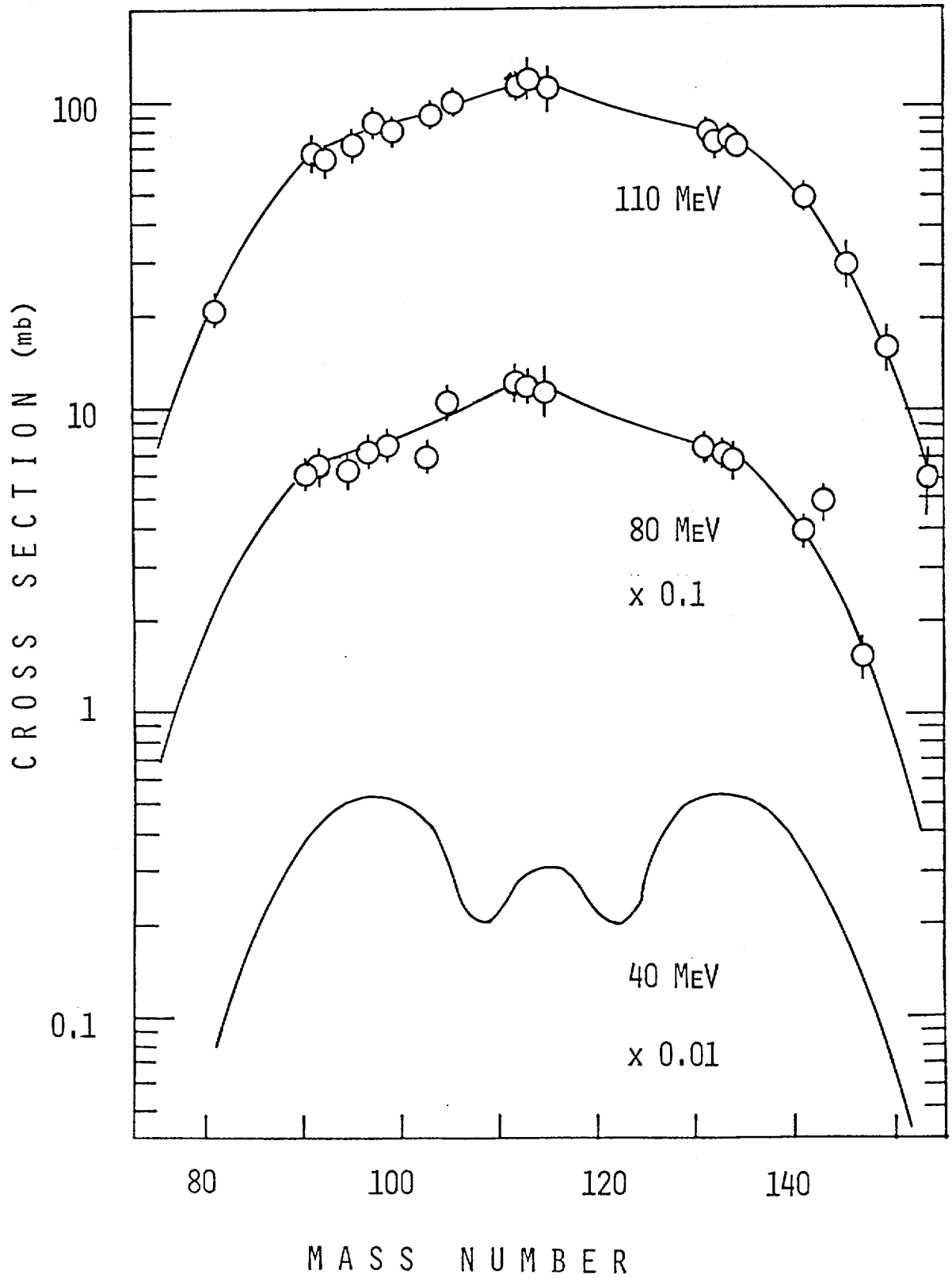

Fig. 2. Mass yield curve for α-particle induced fission of ^{232}Th.

B. Research Reactor Institute

II-B-1

ASSESSMENT OF GROUP CONSTANTS THROUGH MEASUREMENT AND ANALYSIS OF ENERGY SPECTRA OF NEUTRONS FROM A SLAB SCATTERER

Takamasa Mori, Katsuhei Kobayashi, Shu A. Hayashi,
Shuji Yamamoto, Itsuro Kimura and Hiroshi Nishihara*

Possibility to assess group constants through measurement and analysis of energy spectra of neutrons from a slab scatterer of reactor material has been studied. By this method we can save the quantity of sample material, as well as the case of the small sample pile with a reflector[1].

We have carried out the sensitivity analysis of group constants to neutron spectrum. The details of the analysis are described elsewhere[1]. The result for the polytetra fluoroethylene ($(CF_2)_n$, Teflon) slab is tabulated in Table 1, comparing with that for the 14-hedral $(CF_2)_n$ pile of 49 cm in mean radius. Similar results have been found for iron and lithium slabs.

Experimental arrangements and the results of the neutron spectra for the lithium slab and the Teflon slab are shown in Figs 1 and 2, where the calculated ones are also given.

---

* Department of Nuclear Engineering, Faculty of Engineering
Kyoto University, Yoshida-Honmachi, Sakyo-ku, Kyoto

The measured spectrum for the lithium slab agrees well with the calculated except around the dip at about 250 keV. On the other hand the agreement between the measured and the predicted is rather poorer for the Teflon slab. Similar tendency was also seen for the case of the Teflon pile[2].

A part of this work will be presented at the International Conference on Nuclear Cross Sections for Technology in Knoxville October 23, 1979.

References :

1) I. Kimura et al., J. Nucl. Sci. Technol., 15 (1978) 183.

2) I. Kimura et al., NEANDC(J)-56/U, INDC(JAP)-42/U (1978) p.37.

Table 1 Sensitivity coefficient of polytetra fluoroethylene slab

Varied flux group	Varied group const.	Sensitivity coefficient	
		scatterer	pile
8 (166 ~ 302 keV)	Σ_{T5}	-o.062	-0.732
	Σ_{T8}	-1.538	-1.385
	$\Sigma_{es(8\to8)}$	0.885	1.025
	$\Sigma_{is(8\to8)}$	0.208	-0.050
10 (41 ~ 87 keV)	Σ_{T5}	-0.037	-0.610
	Σ_{T10}	-2.169	-2.907
	$\Sigma_{es(10\to10)}$	1.620	2.461
	$\Sigma_{is(10\to10)}$	0.069	-0.054

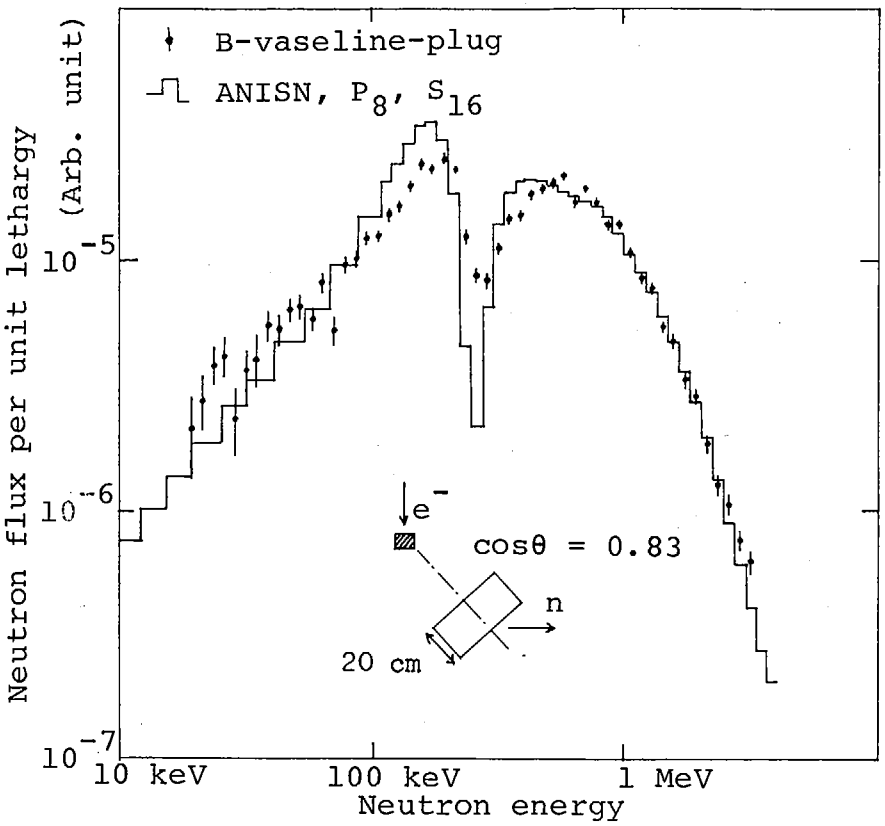

Fig. 1 Experimental arrangement and neutron spectra from lithium slab

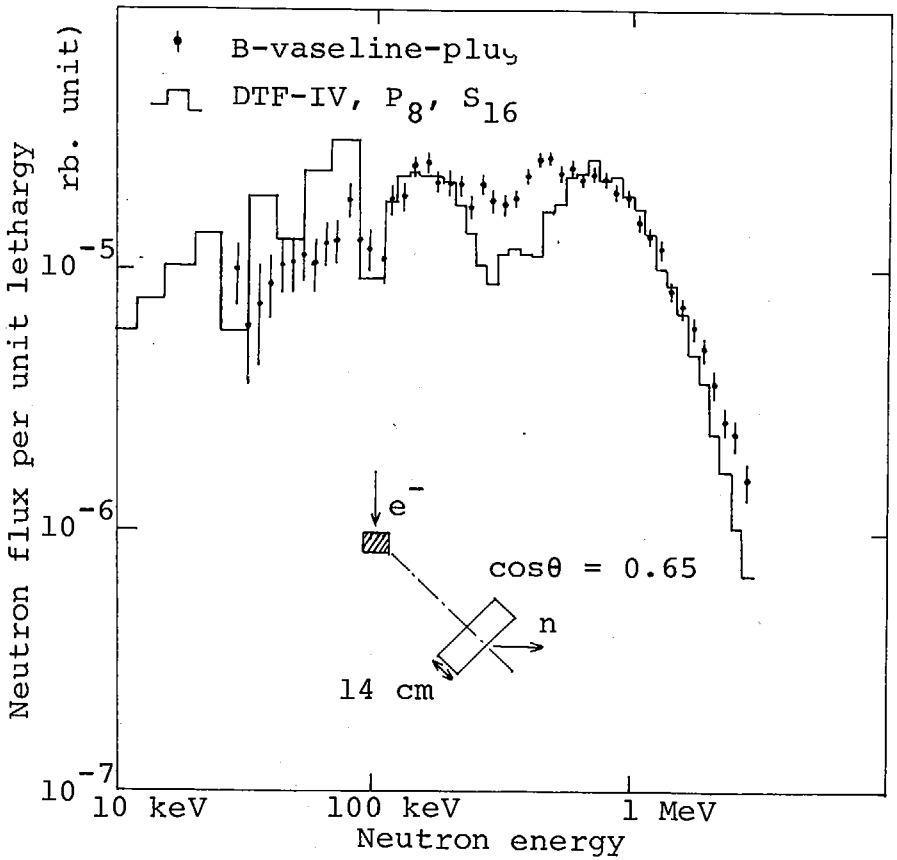

Fig. 2 Experimental arrangement and neutron spectra from Teflon slab

II-B-2

SPECTRUM OF NEUTRONS SCATTERED BY THORIUM SLAB

Katsuhei Kobayashi, Takamasa Mori and Itsuro Kimura

The energy spectrum of neutrons scattered by a slab of thorium metal was measured by the time-of-flight method with an electron linear accelerator and the result was compared with the theoretically calculated. The neutron spectrum in a pile of thoria was similarly measured before[1]. By the slab-scatterer method, we can save the quantity of sample material. In order to investigate the usefulness of this method, we have carried out the sensitivity analysis of group constants to neutron spectrum. The details of the analysis are described elsewhere[2]. The result for the thorium slab 5 cm thick is given in Table 1, comparing with that in the thoria pile which we investigated before. From this table, it can be seen that the sensitivity coefficients for both the thoria pile and the thorium slab are generally comparable in order.

Experimental arrangement and the result of the neutron spectrum are shown in Fig. 1, where the calculated ones are also given. Neutron source spectrum for the calculation was determined by the separate experimental runs with a ^{6}Li glass scintillator and a NE-213 scintillator, as shown in Fig. 2. The measured spectrum and the calculated ones by ANISN code (slab geometry) with group constants processed from ENDF/B-IV and DFT-IV code (shell geometry) with JAERI-FAST, Version-II, generally agree from about 15 keV to about

2 MeV.

A part of this work will be presented at the International Conference on Nuclear Cross Sections for Technology in Knoxville October 23, 1979.

References :

1) Hiroshi Nishihara et al., J. Nucl. Sci. Technol., 14 (1977) 426.

2) I. Kimura et al., ibid., 15 (1978) 183.

Table 1 Comparison of the sensitivity coefficient of thoria pile and thorium scatterer

Varied flux group	Varied group const.	Thoria pile	Thorium scatterer	
		R=30 cm r=15 cm, μ=0	μ=0.83 slab	shell
6 (400 ~ 800 keV)	Σ_{T3}	-0.042	-0.105	-0.117
	Σ_{T6}	-1.019	-1.614	-2.877
	$\Sigma_{es}(6\to6)$	1.190	1.682	2.884
	T3	-0.051	-0.194	-0.171
10 (21.5 ~ 46.5 keV)	Σ_{T6}	-0.121	-0.007	-0.074
	Σ_{T10}	-2.939	-3.217	-6.249
	$\Sigma_{es}(6\to6)$	0.198	0.007	0.081
	$\Sigma_{es}(10\to10)$	3.068	3.177	5.914

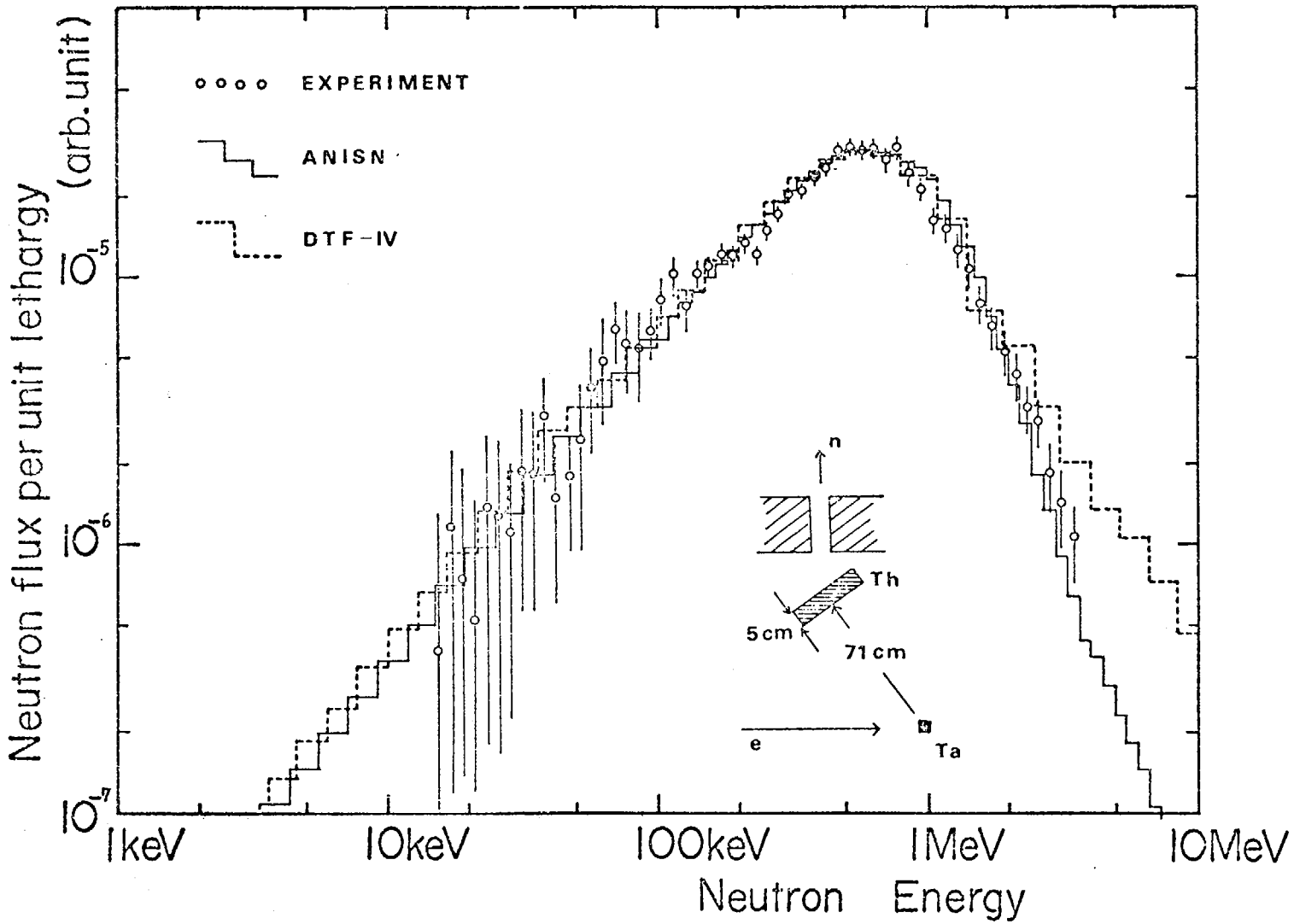

Fig. 1 Experimental arrangement and neutron spectra from thorium scatterer

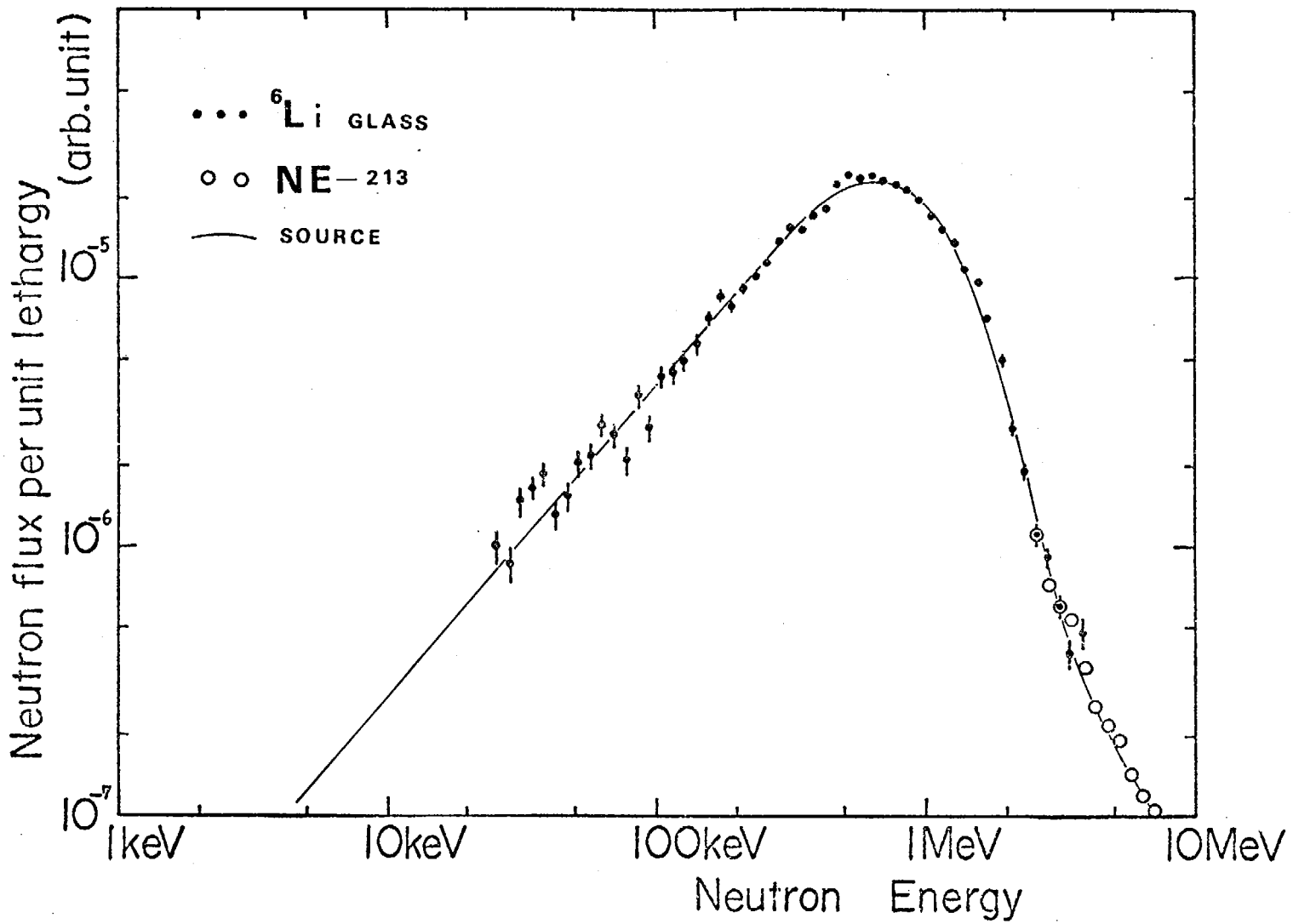

Fig. 2 Neutron source spectrum used for the transport calculation (solid line is the input for the calculation)

II-B-3

FISSION AVERAGED CROSS SECTIONS FOR THE $^{93}Nb(n,n')^{93m}Nb$ AND $^{199}Hg(n,n')^{199m}Hg$ REACTIONS

Katsuhei Kobayashi and Itsuro Kimura

Since the $^{93}Nb(n,n')^{93m}Nb$ reaction has advantages of low threshold energy ($E_{eff} \simeq 1$ MeV) and a long half life ($\sim$14 years), a large amount of attention has been given to the use of niobium in a fast neutron fluence monitor. The $^{199}Hg(n,n')^{199m}Hg$ reaction also has a low threshold energy ($\sim$500 keV). A large ^{235}U fission plate and the core of a fast reactor, YAYOI, were used to measure the fission averaged cross sections for these reactions. Experimental procedures are almost the same as in the previous experiment[1]. Neutron fluence during irradiation was monitored by the $^{27}Al(n,\alpha)^{24}Na$, $^{58}Ni(n,p)^{58}Co$ and $^{115}In(n,n')^{115m}In$ reactions as in the previous measurement[1].

The niobium sample used was a film about 0.01 mm thick ($\sim$10 mg/cm^2). The 16.6 keV and 18.7 keV X-rays from ^{93m}Nb were measured by a NaI(Tl) scintillator 3 mm thick and 2.5 cm in diameter with a Be-window. The mercury sample was powder of Hg_2SO_4, pressed into a pellet of 10 mm diameter and about 3.5 mm thick ($\sim$1.5 g). The gamma-rays of 158 keV and 375 keV from ^{199m}Hg were measured with a Ge(Li) detector. Detection efficiency of these detectors was calibrated with the standard gamma-ray sources of ^{54}Mn, ^{57}Co, ^{60}Co, ^{133}Ba, ^{137}Cs, ^{241}Am, etc. which had been purchased from the Radiochemical Centre.

Fission averaged cross section for the $^{93}Nb(n,n')^{93m}Nb$ reaction is shown in Table 1, as well as previously reported values. The main problem in the cross section measurement is due to the uncertainties of the half life and the branching ratio for the decay of the ^{93m}Nb state.

Induced activities of ^{199m}Hg produced by the $^{198}Hg(n,\gamma)$ and $^{200}Hg(n,2n)$ reactions compete with those of the $^{199}Hg(n,n')^{199m}Hg$ reaction. In a thermal reactor, contamination by the (n,γ) reaction would be up to about 15 % for the (n,n') reaction. However, with a fission plate and in the YAYOI core, the contamination is less than 1 %, because the thermal neutron flux is much lower than the fast neutron flux. We also calculated the average cross section for the (n,2n) reaction using the statistical model by Pearlstein[2]. In the case of the $^{200}Hg(n,2n)^{199m}Hg$ reaction, the calculated value was normalized to the average data at 14 MeV measured by Hankla[3] and Temperley[4]. Vlasov showed the effective cross section was 480 mb for E_{eff}=1.9 MeV[5]. The fission averaged cross sections for the $^{199}Hg(n,n')^{199m}Hg$ reaction are shown in Table 2. Present values with a fission plate and in the YAYOI core are in good agreement with each other.

References :

1) I. Kimura et al., Proc. of the 1st ASTM-EURATOM Symp. on Reactor Dosimetry, Petten (1975) EUR 5667 e/f, Part II, p.142.

2) S. Pearlstein, Nucl. Sci. Eng., 23 (1965) 238.

3) A. K. Hankla et al., Nucl. Phys., A180 (1972) 157.

4) J. K. Temperley, Phys. Rev., 178 (1969) 1904.

5) M. F. Vlasov, Neutron Cross Sections for Reactor Dosimetry, IAEA-208, Vol.II (1976) p.353.

Table 1 Fission averaged cross section for the $^{93}Nb(n,n')^{93m}Nb$ reaction

CROSS SECTION(mb)	HALF LIFE(y)	REFERENCE
122 ± 9	13.6	Present(fission plate)
97 (calc.)	11.4	Hegedus
97 ± 35	11.4	Hegedus($\bar{\sigma}_{Rh}$=595 mb)
102 ± 30	11.4	Hegedus($\bar{\sigma}_{Ni}$=101 mb)
87 ± 14	16.4	NUREG/CP-0004, p.904

Table 2 Fission averaged cross section for the $^{199}Hg(n,n')^{199m}Hg$ reaction

CROSS SECTION(mb)		REFERENCE
285 ± 27	(158 keV)	Present(fission plate)
278 ± 19	(375 keV)	Present(fission plate)
279 ± 26	(158 keV)	Present(YAYOI core)
273 ± 19	(375 keV)	Present(YAYOI core)
σ_{eff} = 480 mb for E_{eff}=1.9 MeV		Vlasov
3.03 mb for $^{200}Hg(n,2n)^{199}Hg$		Present calc.
1.12 mb for $^{200}Hg(n,2n)^{199m}Hg$		Present calc.

II-B-4

MEASUREMENT OF AVERAGE CROSS SECTION FOR ^{235}U AND ^{252}Cf FISSION NEUTRONS

Katsuhei Kobayashi and Itsuro Kimura

Precise knowledge of the average cross sections measured in a standard neutron field is of much importance from the standpoints of eliminating the discrepancies among the average cross sections and of evaluating the energy dependent cross sections. In the present work, the average cross sections for both the neutrons from the thermal neutron induced fission of ^{235}U and those from the spontaneous fission of ^{252}Cf have been measured and compared with each other.

Average cross sections for the ^{235}U fission neutrons have been measured with a large fission plate and in the core of the fast source reactor, YAYOI[1]. The experimental procedures are almost the same as in previous work[2]. The beta-ray from ^{32}P induced by the $^{32}S(n,p)$ reaction has been measured with a liquid scintillator, whose detection efficiency had been calibrated by the standard ^{32}P source made at the Radiochemical Centre. Present results of the fission averaged cross sections are shown in Table 1. Values obtained with the plate and in the YAYOI core are in good agreement and they also agree well with those of the previous work[2] within the experimental error.

The needle-type californium source containing about 500 μg of ^{252}Cf ($\sim 1 \times 10^9$ n/sec) was implanted in a small capsule of 0.08 inch inner diameter. Irradiations were carried out

at the distance of 6 cm from the source. It has been found that the effect of the room-returned neutrons is negrigibly small. Neutron flux at the irradiation sample was monitored by using the $^{27}Al(n,\alpha)^{24}Na$ reaction, whose average cross section was normalized to 1.00 mb which is a recent value obtained by Mannhart[3]. The present results are summarized in Table 2. The average cross section for the $^{32}S(n,p)^{32}P$ reaction has not measured before. The present values are close to most of the recent results by Mannhart[3] and Dezsö[4].

We calculated the ratio $\bar{\sigma}(^{252}Cf)/\bar{\sigma}(^{235}U)$ of the average cross section from the values in Table 1 and Table 2, and those we had obtained before[2]. Figure 1 shows the ratio versus the effective threshold energy, E_{eff}, respectively. The solid line was obtained from the following relation :

$$\bar{\sigma}(^{252}Cf)/\bar{\sigma}(^{235}U) \text{ ratio} = \int_{E_{eff}}^{\infty} \chi_{252}(E)\,dE \Big/ \int_{E_{eff}}^{\infty} \chi_{235}(E)\,dE$$

where $\chi_{252}(E)=0.6672\sqrt{E}\,\exp(-1.5E/2.13)$,

$\chi_{235}(E)=0.7501\sqrt{E}\,\exp(-1.5E/1.97)$.

The plotted data generally agree well each other and with the solid curve. Effective threshold energy dependence of the $\bar{\sigma}(^{252}Cf)/\bar{\sigma}(^{235}U)$ ratio is useful for comparing the values of the average cross section or evaluating the effective threshold energy.

References :

1) I. Kimura et al., Neutron Cross Sections for Reactor Dosimetry, IAEA-208, Vol.II (1976) p.265.

2) I. Kimura et al., Proc. of the 1st ASTM-EURATOM Symp. on Reactor Dosimetry, Petten (1975) EUR 5667 e/f, Part II, p.142.

3) W. Mannhart, PTB-FMRB-72 (1978), and Nucl. Sci. Eng., 69 (1979) 333.

4) Z. Dezsö et al., INDC(NDS)-103/M (1979) p.176.

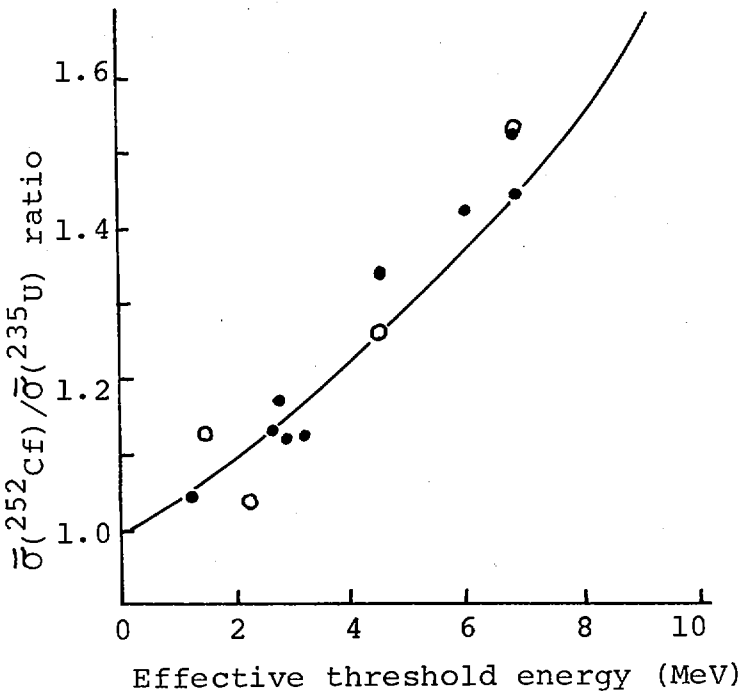

Fig. 1 $\bar{\sigma}(^{252}Cf)/\bar{\sigma}(^{235}U)$ ratio versus the effective threshold energy. Solid line is our present calculation. Data with ● mark have been obtained from Table 1 and Table 2. Data with o mark have been obtained from Table 2 and Ref. 2)

Table 1 Average cross sections for ^{235}U fission neutrons

REACTION	^{235}U plate $\bar{\sigma}$ (mb)	YAYOI core $\bar{\sigma}$ (mb)
$^{24}Mg(n,p)^{24}Na$	1.38 ± 0.07	1.35 ± 0.07
$^{27}Al(n,p)^{27}Mg$	3.65 ± 0.20	3.64 ± 0.21
$^{31}P(n,p)^{31}Si$	33.5 ± 2.0	34.0 ± 2.5
$^{32}S(n,p)^{32}P$	64.7 ± 3.8	- - - - -
$^{52}Cr(n,p)^{52}V$	1.06 ± 0.11	1.07 ± 0.07
$^{53}Cr(n,p)^{53}V$	- - - - -	0.306 ± 0.027
$^{54}Fe(n,p)^{54}Mn$	78.1 ± 3.7	76.7 ± 4.6
$^{56}Fe(n,p)^{56}Mn$	1.02 ± 0.05	0.997 ± 0.06
$^{59}Co(n,\alpha)^{56}Mn$	- - - - -	0.143 ± 0.008
$^{113}In(n,n')^{113m}In$	- - - - -	155 ± 13
$^{197}Au(n,2n)^{196}Au$	3.00 ± 0.16	3.09 ± 0.17

Table 2 Average cross sections for ^{252}Cf spontaneous fission neutrons, when the $^{27}Al(n,\alpha)^{24}Na$ reaction cross section was normalized to 1.00 mb

REACTION	CROSS SECTION(mb)
$^{24}Mg(n,p)^{24}Na$	1.95 ± 0.12
$^{27}Al(n,p)^{27}Mg$	4.90 ± 0.32
$^{32}S(n,p)^{32}P$	72.4 ± 4.8
$^{51}V(n,p)^{51}Ti$	0.71 ± 0.11
$^{54}Fe(n,p)^{54}Mn$	87.0 ± 5.4
$^{56}Fe(n,p)^{56}Mn$	1.43 ± 0.08
$^{58}Ni(n,p)^{58}Co$	119 ± 6
$^{59}Co(n,\alpha)^{56}Mn$	0.217 ± 0.015
$^{64}Zn(n,p)^{64}Cu$	41.7 ± 2.7
$^{113}In(n,n')^{113m}In$	170 ± 10
$^{115}In(n,n')^{115m}In$	201 ± 10
$^{197}Au(n,2n)^{196}Au$	5.25 ± 0.31

III. KYUSHU UNIVERSITY

A. Department of Nuclear Engineering

Faculty of Engineering

III-A-1 Multi-Step-Direct-Reaction Analysis of 14 MeV-Neutron Reaction (I) (n,n') Reaction

K. Fukuda, M. Matoba and I. Kumabe

The pre-equilibrium model has succeeded in reproducing the high energy tail of angle-integrated energy spectrum in the reactions by neutrons, protons and alpha-particles in the energy range of 10~60 MeV. This model, however, can not predict the angular distribution of emitted particles because the effect of angular momentum is not taken into account.

Recently Tamura et al.[1,2] proposed a multi-step direct reaction (MSDR) theory to describe reactions that leave the residual nucleus in a highly excited continuum state. They demonstrated the capability of this approach by succeessfully fitting spectra of the (p,p') and (p,α) reactions at 65 MeV.

In the present report we apply the MSDR analysis to the 14 MeV (n,n') reaction with some improvements. Since Tamura et al. have analyzed the data in the excitation energy higher than 10 MeV, they have assumed that the target is an even-even 0^+ nucleus with a doubly closed (sub-) shell configuration for simplicity of presentation. Since in our case the data in the excitation energies between 3 and 10 MeV are analyzed, following three effects which are expected to affect the low-lying continuum state are taken into account.

1) extension from a completely filled shell to the partly filled shells.
2) pairing correlation

3) difference between the strengths of n-p and n-n interactions Moreover renormalization of the absolute cross sections was performed using the strength of the low-lying 2^+ states which are well known.

We carried out the MSDR analysis for the 14.1 MeV (n,n') reactions on Fe, Cu, As, Nb and Ag with the improvements mentioned above. The experimental data have been measured[3)] by two of the authors and others. We first consider a one-step process only. For an example a comparison of the experimental to calculated energy spectrum for Ag is shown in Fig. 1. The histogram shows the energy spectrum calculated by MSDR process. The results of the pre-equilibrium calculation are also shown in this figure. Since the one-step direct reaction is considered to correspond to the pre-equilibrium process for n=3, the histogram should be compared with the pre-equilibrium calculation for n=3. The histogram is in fairly good agreement with the pre-equilibrium calculation for n=3 for both the shape and the absolute value.

Comparisons of the experimental and calculated angular distributions are shown in Fig. 2. In Fig. 2 there are presented angular distributions of the cross sections integrated over 4 MeV energy bins in En'=4~8 MeV. The experimental angular distributions in this figure were obtained by the subtraction of the compound contribution from the total experimental angular distributions. The calculated angular distributions are the results with the one-step process only. The solid curves present the absolute values, while the dashed curves present the fit to the experimental data.

Numerical calculations for two-step process were made for En'=5.5~6.5 MeV in ^{93}Nb. The results are shown in Fig. 3. The dot-dashed curve presents the two-step cross sections. It was seen in this figure that the two-step cross sections are about 10 % of the one-step cross sections.

References

1) T. Tamura, T. Udagawa, D.H. Feng and K.K. Kan : Phys. Lett. 66B (1977) 109.

2) T. Tamura and T. Udagawa : Phys. Lett. 71B (1977) 273.

3) Y. Irie, M. Hyakutake, M. Matoba, I. Kumabe and M. Sonoda : Mem. Fac. Eng. Kyushu Univ. 37 (1977) 19.

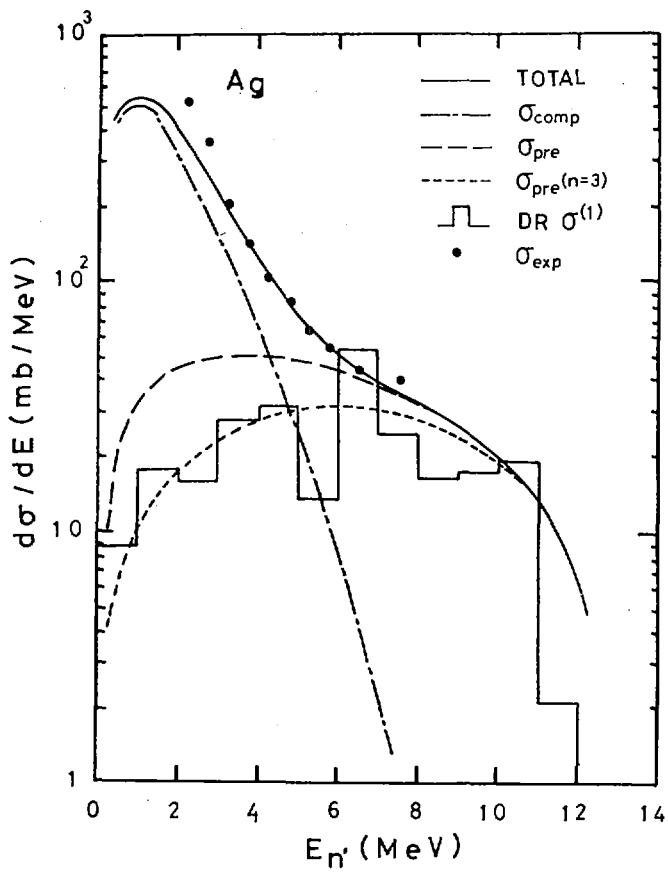

Fig. 1 Comparison of experimental to calculated energy spectrum. Histogram shows the present MSDR calculation.

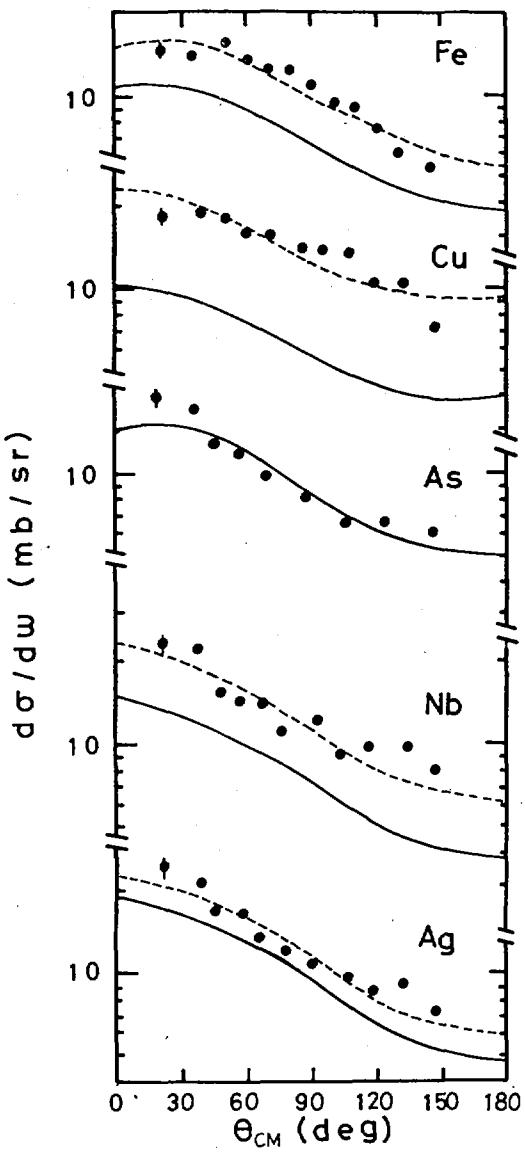

Fig. 2 Comparison of calculated angular distributions with experimental ones of cross sections integrated over 4 MeV bins in En'=4~8 MeV.

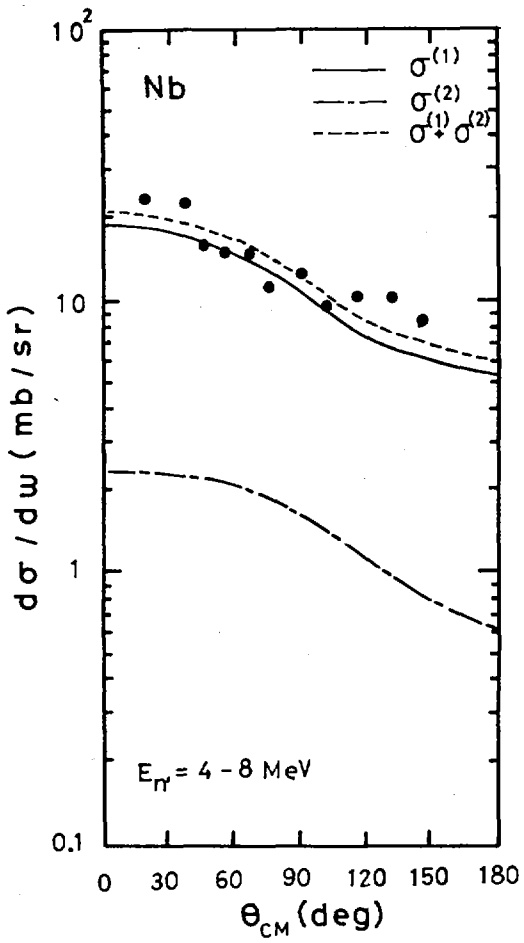

Fig. 3 Comparison of experimental to calculated angular distributions. Solid and dot-dashed curves present the one-step and two-step cross sections, respectively.

III-A-2

Multi-Step-Direct-Reaction Analysis of 14 MeV-Neutron Reaction (II) (n,p) Reaction

K. Fukuda, M. Matoba and I. Kumabe

In the preceding report, we have reported that the application of the multi-step-direct-reaction theory[1] to 14 MeV-neutron reaction is demonstrated by successfully fitting continuum energy and angular distributions of 14 MeV (n,n') reaction. In this report we extend the MSDR analysis to 14 MeV (n,p) reaction.

We consider a one-step process only. We carried out the MSDR analysis for the 14.1 MeV (n,p) reaction on ^{115}In with the similar manner to the preceding report. In the present calculation the derivative of Wood-Saxon optical potential was used as a form factor.

A comparison of the calculated energy spectrum with experiment[2] for ^{115}In is shown in Fig. 1. The histogram shows the energy spectrum calculated by MSDR process. The results of the pre-equilibrium calculation are also shown in this figure. The histogram is in fairly good agreement with the pre-equilibrium calculation for n=3 for both the shape and the absolute value.

A comparison of the calculated angular distribution with the experiment for ^{115}In is shown in Fig. 2. The angular distribution of the cross sections integrated over all energies is shown in this figure. The calculated angular distribution is in good agreement with the experimental one for both the shape and the absolute value.

References

1) T. Tamura, T. Udagawa, D.H. Feng and K.K. Kan : Phys. Lett. 66B (1977) 109.

2) J. Niidome, M. Hyakutake, N. Koori, I. Kumabe and M. Matoba : Nucl. Phys. A245 (1975) 509.

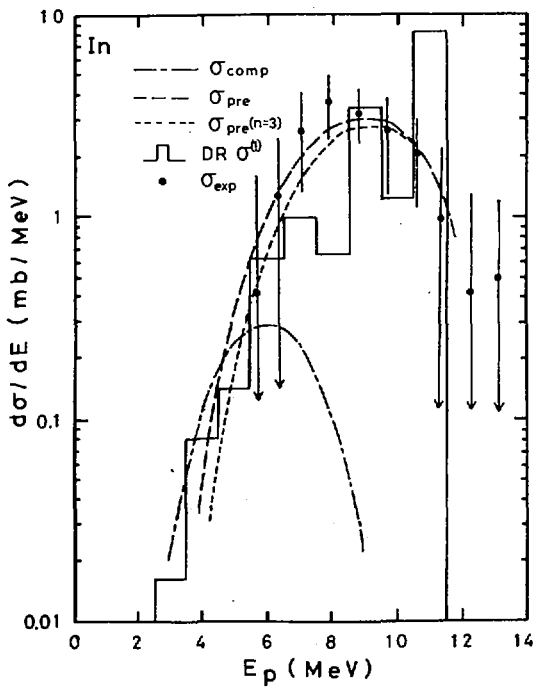

Fig. 1 Comparison of experimental to calculated energy spectrum for In. Histogram shows the present MSDR calculation.

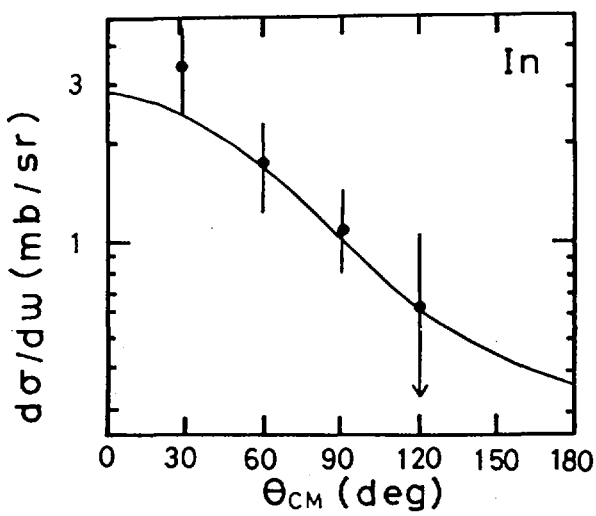

Fig. 2 Comparison of calculated angular distribution with experimental one of cross sections integrated over all energies.

III-A-3

Analysis of Total (n,p) Cross Sections with Pre-Equilibrium model and Effective Q-Values

I. Kumabe

Recently, we have analyzed[1)] the 14 MeV (n,p) cross sections in terms of the pre-equilibrium exciton model, and found gross mass-number dependence of the ratios of the experimental to calculated cross sections $\sigma_{exp}/\sigma_{cal}$. We also found the correlation between the gross mass-number dependence of $\sigma_{exp}/\sigma_{cal}$ and $a/\bar{a}$, where a is the level density parameter and $\bar{a}$ the mean level density parameter which is equal to A/7.5.

In trying to obtain a better agreement between the experimental and calculated cross sections, we have attempted to correct σ_{cal} by $(a/\bar{a})^2$. The deviation of the values of $(\sigma_{exp}/\sigma_{cal})/(a/\bar{a})^2$ from 1.0 were considerably reduced.

In this report the result of the analysis using an effective Q-value is reported.

Pairing correlations which depress the ground state are generally assumed to become negligible at excitation energies of 4~10 MeV (the energies important for pre-equilibrium proton emission induced by 14 MeV neutrons). Therefore level densities corresponding to one-particle one-hole states are calculated using excitation energies [U-δ, (δ=-P)] measured from fictitious ground states whose masses show no odd-even fluctuations. If the depression of the ground state by a closed shell -S is treated in the same way, and if shells have negligible influence on level densities at the excitation energies mentioned above, one should use δ=-P-S .

Thus we define the quantity $Q'_{np}=Q_{np}-\delta_r+\delta_t$ as the effective Q-value for the (n,p) reaction at excitation energies for which pairing and shell correlations do not affect. Here δ_t and δ_r are δ-values for the target and

residual nuclei, respectively. If pairing and shell energies are taken from Cameron and Elkin[2], the effective Q-values do not vary smoothly with the mass number A. Therefore we used the effective Q-value, derived from a semi-empirical mass formula[3,4] whose parameters are smooth functions of mass number and free of fluctuations near closed shells.

The ratios of the experimental to theoretical cross sections calculated using true Q-values are plotted in the upper part of Fig. 1. In this figure gross mass-number dependence of the ratios is seen. The ratios of the experimental to theoretical cross sections calculated using the effective Q-values are plotted in the lower part of Fig. 1. The deviations of the points from 1.0 are remarkably reduced.

Similar analysis for the 14 MeV (n,α) reaction is now in process.

References :

1) I. Kumabe, M. Hyakutake and Y. Fujino : J. Nucl. Sci. Technol. 14 (1977) 73

2) A.G.W. Cameron and R.M. Elkin : Can. J. Phys. 43 (1965) 1288

3) J.W. Dewdney : Nucl. Phys. 43 (1963) 303

4) H.L. Pai, R.L. Clarke and W.G. Cross : Nucl. Phys. A164 (1971) 526.

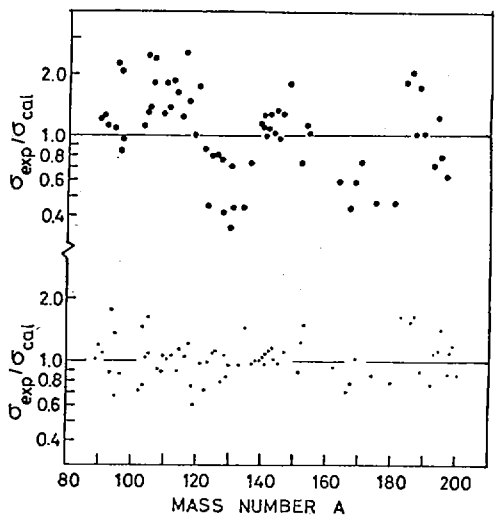

Fig. 1 Ratios of experimental to theoretical cross sections calculated using true Q-values and using effective Q-values plotted in upper and lower parts, respectively.

III-A-4

Activation Cross Sections on Ti, Mn, Cu, Zn, Sr, Y, Cd, In and Te for 14.6 MeV neutrons

K. Kayashima, A. Nagao and I. Kumabe

Many workers have measured the activation cross sections for 14 MeV neutrons. However relatively a few data have been reported for the reactions leading to the long-lived nuclei. Therefore we have measured the reaction cross sections leading to the long-lived nuclei on Ti, Mn, Cu, Zn, Sr, Y, Cd, In and Te for 14.6 MeV neutrons.

In the present experiment 0.3~1.5 g of samples covered with Cd-plates of 0.5 mm thick were bombarded. Thin monitor Aℓ-foils of about 50 mg were placed in the front and back of samples. After cooling period of 14~30 days, long-lived activities were measured with a 60 cm^3 coaxial Ge(Li) detector shielded with iron-plates of 30 mm thick and lead-plates of 70 mm thick. By using this shield, background was reduced by a factor of 40.

Tables 1 and 2 show the results obtained from the present work.

Table 1 Cross sections for (n,p) and (n,α) reactions with 14.6 MeV neutrons

REACTION	$T_{1/2}$		E_γ(KeV)	η(%)	σ(mb)
$^{46}Ti(n,p)\,^{46}Sc$	83.8	d	1120.5	100	230 ± 50
$^{48}Ti(n,p)\,^{48}Sc$	43.7	h	983.3	100	55.0 ± 5.0
$^{86}Sr(n,p)\,^{86}Rb$	18.65	d	1076.6	8.76	34.9 ± 8.4
$^{110}Cd(n,p)\,^{110m}Ag$	253	d	657.7	94.4	27.1 ± 4.7
$^{115}In(n,p)\,^{115g}Cd$	53.5	h	527.9	27.5	5.1 ± 0.8
$^{122}Te(n,p)\,^{122}Sb$	2.72	d	564.1	63	14.5 ± 3.1
$^{124}Te(n,p)\,^{124g}Sb$	60.3	d	602.7	98.1	8.4 ± 1.1
$^{50}Ti(n,\alpha)\,^{47}Ca$	4.54	d	1296.8	75	11.5 ± 5.3
$^{63}Cu(n,\alpha)\,^{60g}Co$	5.272	y	1332.5	100.00	50.4 ± 5.7
$^{89}Y\,(n,\alpha)\,^{86g}Rb$	18.65	d	1076.6	8.76	4.8 ± 2.1
$^{128}Te(n,\alpha)\,^{125g}Sn$	9.65	d	1066.6	9	0.78± 0.45

η= Intensity of γ-rays per disintegration

Table 2 Cross sections for (n,2n) reaction with 14.6 MeV neutrons

REACTION	$T_{1/2}$	E_γ(keV)	η(%)	σ(mb)
$^{55}Mn(n,2n)\ ^{54}Mn$	312.5 d	834.8	100	884 ± 58
$^{66}Zn(n,2n)\ ^{65}Zn$	243.7 d	1115.5	49.8	588 ± 65
$^{86}Sr(n,2n)\ ^{85g}Sr$	65.2 d	514	99.3	918 ± 74
$^{89}Y\ (n,2n)\ ^{88}Y$	106.6 d	898	93	962 ± 78
$^{116}Cd(n,2n)^{115m}Cd$	44.6 d	934.1	1.9	799 ± 82
$^{116}Cd(n,2n)^{115g}Cd$	53.5 h	527.9	27.5	842 ± 70
$^{115}In(n,2n)^{114m}In$	49.51 d	189.9	17.7	1331 ± 110
$^{120}Te(n,2n)^{119m}Te$	4.7 d	1212.6	67	673 ± 74
$^{120}Te(n,2n)^{119g}Te$	16 h	644.1	88	679 ± 121
$^{122}Te(n,2n)^{121m}Te$	150 d	212.2	81	906 ± 73
$^{122}Te(n,2n)^{121g}Te$	17 d	573.1	79.1	721 ± 60
$^{124}Te(n,2n)^{123m}Te$	119.7 d	159	83.5	863 ± 69
$^{130}Te(n,2n)^{129m}Te$	33.4 d	696	2.9	1203 ± 97

III-A-5

Evaluation of Neutron Cross Sections of Thorium-232

Takaaki OHSAWA and Masao OHTA

The neutron cross sections of thorium-232 were evaluated in the energy range from thermal to 20 MeV with the aim of providing consistent set of data to be stored in the Japanese Evaluated Nuclear Data Library, Version-2 (JENDL-2). This work revises our previous evaluation registered in JENDL-1.

a) Total Cross Section

Our previous evaluation of the total cross section was based on the data of Foster et al.[1] and Fasoli et al.[2] in the energy range between 1.5 and 5.0 MeV, and those of Uttley et al.[3] below 1.5 MeV. Recent measurement of Whalen and Smith [4] provided data that agree fairly well with JENDL-1 evaluation. Thus previous evaluation was adopted without essential change, except partial correction made at lower energies to be sure that evaluated curve should pass through the recent data point of Kobayashi et al.[5] at 24 keV.

b) Radiative Capture Cross Section

In order to eliminate the ambiguities relevant to the reference data, the ratio data were resorted to renormalization by means of unified reference data: Matsunobu's new evaluation[6] for $^{235}U(n,f)$, and Kanda's[7] for $^{238}U(n,\gamma)$.

Marked aspect in the trend of measurements of radiative capture cross section is that experiments performed after 1976 tend to yield systematically lower values than ENDF/B-IV and JENDL-1 evaluations in the region 0.5-1.0 MeV. In the present evaluation, we relied primarily on the data of Kobayashi et al.[8]

in the region 3.5 - 450 keV, and those of Lindner et al.[9] above 450 keV.

c) Fission Cross Section

Extensive measurement of fission cross section of ^{232}Th relative to that of ^{235}U was recently made by Behrens et al.[10] The cross section values obtained by multiplying them with Matsunobu's evaluation for $^{235}U(n,f)$ were found to give data 10% higher than JENDL-1 evaluation. This new data improved agreement between calculated and measured values of the fission-neutron spectrum averaged cross section.

d) Inelastic Scattering Cross Section

Existing measured data are sparse and far from enabling evaluation on the basis of the exprimental information only. We thus resorted to theoretical calculation based on the Hauser-Feshbach formalism combined with Moldauer's corrections. The excitation functions for the 1st, 2nd and 3rd excited states were corrected so as to fit the experimental points for each level. This correction takes approximately into account the effect of direct excitation of collective modes of the deformed nucleus.

e) (n,2n) and (n,3n) Reaction Cross Sections

In the conventional prescription of the (n,2n) cross section, σ_{2n} is factored into three parts:

$$\sigma_{2n} = \sigma_{ne} \times (\sigma_{nM}/\sigma_{ne}) \times (\sigma_{2n}/\sigma_{nM})$$

Pearlstein used for σ_{ne} and σ_{nM}/σ_{ne} empirical formulas of Flerov-Talyzin[11] and Barr et al.[12], respectively. In the present

work, we instead used Segev-Caner's method[13] for σ_{2n}/σ_{nM}, and Kondaiah et al.'s formula[14] for σ_{nM}/σ_{ne}. Nonelastic cross section σ_{ne} was obtained by subtracting fission cross section from the reaction cross section σ_R calculated by means of the optical model.

f) Elastic Scattering Cross Section

Experimental data are very sparse, thus elastic scattering cross section was calculated from $\sigma_{el}=\sigma_t-(\sigma_{in}+\sigma\ +\sigma_f+\sigma_{2n}+\sigma_{3n})$. The values thus obtained were in good agreement with measurements within the uncertainty of the data.

The cross sections obtained in this work are shown in Fig.1 together with our earlier evaluation stored in JENDL-1.

References:

1) D.G.Foster et al., Private communication (1967); see also Phys. Rev. C3,576 (1971)
2) U.Fasoli et al., Nucl.Phys. A151,369 (1970)
3) C.A.Uttley et al., EANDC Conf. on the TOF-Methods,Saclay (1961) p.109; Ist Conf. on Nucl. Data for Reactors, Paris (1966)
4) J.F.Whalen and A.B.Smith, Nucl. Sci. Eng. 67, 129 (1978)
5) K.Kobayashi et al., Nucl. Sci.Eng. 65, 347 (1978)
6) H.Matsunobu et al., Proc. of the 1978 seminar on Nuclear Data, JAERI-M-8163, p.209.
7) Y.Kanda, Private communication, (1973)
8) K.Kobayashi et al., Fall Meeting of the Atom. Ener. Soc. Japan D27 (1978)

9) M.Lindner et al., Nucl. Sci. Eng. 59, 389 (1976)

10) J.W.Behrens et al., Phys. Lett. 69B,278 (1977); UCID-17442 (1977)

11) N.N.Flerov et al., J. Nucl. Ener. 4, 529 (1957)

12) D.W.Barr et al., Phys. Rev. 123, 859 (1961)

13) M.Segev et al., Ann. Nucl. Ener. 5, 239 (1978)

14) E.Kondaiah et al., J.Phys. A7, 1457 (1974)

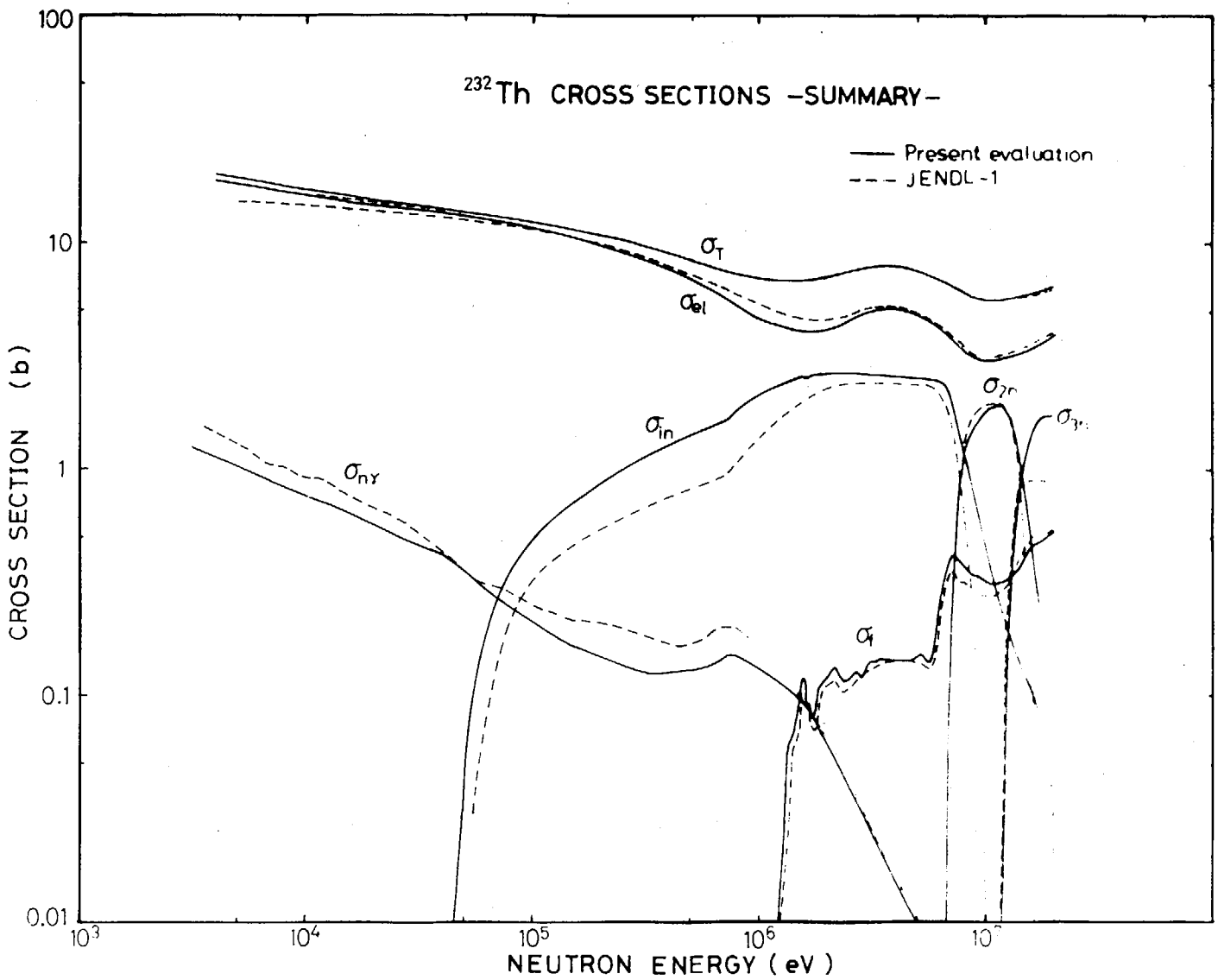

Fig.1 Summary of evaluated neutron cross sections of Th-232 compared with JENDL-1 evaluation.

B. Graduate School of Engineering Sciences

III-B-1 Neutron Capture Cross Section Measurements of ^{133}Cs

T.Kawano, Y.Kanda, A.Asami*, N.Nakajima*, Y.Kawarasaki* and Y.Furuta*

The neutron capture cross section of ^{133}Cs have been measured in the energy range between 5 and 300 keV with a large liquid scintillator, 3,500 l volume, on a 52 m flight path of the Japan Atomic Energy Research Institute 120-MeV linac neutron time-of-flight spectrometer. The neutron flux are monitored with a ^{6}Li-glass scintillation counter at lower neutron energies or a ^{10}B-NaI(Tl) scintillation counter at higher energies. Samples are powder of caesium carbonate with the thickness of 5.56×10^{-3} atoms/barns.

Attention is particularly paid to background determination in order to obtain accurate cross section data. Eight kinds of time-of-flight spectra of incident neutrons and neutron captures are measured for the combination of the detectors, the samples and the blank-samples-in or -out. Data analysis is in progress.

---

* Linac Laboratory, Division of Physics, Japan Atomic Energy Research Insitute

III-B-2

Evaluation of Neutron Nuclear Data for ^{237}Np

N.Wachi and Y.Kanda

Neutron nuclear data for ^{237}Np have been evaluated below 20 MeV. Since the fission cross sections of ^{237}Np are important data in neutron dosimetry, a main theme in this work is the evaluation of the threshold energy and cross sections of $^{237}Np(n,f)$.

The fission cross sections are determined by using the reported experimental data. The evaluated values are checked up with experimental data of integral cross sections in fission neutron spectra. The cross sections of (n,2n) and (n,3n) reactions are obtained semiempirically from Segev's method[1] and experimental data. The optical model and statistical model are used to calculate total cross sections and cross sections of (n,n), (n,n'), and (n,γ), taking account of the evaluated (n,f), (n,2n), and (n,3n) cross sections and few available experimental data. Resonance parameters of Plattard[2] are adopted.

The results are shown in Fig. in the fast neutron region. They are submitted to the compilation group of Japanese Evaluated Nuclear Data Library (JENDL) for storing in JENDL Version 2.

References

1) M.Segev et al. ; Ann. Nucl. Energy, 5, 239 (1978)

2) S.Plattard ; Nucl. Sci. Eng. 61, 477 (1976)

3) M.Lindner, R.J.Nagle, and J.H.Landrum ; Nucl. Sci. Eng. 59, 381 (1976)

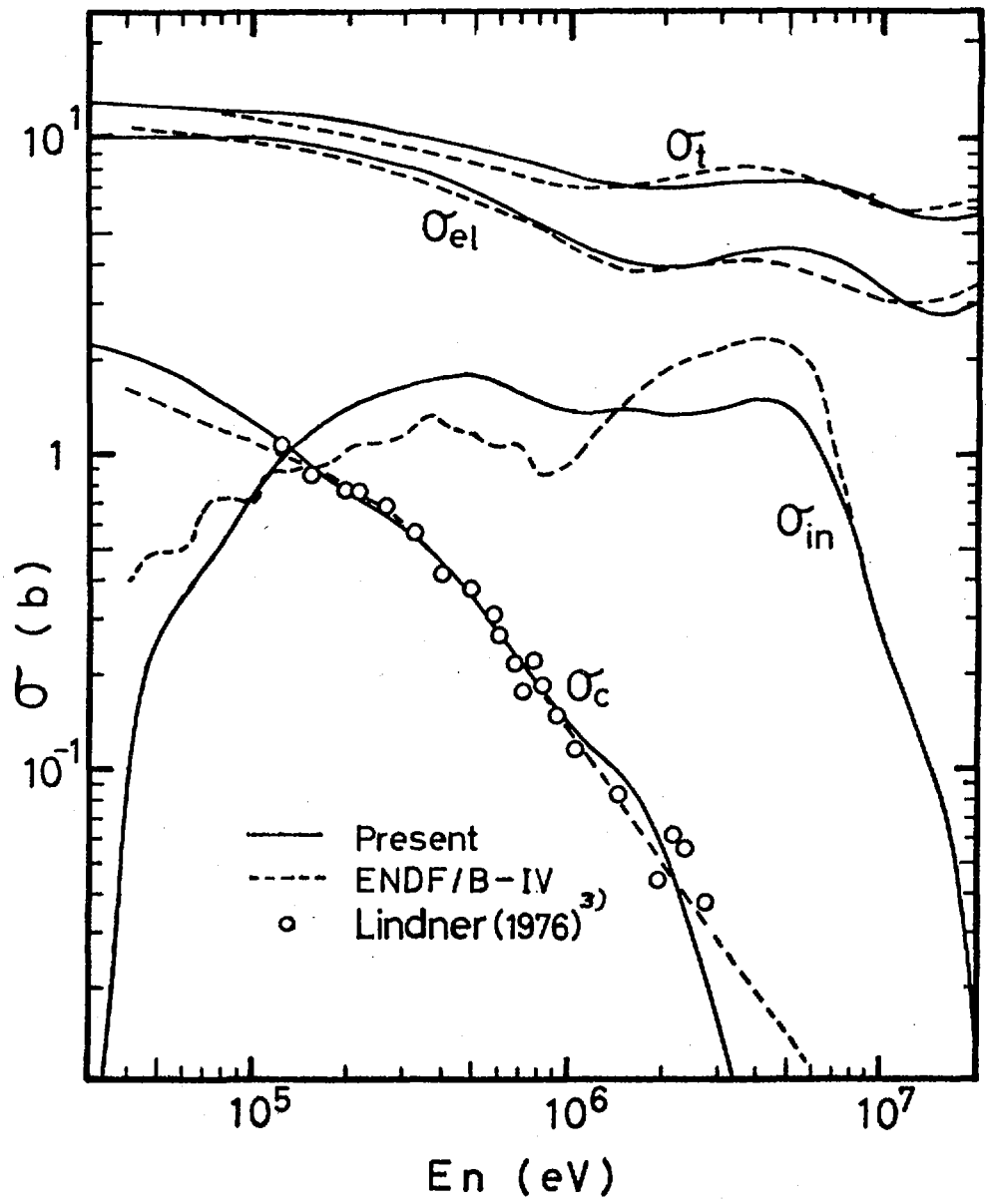

Fig. σ_t, σ_{el}, σ_{in}, σ_c.

III-B-3

Calculation of Emission Probabilities of Recoiled Nuclei from Metal Samples in Neutron-Induced Reactions

T.Shibayama and Y.Kanda

A recoil sputtering ratio which is defined as a ratio of the number of nuclei emitted from metal sample in neutron-induced reactions to the number of incident neutrons is interested in the field of the fusion reactor developement. Especially, in the case that the recoiled nucleus is radioactive, the ratio is demanded.

Harling et al.[1] measured the radioactive recoil-sputtering-ratios for the candidate metals of the first wall of the fusion reactor by 14-MeV neutrons.

We have studied to calculate the ratios by Monte Carlo method on the assumptions that the energy spectra of reaction products can be deduced from the evaporation model and the energy loss and range of the recoiled nucleus in the sample can be estimated from Lindhard Scharff and Schiott theory[2].

Preliminary results are shown in Fig.. The "forward" and "backward" mean the forward sputtering ratio and the backward sputtering ratio, respectively. The forward sputtering is that the recoiled nuclei are emitted in the direction of the incident neutrons.

References

1) O.K.Harling, M.T.Thomas, R.L.Brodzinski, and L.A.Rancitelli ; J.Appl.Phys. 48, 4328 (1977)

2) J.Lindhard, M.Scharff and H.Schiott ; Kgl.Danske Videnskab. Selskab, Mat-Fys. Medd. 33, no.14

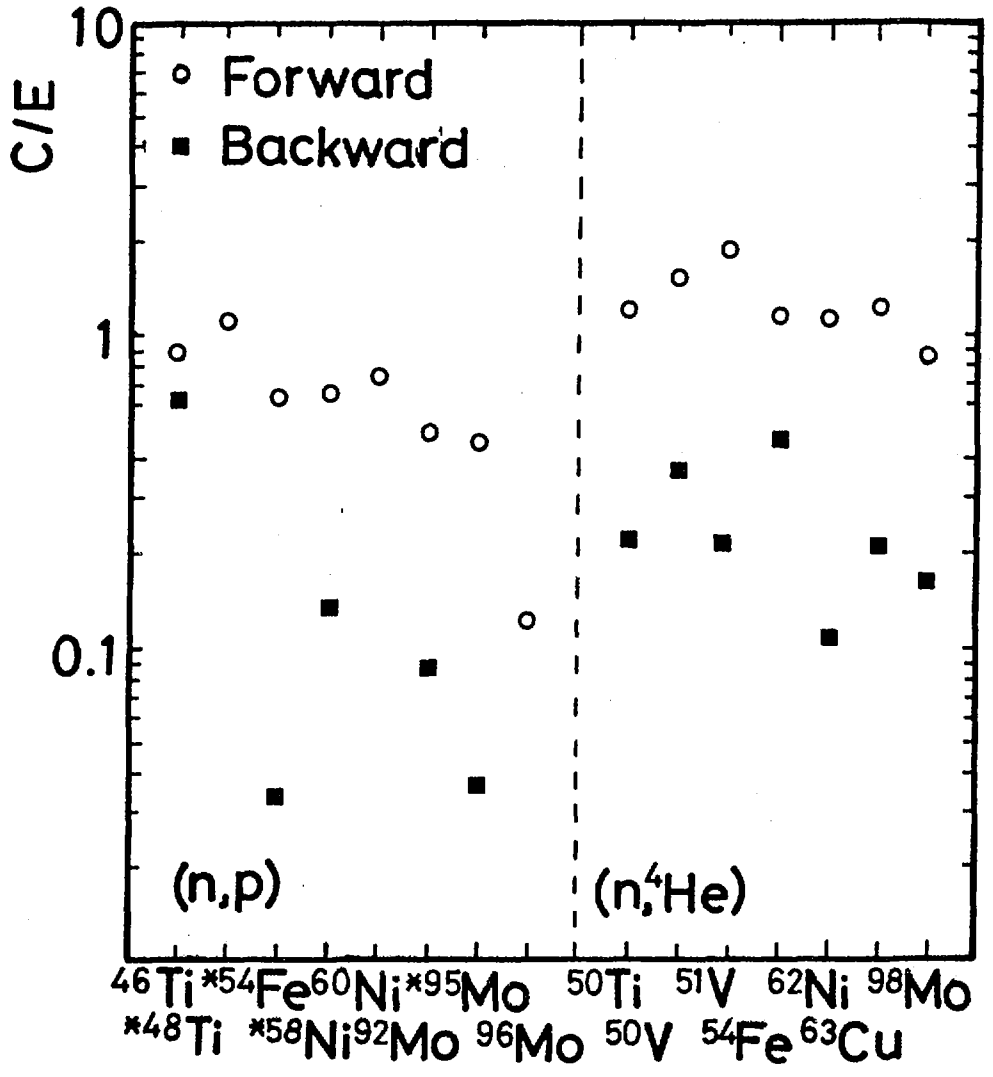

Fig. Calculation/Experiment

IV. NAGOYA UNIVERSITY

Department of Nuclear Engineering

IV-1 Level Properties of ^{146}Nd in the Decay of ^{146}Pr

Y. Ikeda, H. Yamamoto, K. Kawade, T. Katoh and T. Nagahara*

A paper on this subject was published in J. Phys. Soc. Japan 45 p.725(1978).

The decay of 24 min ^{146}Pr has been studied with Ge(Li), pure Ge(Li), NaI(Tl) and plastic detectors in singles and coincidence modes. Sources were prepared by the chemical separation called a rapid paper electrophoresis, from the fission products of ^{235}U. A total of 104 γ-ray transitions, 64 of them not reported before, have been observed and 88 transitions of them are incorporated into a level scheme comprising 32 excited states of ^{146}Nd. Observed Q_β value was 4.15 ± 0.15 MeV. Gamma-gamma derectional angular correlation measurements in ^{146}Nd have been performed with 12 cascades, each including 453.9 keV $2^+ \rightarrow 0^+$ ground state transition. Spin assignments of 13 levels in ^{146}Nd were deduced. The low lying states in ^{146}Nd are discussed in terms of the quasi band.

---

* Institute for Atomic Energy, Rikkyo University

IV-2 Decay of ^{148}Pr Isomers to Levels of ^{148}Nd

Y. Ikeda, H. Yamamoto, K. Kawade, T. Takeuchi, T. Katoh and T. Nagohara*

A paper on this subject was submitted to J. Phys. Soc. Japan, and will be published in vol. 47, no. 4.

The decay of ^{148}Pr to levels of ^{148}Nd has been investigated with Ge(Li) and plastic detectors in singles and coincidence modes. Sources were prepared by a chemical separation from the fission products of ^{235}U. Forty γ-rays assosiated with ^{148}Pr decay have been observed and thirty four of them are incorporated into a level scheme including six new levels at 723.7, 1275.0, 1512.4, 1687.5, 2543.0 and 3129.6 keV. In comparison with the decay study of ^{148}Pr produced by the ^{148}Nd(n,p) reaction, this work, for the first time, could make clear the existence of ^{148}Pr isomers by γ-ray intensity ratios and their half-lives which are 2.27 ± 0.04 and 2.0 ± 0.1 min. A low lying level at 723.7 keV is assigned a 0^+ state from the γ-γ anisotropy measurements and low lying levels in the transitional nuclide ^{148}Nd are discussed in terms of the quasi band description.

---

* Institute for Atomic Energy, Rikkyo University

V. RIKKYO (ST. PAUL'S) UNIVERSITY

Department of Physics

V-1 Measurement of the α-α Correlation Spectrum from the $^{9}Be(n,\alpha\alpha)nn$ Reaction at 14.1 MeV*

S. Shirato, K. Shibata and M. Saito

Since a previous report[1], we have continued to measure the correlation energy-spectrum of two α-particles from the four-body breakup reaction of ^{9}Be bombarded with 14.1 MeV neutrons.

A self-supporting beryllium target of 1.7 mg/cm^2 thick and two counter telescopes were mounted in a specially designed reaction chamber, in which the counter gas (Ar + 4.9% CO_2 of 100 Torr) was filled outside the neutron-source part. Each counter telescope consists of two gas-proportional counters and a silicon detector. Four ΔE and two E linear signals from the telescopes 1 and 2 and the output signal of a time-to-amplitude converter were analyzed through a CAMAC data acquisition system.[2]

The event data were taken in three separate times, each (∿ 500 hours) with the identical setup of $\theta_1 = 40^{\circ}$ and $\theta_2 = -102^{\circ}$. After separation between ^{4}He and ^{6}He and correction for energy losses of the breakup α-particles in the counter gas and the target, we obtained for the first time the α-α correlation spectrum in the $^{9}Be(n,\alpha\alpha)nn$ reaction. The result is shown in Fig. 1, in steps of the associated α-particle energy interval $\Delta E_2 = 1.2$ MeV.

The top figure in Fig. 1 shows a part of the three-body

---

* This work was supported in part by a Grant-in-Aid for Scientific Research from the Ministry of Education.

kinematic locus (the solid curve) solved under the zero relative energy between two unobserved neutrons ($E_{nn} = 0$). The arrows indicate the kinematic regions corresponding to the sequential decay processes (A) $^9Be + n \rightarrow \alpha_1 + {}^6He^* \rightarrow \alpha_1 + \alpha_2 + 2n$ and (B) $^9Be + n \rightarrow {}^6He^* + \alpha_2 \rightarrow \alpha_1 + 2n + \alpha_2$, where α_1 and α_2 represent the α-particles detected by the E_1 and E_2 detectors, respectively. The subscripts 1, 2 and 3 in (A) and (B) stand for the first (1.797 MeV), second (3.4 MeV?) and third (6.0 MeV?) excited states in ^6He, respectively. The somewhat enhanced yields seen in the corresponding energy regions of the measured spectra seem to be due to sequential decay via the above excited states, but further studies are needed to confirm the possible existence[3] of the second and the third excited states in ^6He.

The dashed curves in Fig. 1 represent the calculated shape of the phase-space factor, which is proportional to $\sqrt{E_1 E_2 E_{nn}}$, after normalization to the datum at $E_1 = 5$ MeV in Fig. 1-a. The dash-dotted curves are the Watson-Migdal form[4] $\sqrt{E_1 E_2 E_{nn}}/\{E_{nn} + (1/a_{nn} - \frac{1}{2} r_o E_{nn} m/\hbar^2)^2 \hbar^2/m\}$, using the scattering length $a_{nn} = -17$ fm and the effective range $r_o = 2.8$ fm for the two unobserved neutrons with the relative energy E_{nn}. Thus, the enhanced yield seen at the high energy end ($E_{nn} \sim 0$) of the measured spectra is considered to be the effect of the n-n final state interaction.

Now we are taking the data at other angle pairs such as forward-forward angles, where the detection of the events from sequential decay should be kinematically impossible through $^6He^*$ but possible or impossible through only $^8Be^*$. Compared with the present forward-backward data, these preliminary results

seem to show that the direct breakup contribution is not remarkable in the geometry of our α-α correlation detection, as was so in the proton-induced ^{9}Be breakup case[5].

References:

1) S. Shirato, K. Shibata and M. Saito, Progress Report submitted to the Japanese Nuclear Data Comittee, Japan Atomic Energy Research Institute, 1978 (unpublished), NEANDC (J)-56/U, INDC(JAP)-42/U, p. 54.

2) S. Shirato, K. Shibata and M. Saito, Rikkyo University Report RUP-78-16 (1978, unpublished).

3) N. Gangas, S. Kosionides, R. Rigopoulos and M.L. Ahmad, Phys. Letters 12 (1964) 233.
G. Paić, D. Rendić and P. Tomaš, Nuclear Phys. A96 (1967) 476.
K. Ogino and K. Maeda, J. Phys. Soc. Japan 26 (1969) 852.

4) K.M. Watson, Phys. Rev. 88 (1952) 1163.
A.B. Migdal, ZhETF (USSR) 28 (1955) 3; JETP (Sov. Phys.) 1 (1955) 2.

5) S.T. Emerson, V. Valković, W.R. Jackson, C. Joseph, A. Niiler, W.D. Simpson and G.C. Phillips, Nuclear Phys. A169 (1971) 317.

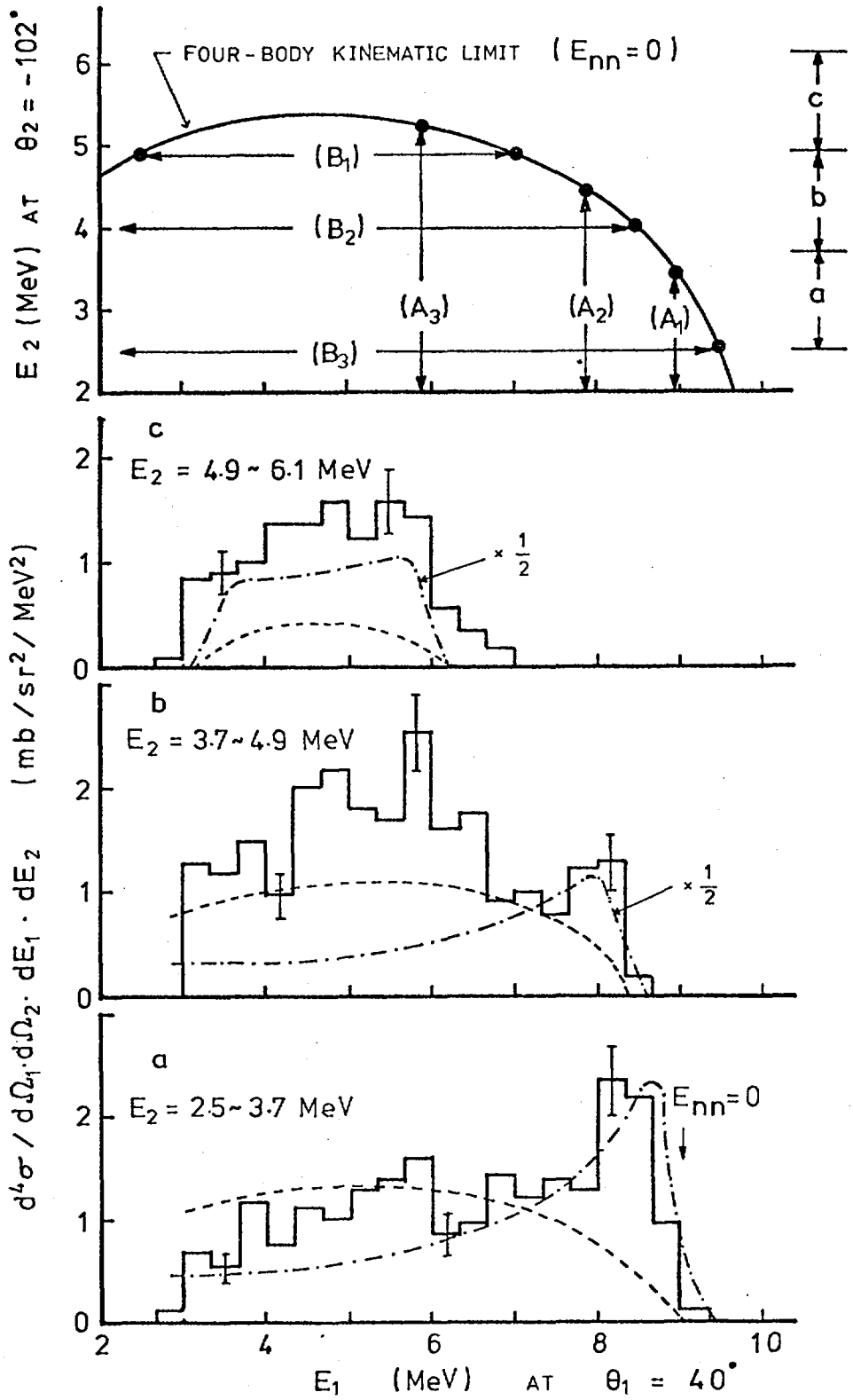

Fig. 1. α-α correlation spectra projected onto the E_1 axis in steps of the indicated E_2 interval for the reaction $^9Be(n,\alpha\alpha)nn$ at 14.1 MeV.

VI. TOHOKU UNIVERSITY

Department of Nuclear Engineering, Faculty of Engineering

VI-1 Studies of the Cross Sections for the (n,xγ) Reactions

Y. Hino, T. Yamamoto*, S. Itagaki and K. Sugiyama

Studies of gamma-ray production cross sections for fast neutron interactions have been continuing in this year. Measurements have been carried out for Al, Ni, Cu and Nb at the neutron energies of 5.3, 5.9, 6.4 and 7.0 MeV. The Dynamitron accelerator and a deuterium gas target were used to produce pulsed monoenergetic neutrons[1]. Gamma-rays were detected with a heavily shielded 70 cm^3 coaxial Ge(Li) detector at an angle of 125°. Absolute cross sections of resolved gamma-ray lines are obtained. Total and unresolved gamma-ray production cross sections are also deduced by unfolding the pulse height spectra with a modified "FERDOR" code. Typical results for aluminum and copper are shown in Fig. 1 and 2.

Reference:

1) Y. Hino, T. Yamamoto, T. Saito, Y. Arai, S. Itagaki and K. Sugiyama, J. Nucl. Sci. and Technol., 15, 85 (1978)

---

* Present Address: Toshiba Electric Co. Ltd.

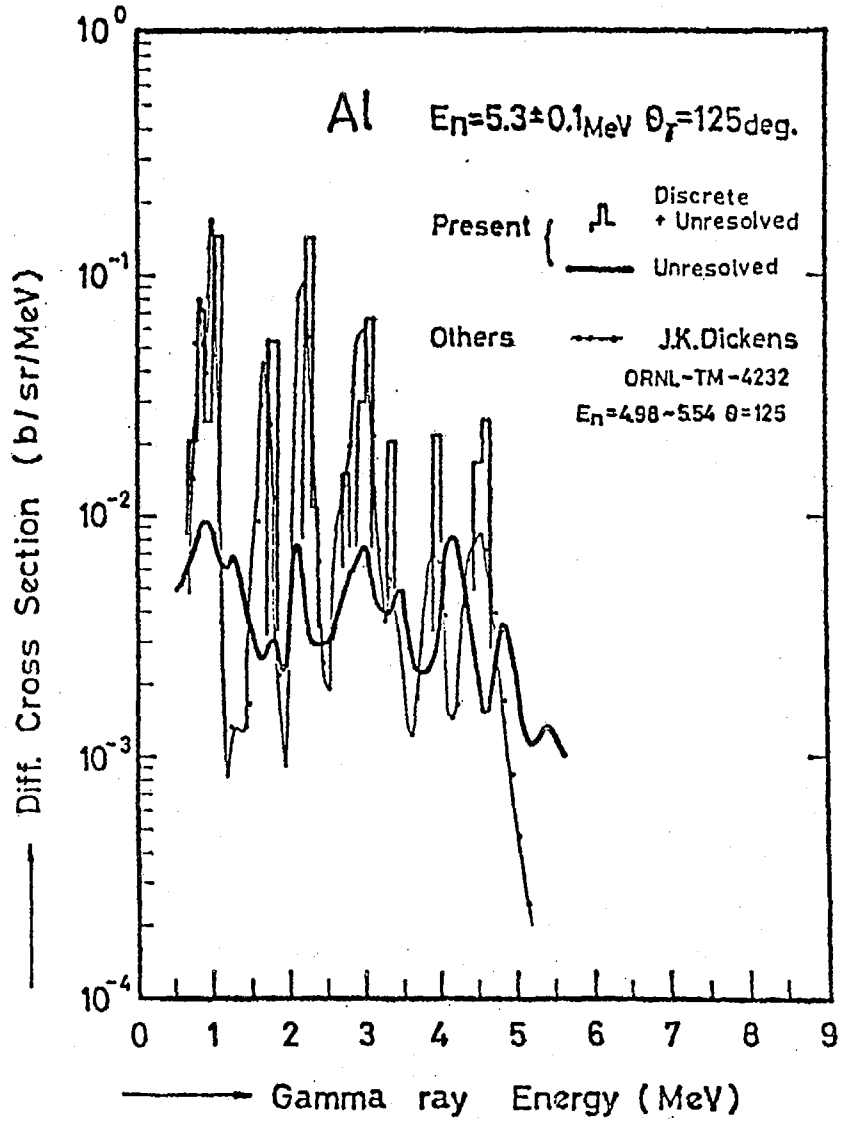
Al
En=5.3±0.1MeV θγ=125deg.
Present
Discrete + Unresolved
Unresolved
Others
J.K.Dickens
ORNL-TM-4232
En=4.98~5.54 θ=125
Diff. Cross Section (b/sr/MeV)
Gamma ray Energy (MeV)

Fig. 1 (a)

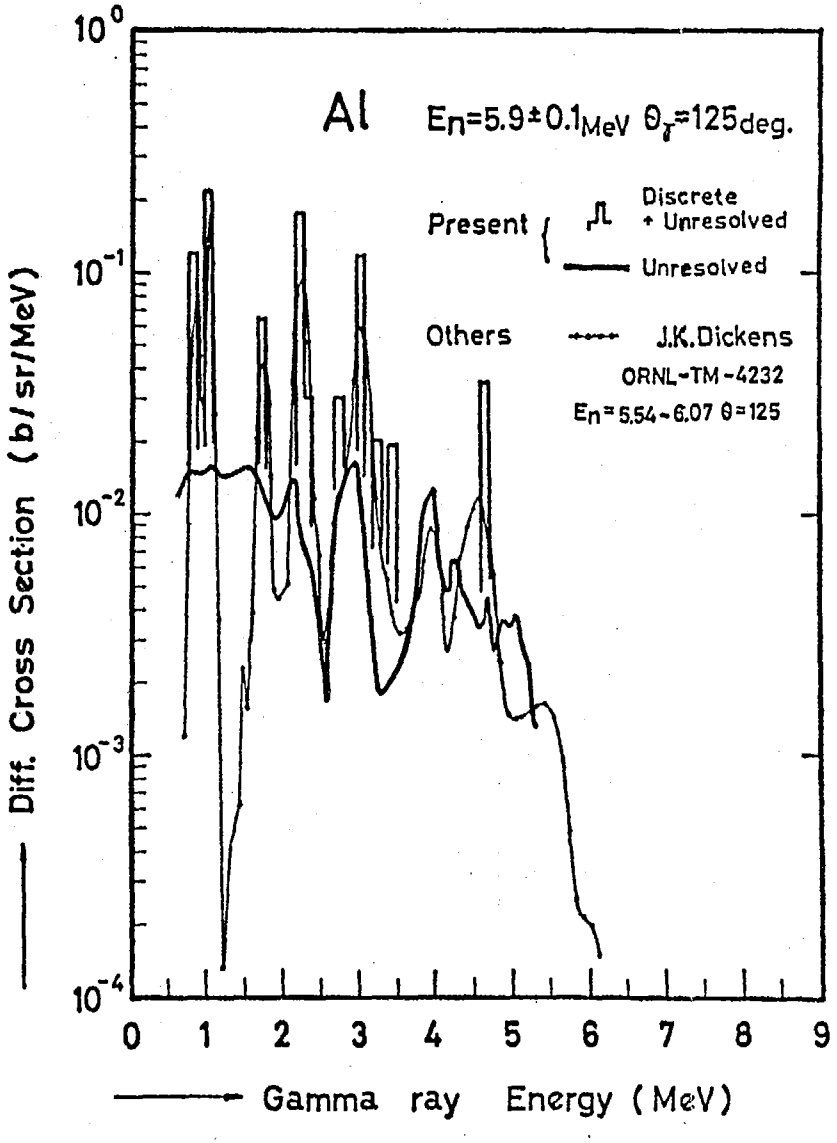
Al
En=5.9±0.1MeV θγ=125deg.
Present
Discrete + Unresolved
Unresolved
Others
J.K.Dickens
ORNL-TM-4232
En=5.54~6.07 θ=125
Diff. Cross Section (b/sr/MeV)
Gamma ray Energy (MeV)

Fig. 1 (b)

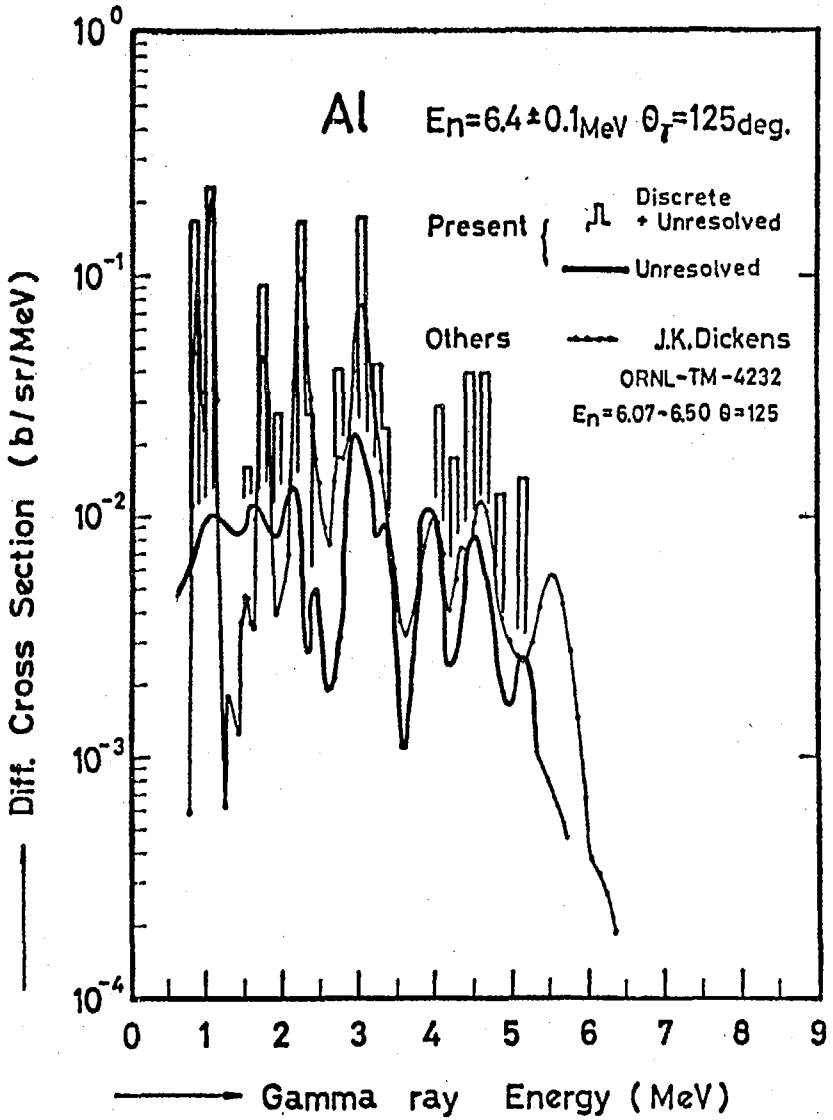
Al
En=6.4±0.1MeV θγ=125deg.
Present
Discrete + Unresolved
Unresolved
Others
J.K.Dickens
ORNL-TM-4232
En=6.07~6.50 θ=125
Diff. Cross Section (b/sr/MeV)
Gamma ray Energy (MeV)

Fig. 1 (c)

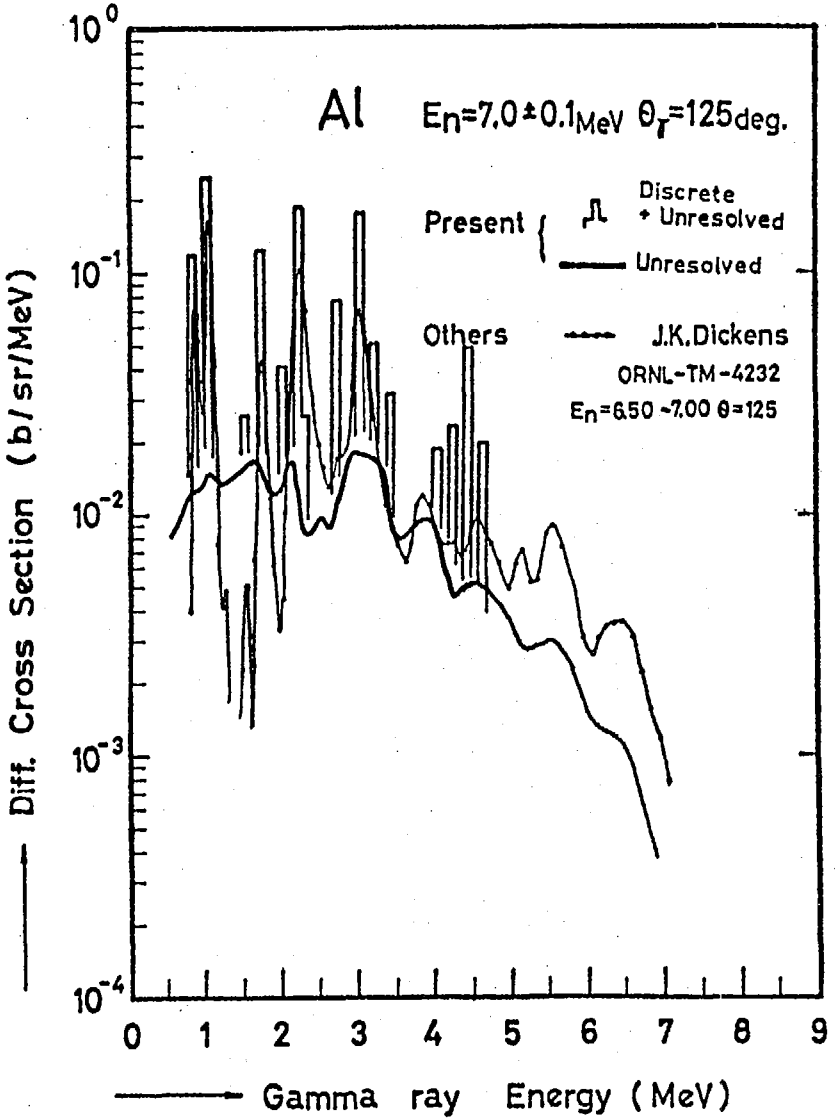
Al
En=7.0±0.1MeV θγ=125deg.
Present
Discrete + Unresolved
Unresolved
Others
J.K.Dickens
ORNL-TM-4232
En=6.50~7.00 θ=125
Diff. Cross Section (b/sr/MeV)
Gamma ray Energy (MeV)

Fig. 1 (d)

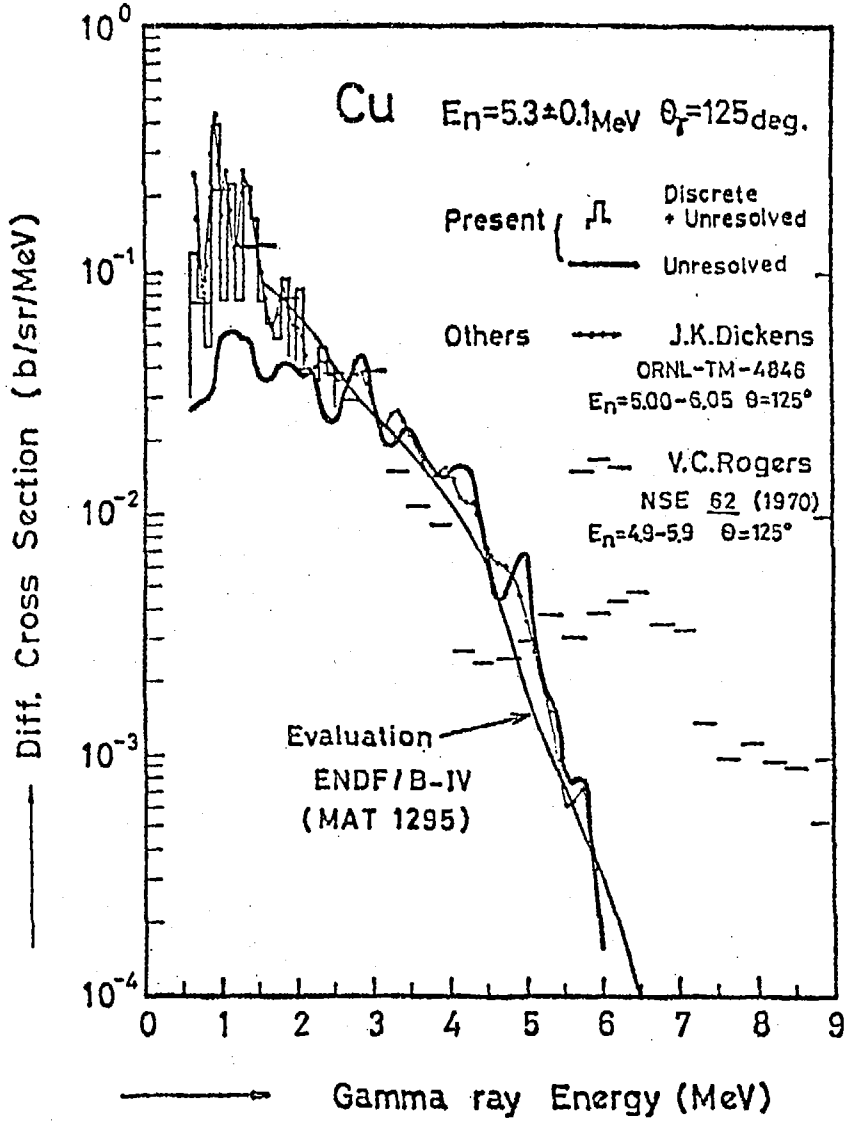
Cu
En=5.3±0.1MeV θγ=125deg.
Present
Discrete + Unresolved
Unresolved
Others
J.K.Dickens
ORNL-TM-4846
En=5.00-6.05 θ=125°
V.C.Rogers
NSE 62 (1970)
En=4.9-5.9 θ=125°
Evaluation
ENDF/B-IV
(MAT 1295)
Diff. Cross Section (b/sr/MeV)
Gamma ray Energy (MeV)

Fig. 2 (a)

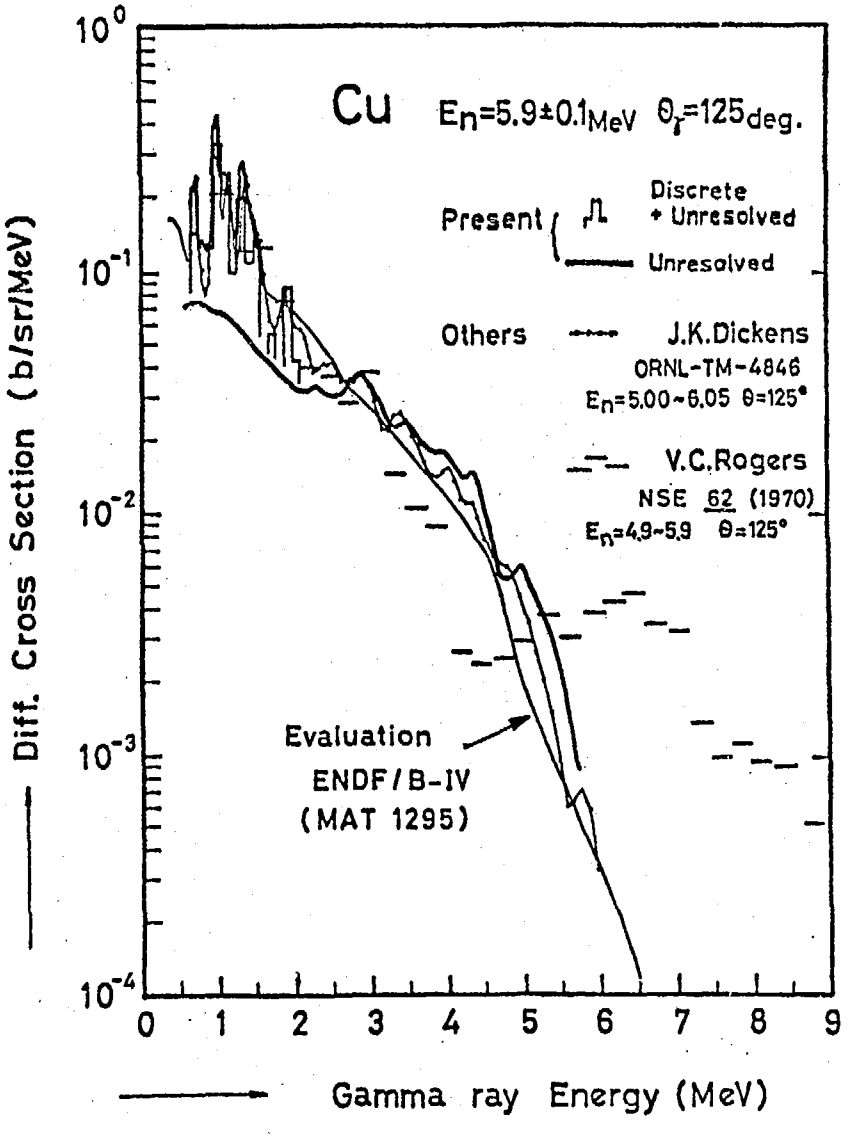
Cu
En=5.9±0.1MeV θγ=125deg.
Present
Discrete + Unresolved
Unresolved
Others
J.K.Dickens
ORNL-TM-4846
En=5.00-6.05 θ=125°
V.C.Rogers
NSE 62 (1970)
En=4.9-5.9 θ=125°
Evaluation
ENDF/B-IV
(MAT 1295)
Diff. Cross Section (b/sr/MeV)
Gamma ray Energy (MeV)

Fig. 2 (b)

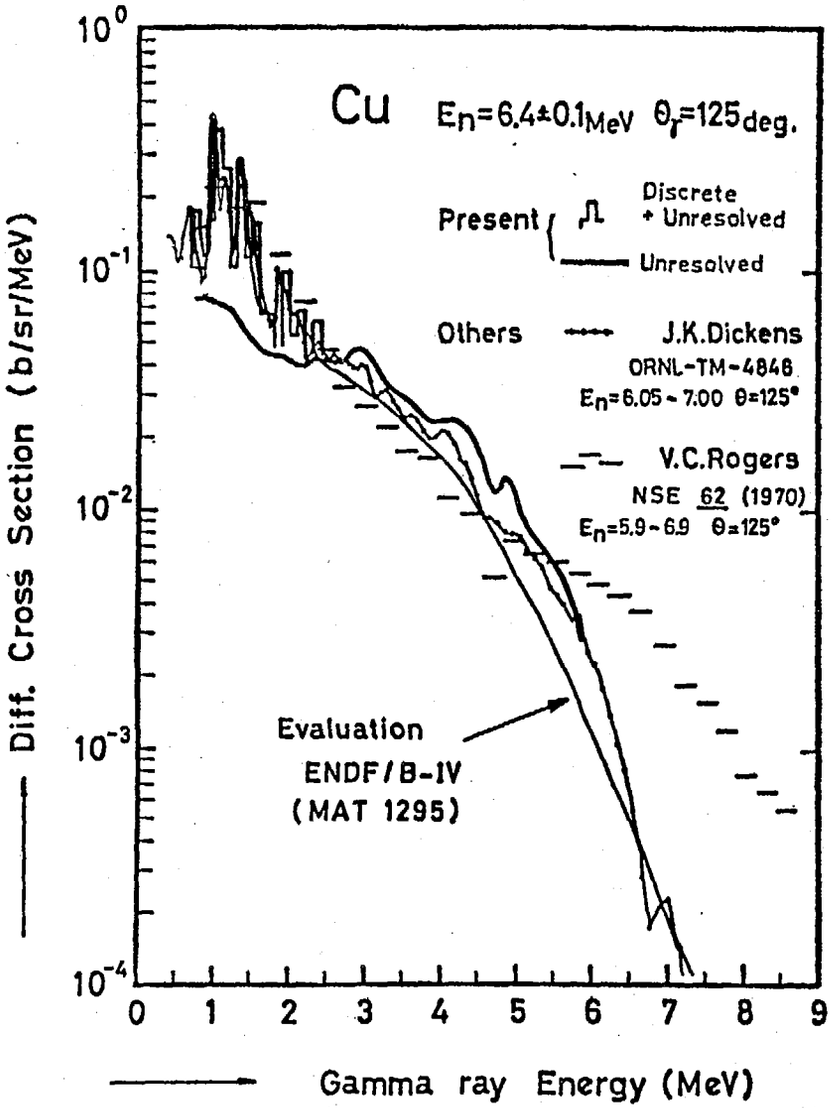
Cu
En=6.4±0.1MeV θγ=125deg.
Present
Discrete + Unresolved
Unresolved
Others
J.K.Dickens
ORNL-TM-4846
En=6.05~7.00 θ=125°
V.C.Rogers
NSE 62 (1970)
En=5.9~6.9 θ=125°
Evaluation
ENDF/B-IV
(MAT 1295)
Diff. Cross Section (b/sr/MeV)
Gamma ray Energy (MeV)

Fig. 2 (c)

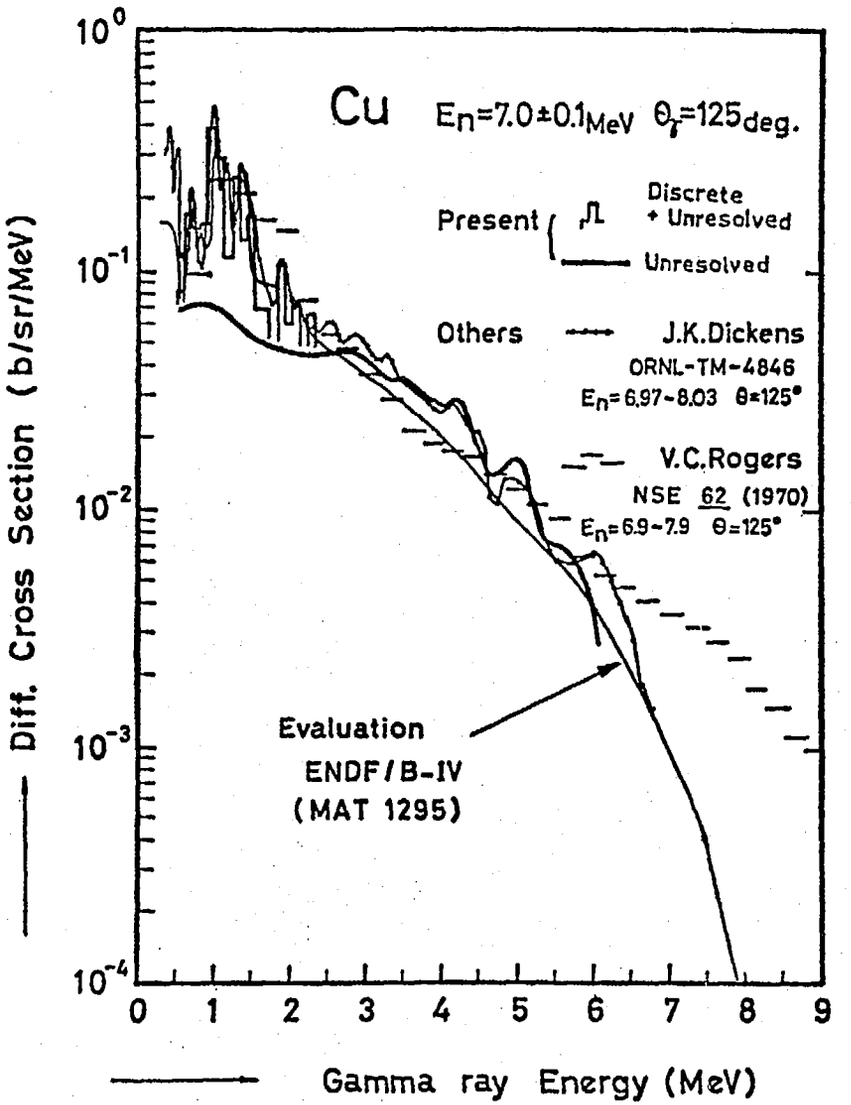
Cu
En=7.0±0.1MeV θγ=125deg.
Present
Discrete + Unresolved
Unresolved
Others
J.K.Dickens
ORNL-TM-4846
En=6.97~8.03 θ=125°
V.C.Rogers
NSE 62 (1970)
En=6.9~7.9 θ=125°
Evaluation
ENDF/B-IV
(MAT 1295)
Diff. Cross Section (b/sr/MeV)
Gamma ray Energy (MeV)

Fig. 2 (d)

VI-2 Secondary Neutron Energy and Angular Distributions for ^{93}Nb(n,xn) Reaction at 15.6 MeV.

S. Iwasaki, T. Tamura, M. Sugimoto, T. Suzuki
H. Takahashi, and K. Sugiyama

In the fusion reactor the 14 MeV neutrons interact with first wall materials by various types of neutron producing reaction, such as (n,n),(n,n'),(n,2n),(n,pn), and (n,αn) etc. The cross section data for these reactions have become more important in the fusion reactor design. In the present work the energy and angular distributions of the secondary neutrons for the (n,xn) reaction on niobium have been measured at the incident neutron energy of 15.6 MeV.

A cylindrical sample (2 cm dia. and 3 cm height) of niobium metal was bombarded by the nano-second pulsed neutrons. The source neutrons were produced by the T + d reaction with the 4.5 MV Dynamitron accelerator. A conventional time-of-flight spectrometer was used for the measurement. Main detector of the spectrometer was a 5"Ø x 2" NE213 scintillator coupled to a photomultiplier tube XP1040. A neutron monitor, the 2"Ø x 2" NE213 scintillator was placed at the angle of 30 deg. to the incident deuteron beam, and used to normalize the scattering experiment at each angle to the constant source flux.

The secondary emission neutrons were measured at thirteen angles from 25° to 150°. Background level for each measuremnt was estimated from the result of the corresponding sample-out measurement. The detection efficiency of the spectrometer was calculated by a Monte-Carlo code O5S[1]. The calculated

values of the efficiency were checked by the measurement of the hydrogen scattering cross section, which was performed using a polyethylene sample under the same experimental condition. The effect of neutron multiple scattering and attenuation in the sample were corrected by a Monte-Carlo calculation [2].

Eight angular distributions for continuum neutrons have been obtained for every 1 MeV bin of the secondary neutron energy from 2 to 10 MeV. Angular distribution for elastic scattering has also been obtained. In the case of the continuum neutrons, the higher energy neutron shows the more enhanced forward peaked distribution which suggests that the reaction proceeds in a direct-like reaction mechanism. The present data are generally consistent with those by Hermsdorf et al.[3] at 14 MeV.

The angle integrated spectrum obtained from above data is shown in Fig. 1. In this figure other two experimental results [3),5)], ENDF/B values and a theoretical curve are also presented. The three experimental results are in good agreement with each other except for the high energy region above 7 MeV. Hermsdorf et al.'s data show smooth decrease with the energy of neutron but others show a structure. The dashed line shows the evaluation made by Hermsdorf et al.[4] by mean of the equilibrium plus preequilibrium model which could rather well reproduce the experimental results. The solid curve in the figure taken from the ENDF/B-IV file is much lower than the experimental ones, especially for 6 MeV region by factor of two. This probably means that the preequilibrium process was underestimated in the evaluation of the file.

References:

1) R. Textor, and V. Verbinski, ORNL-4160 (1968)

2) T. Tamura, Grad. Thesis, Tohoku Univ. (1979)

3) D. Hermsdorf, A. Meister, S. Sassonoff, D. Seeliger, K. Seidel, and F. Shakin, Zfk-277 (Ü) (1975)

4) D. Hermsdorf, G. Kiessig, and D. Seeliger, Kernenergie, 20 166 Jahrgan Heft 6/1977

5) J. Karmmerdiener, UCRL-51232 (1972)

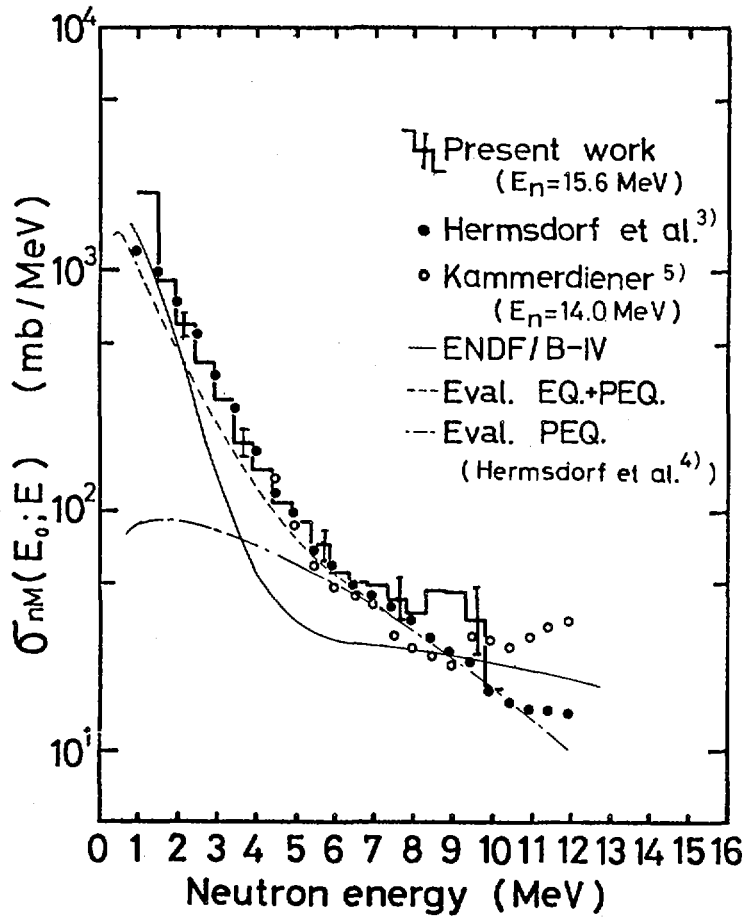

Fig. 1. Measured and evaluated total neutron emission spectra for ^{93}Nb+n reaction.